

WL-TR-96-4084

**NONCHEMICAL SURFACE TREATMENT
FOR ALUMINUM ALLOYS**



**GERHARDUS H. KOCH, GARY L. TODD
ARNOLD DEUTCHMAN, ROBERT PARTYKA**

**CC TECHNOLOGIES LABORATORIES, INC.
6141 AVERY ROAD, DUBLIN, OH 43016-8761
BEAMALLOY CORP., 6360 DUBLIN
INDUSTRIAL LANE, DUBLIN, OH 43017**

SEPTEMBER 1996

FINAL REPORT FOR 04/01/96 – 09/01/96

APPROVED FOR PUBLIC RELEASE; DISTRIBUTION UNLIMITED

19990701 053

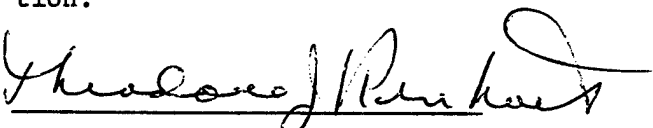
**MATERIALS DIRECTORATE
WRIGHT LABORATORY
AIR FORCE MATERIEL COMMAND
WRIGHT-PATTERSON AIR FORCE BASE OH 45433-7734**

NOTICE

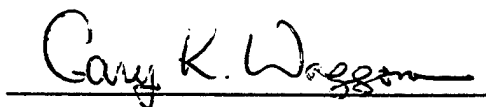
When Government drawings, specifications, or other data are used for any purpose other than in connection with a definitely Government-related procurement, the United States Government incurs no responsibility or any obligation whatsoever. The fact that the government may have formulated or in any way supplied the said drawings, specifications, or other data, is not to be regarded by implication, or otherwise in any manner construed, as licensing the holder, or any other person or corporation; or as conveying any rights or permission to manufacture, use, or sell any patented invention that may in any way be related thereto.

This report is releasable to the National Technical Information Service (NTIS). At NTIS, it will be available to the general public, including foreign nations.

This technical report has been reviewed and is approved for publication.



THEODORE J. REINHART, Chief
Materials Engineering Branch
Systems Support Division
Materials Directorate



GARY K. WAGGONER, Chief
Systems Support Division
Materials Directorate

If your address has changed, if you wish to be removed from our mailing list, or if the addressee is no longer employed by your organization please notify WL/MLSE, WPAFB, OH 45433-7718 to help us maintain a current mailing list.

Copies of this report should not be returned unless return is required by security considerations, contractual obligations, or notice on a specific document.

REPORT DOCUMENTATION PAGE			Form Approved OMB No. 0704-0188	
Public reporting burden for this collection of information is estimated to average 1 hour per response, including the time for reviewing instructions, searching existing data sources, gathering and maintaining the data needed, and completing and reviewing the collection of information. Send comments regarding this burden estimate or any other aspect of this collection of information, including suggestions for reducing this burden, to Washington Headquarters Services, Directorate for Information Operations and Reports, 1215 Jefferson Davis Highway, Suite 1204, Arlington, VA 22202-4302, and to the Office of Management and Budget, Paperwork Reduction Project (0704-0188), Washington, DC 20503.				
1. AGENCY USE ONLY (Leave blank)	2. REPORT DATE SEP 1996	3. REPORT TYPE AND DATES COVERED FINAL 04/01/96--09/01/96		
4. TITLE AND SUBTITLE NONCHEMICAL SURFACE TREATMENT FOR ALUMINUM ALLOYS		5. FUNDING NUMBERS C F33615-93-C-5323 PE 62102 PR 2418 TA 04 WU FP		
6. AUTHOR(S) GERHARDUS H. KOCH, GARY L. TODD ARNOLD DEUTCHMAN, ROBERT PARTYKA				
7. PERFORMING ORGANIZATION NAME(S) AND ADDRESS(ES) CC TECHNOLOGIES LABORATORIES, INC. 6141 AVERY ROAD DUBLIN OH 43016-8761 BEAMALLOY CORP, 6360 DUBLIN INDUSTRIAL LANE, DUBLIN OH 43017		8. PERFORMING ORGANIZATION REPORT NUMBER		
9. SPONSORING/MONITORING AGENCY NAME(S) AND ADDRESS(ES) MATERIALS DIRECTORATE WRIGHT LABORATORY AIR FORCE MATERIEL COMMAND WRIGHT PATTERSON AFB OH 45433-7734 POC: JAMES J. MAZZA, WL/MLSE, 937-255-7778		10. SPONSORING/MONITORING AGENCY REPORT NUMBER WL-TR-96-4084		
11. SUPPLEMENTARY NOTES				
12a. DISTRIBUTION AVAILABILITY STATEMENT APPROVED FOR PUBLIC RELEASE; DISTRIBUTION IS UNLIMITED.		12b. DISTRIBUTION CODE		
13. ABSTRACT (Maximum 200 words) The state-of-the-art chemical surface treatments for adhesive bonding of aluminum alloys, such as phosphoric acid anodizing (PAA) are the basis of the present high-strength and durable adhesive bonds. Because of increasingly strict regulations on the use of wet chemicals, the Materials Directorate at Wright Laboratories initiated a research program to develop alternative non-chemical techniques that do not produce waste and are not detrimental to health and environment. This report describes the development of a non-chemical process, based on ion beam enhanced deposition (IBED). The process consists of various steps, the major ones being grit blasting with 50 μm Al_2O_3 grit and deposition of α - Al_2O_3 with IBED. The resulting surface is dense and corrosion resistant, and provides an excellent basis for adhesive bonding. Strength and durability studies on peel and wedge type specimens is equivalent to that of anodized specimens. Surface analytical studies, Scanning Electron Microscopy (SEM), Transmission Electron Microscopy (TEM), X-ray Photoelectron Spectroscopy (XPS), Fourier Transform Infrared Spectroscopy (FTIR), and Atom Force Microscopy (AFM), as well as electrochemical studies were used to characterize the surface and determine the mechanism of adhesion.				
14. SUBJECT TERMS ION BEAM ENHANCED DEPOSITION, PHOSPHORIC ACID ANODIZING, ADHESIVE BONDING, STRENGTH, DURABILITY SURFACE ANALYSIS ELECTROCHEMISTRY		15. NUMBER OF PAGES		
		16. PRICE CODE		
17. SECURITY CLASSIFICATION OF REPORT Unclassified	18. SECURITY CLASSIFICATION OF THIS PAGE Unclassified	19. SECURITY CLASSIFICATION OF ABSTRACT Unclassified	20. LIMITATION OF ABSTRACT SAR	

TABLE OF CONTENTS

	<u>Page</u>
1.0 INTRODUCTION	1
2.0 OBJECTIVES	2
3.0 APPROACH	2
4.0 BACKGROUND	3
4.1 Aluminum Oxide Structure And Morphology	3
4.2 Principles Of Adhesion	6
4.3 Adhesive Joint Durability	7
4.3.1 Increasing The Barrier To Water Diffusion Into The Bond Line ..	7
4.3.2 Inhibition Of Hydration Of Surface Oxide	8
4.3.3. Application of Primers	8
4.4 Ion Beam Enhanced Deposition	8
5.0 EXPERIMENTAL APPROACH	10
5.1 Surface Preparation	10
5.2 Phosphoric Acid Anodizing	10
5.3 Grit Blasting	11
5.4 Ion Beam Enhanced Deposition	11
5.4.1 Surface Cleaning	11
5.4.2 Ion Beam Surface Texturing	12
5.4.3 Oxide Film Deposition	12
5.4.4 Oxide Deposition On Grit Blasted Surface	13
5.4.5 Pre-Bond Exposure And Treatment	13
5.5 Adhesive Bonding	13
5.6 Mechanical Testing	14
5.7 Peel Testing	14
5.7.1 Test Specimens	14
5.7.2 Test Apparatus and Procedure	15
5.8 Durability Testing	15
5.8.1 Wedge Testing	15
5.9 Electrochemical Testing	15

TABLE OF CONTENTS (CONT'D)

	<u>Page</u>
5.9.1 Cyclic Potentiodynamic Polarization	16
5.9.2 Electrochemical Impedance Spectroscopy	16
5.10 Surface Analysis	17
6.0 RESULTS	18
6.1 Mechanical Strength	18
6.2 Durability	19
6.3 Electrochemical Testing	22
6.4 Cyclic Potentiodynamic Polarization	22
6.5 Electrochemical Impedance Spectroscopy	22
6.6 Surface Analysis	23
6.6.1 Scanning Electron Microscopy	23
6.6.2 Transmission Electron Microscopy	24
6.6.3 Atomic Force Microscopy	25
6.6.4 Auger Electron Spectroscopy	25
6.6.5 X-Ray Photoelectron Spectroscopy	25
6.6.6 Fourier Transform Infrared Spectroscopy	26
7.0 DISCUSSION AND CONCLUSIONS	26
8.0 REFERENCES	29

LIST OF TABLES

	<u>Page</u>
Table 1. Work Of Adhesion Values For Various Interfaces. ⁽²³⁾	33
Table 2. Sputter Dose Required For Surface Cleaning (Argon On Al ₂ O ₃).	33
Table 3. Sputter Dose Required For Aluminum Layer Removal (Argon On Al)	33
Table 4. Electrochemical Parameters For Anodized, IBED Treated And Bare Aluminum Alloy 2024-T3 In A 3% NaCl Aqueous Solution.	34
Table 5. Atom Percent Surface Composition Of IBED Samples, As Determined By XPS.	34

LIST OF FIGURES

		Page
Figure 1.	Structure Of 120-Volt Phosphoric Acid Coating Constructed On Cross Section Of Cell Base Pattern. The Dimensions Of Pore, Cell, Cell Wall and Barrier are Shown. ¹	35
Figure 2.	Schematic Representation Of Oxide Morphology Of An Aluminum Surface After Pickling With FL Process. ^{10,11}	35
Figure 3.	Schematic Representation Of Oxide Morphology On An Aluminum Surface After Phosphoric Acid Anodizing. ^{10,11}	36
Figure 4.	Schematic Representation Of Oxide Morphology On An Aluminum Surface After Chromic Acid Anodizing. ^{10,11}	36
Figure 5.	Peel Strength After Pickling Aluminum Alloy 5052 In A Sulfuric Acid-Chromic Acid Solution. ²¹	37
Figure 6.	Schematic Drawing Of The Failure Mechanism In An Aluminum/Polymer Joint System During Wedge Testing In Humid Environment. The Original Oxide Is Converted To Hydroxide, Which Adheres Poorly To The Aluminum Substrate. ²⁶	37
Figure 7.	Schematic Drawing Of Ion Beam Enhanced Deposition (IBED) Process.	38
Figure 8.	Schematic Diagram Showing Amorphous Bonding Surface, Resulting From Oxide Growth Under Influence Of Augmenting Ion Beam.	39
Figure 9.	Schematic Diagram Showing Crystalline Bonding Surface, Resulting From Outer Oxide Growth Without The Influence Of The Augmenting Ion Beam.	39

LIST OF FIGURES (CONT'D)

		<u>Page</u>
Figure 10.	Test Panel And Test Specimen For Peel Testing. ³⁵	40
Figure 11.	Roller Drum Peel Test Fixture. ³⁵	40
Figure 12.	Wedge Test Specimen Configuration. ³⁶	41
Figure 13.	Schematic Diagram Of Typical Potentiodynamic Polarization Curve Showing Important Polarization Parameters. E_{cor} = corrosion potential; E_{pit} = potential at which pits form on forward scan; E_{prot} = potential at which pits repassivate on scan; i_{cor} = corrosion current density; i_{max} = current density active peaks; i_{pass} = current density in passivate range.	41
Figure 14.	Analog Circuit For Single Time Constant Corroding Interface.	42
Figure 15.	"Nyquist" Plot Corresponding To Simple Circuit Of Figure 14.	42
Figure 16.	Typical "Bode" Plot Produced By EIS Corresponding To Circuit in Figure 14.	43
Figure 17.	Schematic Drawing Of Atomic Force Microscope.	43
Figure 18.	Peel Strength Diagram Of Aluminum Alloy 2024-T3 With FPL Pickled Surface, HNO_3 - HF Pickled Surface And PAA Treated Surface.	44
Figure 19.	Peel Strength Diagram Of Aluminum Alloy 2024-T3 With Sputter Cleaned Surface (5×10^{16} Ar Atoms/cm ² , 50kev and 1×10^{17} Ar Atoms/cm ² , 50kev).	44
Figure 20.	Peel Strength Diagram Of Aluminum Alloy 2024-T3 With Textured Surface (Sputter Dose 2×10^{17} Ar Atoms/cm ² , Texture Dose 1×10^{17} and 1×10^{18} Ar Atoms/cm ²).	45

LIST OF FIGURES (CONT'D)

	Page
Figure 21. Peel Strength Of Aluminum Alloy 2024-T3 With A 5000Å IBED Film Directly Deposited On Brulin And Acetone - Methanol Cleaned Surface.	45
Figure 22 Peel Strength Diagram Of Aluminum Alloy 2024-T3 With A 5000Å IBED Film Deposited Under Optimal Conditions.	46
Figure 23. Crack Extension Diagram Of IBED And PAA Treated Aluminum Alloy 2024-T3 Wedge Specimens Exposed To 98% RH, 120°F Air. . .	46
Figure 24. Photograph Of Wedge Specimen Fracture Surface Of IBED Treated Aluminum Alloy 2024-T3.	47
Figure 25. Photograph Of Wedge Specimen Fracture Surface Of PAA And Primed Aluminum Alloy 2024-T3.	47
Figure 26. Peel Strength Diagrams After 14 Days Exposure To Humid Air Of IBED Treated Aluminum Alloy 2024-T3 With The Surface Oxides Doped With 30% Silicon, 30% Chromium, And 30% Titanium.	48
Figure 27. Peel Strength Diagram After 14 Days Exposure To Humid Air Of IBED Treated Aluminum Alloy 2024-T3 Where The Surface Oxides Were Doped With 30%, 60% And 100% Silicon.	48
Figure 28. Crack Extension Diagram Of IBED Treated, Silicon Doped Aluminum Alloy 2024-T3 Wedge Specimens, Exposed To 98% RH, 120°F Air.	49
Figure 29. Crack Extension Diagram Of Grit Blasted And IBED Treated Wedge Specimens Exposed To 98% RH, 120°F Air, Comparing Primed And Not-Primed Surfaces.	49

LIST OF FIGURES (CONT'D)

	<u>Page</u>
Figure 30. Crack Extension Diagrams Of PAA Treated Wedge Specimens Exposed To 98% RH, 120°F Air, Comparing Primed And Not-Primed Surfaces.	50
Figure 31. Peel Strength Diagram Of Grit Blasted And IBED Treated Aluminum Alloy 2024-T3 After 14 Days Exposure To 98% RH, 120°F Air. Prior To Bonding, The Surfaces Were Exposed To Boiling Water For 5 Minutes And Dried With Acetone And Methanol Or In A 250°F Oven For 30 Minutes.	50
Figure 32. Crack Extension Diagram Of Grit Blasted And IBED Treated Aluminum Alloys Exposed To 98% RH 120°F, Comparing The Effect Of Different Prebond Drying Treatments (see Figure 31).	51
Figure 33. Crack Extension Diagram Comparing The Optimal Non-Chemical Surface Treatments With PAA. Exposure Environment Is 98% RH, 120°F Air.	51
Figure 34. Crack Extension Diagram Demonstrating The Progression Of IBED Treatment To The Optimal Combination Of Grit Blasting And IBED Treatment Compared With PAA. Exposure Environment Is 98% RH, 120°F Air.	52
Figure 35. Photograph Of Wedge Specimen Fracture Surface Of Grit Blasted IBED Treated, Oven Dried And Primed Aluminum Alloy 2024-T3.	52
Figure 36. Cyclic Potentiodynamic Polarization Curve Of Aluminum Alloy 2024-T3 With Natural Oxide Film. The CPP Test Is Conducted In A Deaerated 3% NaCl Aqueous Solution.	53

LIST OF FIGURES (CONT'D)

		<u>Page</u>
Figure 37.	Cyclic Potentiodynamic Polarization Curve Of Aluminum Alloy 2024-T3 With PAA Surface. The CPP Test Is Conducted In A Deaerated 3% NaCl Aqueous Solution.	53
Figure 38.	Cyclic Potentiodynamic Polarization Curve Of Aluminum Alloy 2024-T3 With IBED Oxide Surface. The CPP Test Is Conducted In A Deaerated 3% NaCl Aqueous Solution.	54
Figure 39.	Impedance (Bode) Diagram Of IBED Treated Surface After Exposure To A 3% NaCl Aqueous Solution For 1 Hour.	54
Figure 40.	Impedance (Bode) Diagram Of PAA Treated Surface After Exposure To A 3% NaCl Aqueous Solution For 1 Hour.	55
Figure 41.	Polarization Resistance (R_p) Of Naturally Oxidized Aluminum Alloy 2024-T3 As A Function Of Exposure Time To and 3%NaCl Aqueous Solution.	55
Figure 42.	Polarization Resistance (R_p) Of PAA Treated Aluminum Alloy 2024-T3 As A Function Of Exposure Time To A 0.5% and 3% NaCl Aqueous Solution.	56
Figure 43.	Polarization Resistance (R_p) Of IBED Treated Aluminum Alloys 2024-T3 As A Function Of Exposure Time To A 0.5% and 3% NaCl Aqueous Solution.	56
Figure 44.	Scanning Electron Micrographs Of IBED Treated Surface.	57
Figure 45.	Scanning Electron Micrograph Of IBED Treated Surface Where The Top Layer Was Allowed To Grow Without Argon Beam Augmentation.	58

LIST OF FIGURES (CONT'D)

		<u>Page</u>
Figure 46.	Scanning Electron Micrograph Of IBED Treated Aluminum Alloy 2024-T3 Exposed To Boiling Water For 15 Minutes.	59
Figure 47.	Scanning Electron Micrographs Of IBED Treated Aluminum Alloy 2024-T3 Exposed To A 3% NaCl Aqueous Solution For 24 Hours.	59
Figure 48.	Scanning Electron Micrograph Of Surface Shown In Figure 45 After 7 Days Of Exposure To A 3% NaCl Aqueous Solution.	60
Figure 49.	TEM Micrograph Of Carbon Replica Of Detergent Cleaned Aluminum Alloy 2024-T3 Surface. (Magnification 80,000 X)	61
Figure 50.	TEM Micrograph Of Carbon Replica Of HNO ₃ - HF Pickled Aluminum Alloy 2024-T3 Surface. (Magnification 80,000 X)	61
Figure 51.	TEM Micrograph Of Carbon Replica Of PAA Treated Aluminum Alloy 2024-T3 Surface. (Magnification 80,000 X)	62
Figure 52.	TEM Micrograph Of Carbon Replica Of Ion Beam Cleaned Surface Of Aluminum Alloy 2024-T3. (Magnification 80,000 X)	62
Figure 53.	TEM Micrograph Of Carbon Replica Of IBED Treated Surface Of Aluminum Alloy 2024-T3. (Magnification 80,000 X)	63
Figure 54.	Electron Diffraction Pattern Of Surface Oxide Resulting From The IBED Process And Oxide Growth Without Augmenting Beam. ...	63
Figure 55.	Profile Of Aluminum Alloy 2024-T3 With 2,000 Å IBED Film, Generated With AFM.	64
Figure 56.	High Magnification Profile Of Area In Figure 55.	64

LIST OF FIGURES (CONT'D)

		<u>Page</u>
Figure 57.	Height Profile Of A Typical Scan Across A-A In Figure 56.	65
Figure 58.	Profile Of Aluminum Alloy 2024-T3 With 3,000 Å IBED Film (2,000 Å Barrier Film And 1,000 Å Top Film)	66
Figure 59.	High Magnification Profile Of Area In Figure 58.	66
Figure 60.	Height Profile Of A Typical Scan Across The Profile In Figure 59.	67
Figure 61.	Auger Electron Spectrograph Depth Profile Across The Aluminum Oxide Indicating Oxide Thickness. A Copper Scan Indicates The Absence Of Copper In The Oxide.	68
Figure 62.	XPS Scan Of IBED Treated Aluminum Alloy 2024-T3.	68
Figure 63.	XPS Scan Of IBED Treated Aluminum Alloy 2024-T3 After Exposure To Boiling Water For 15 Minutes Then Dried In 110°C (230°F) Air.	69
Figure 64.	FTIR Spectra Of IBED Treated Aluminum Alloy 2024-T3 Exposed To Boiling Water And 110°C (230°F) Air.	69
Figure 65.	FTIR Spectra Of IBED Treated Aluminum Alloy 2024-T3 Exposed To Boiling Water And 110°C (230°F) Air.	70
Figure 66.	FTIR Spectra Showing The Effect Of Exposure Time To 110°C (230°F) Air On The Hydroxyl Peak.	70

FOREWORD

This technical report covers work performed under U.S. Air Force Contract No. F33615-93-C-5323 "Non-chemical Surface Treatment For Aluminum, Titanium, and Copper," during April 15, 1993 to September 30, 1996. This work has demonstrated the viability of ion beam enhanced deposition (IBED), as an alternative technique to wet chemical techniques, such as phosphoric acid anodizing (PAA), as pretreatment for adhesive bonding.

The program was administered under the technical direction of Mr. Theodore J. Reinhart, and Mr. James Mazza, Wright Laboratory/MLSE. The contract for this effort was with CC Technologies Laboratories, Inc. with Dr. Gerhardus H. Koch as Program Manager and Principal Investigator. BeamAlloy Corporation, with Dr. Arnold H. Deutchman as Principal Investigator, performed under subcontract to CC Technologies Laboratories.

EXECUTIVE SUMMARY

Adhesively bonded structures are being used extensively as structural components for both military and civilian aircraft. It is essential to achieve a good bonding surface which will be the basis for high strength adhesive bonds with good durability in aggressive operating environments. Surface treatments based on wet chemical processes have been shown to create excellent surfaces for adhesive bonding and coating application, and are widely used throughout the industry. The most common surface treatment as pretreatment for adhesive bonding in the United States is the phosphoric acid anodizing (PAA) process. This anodizing process results in a $\gamma\text{-Al}_2\text{O}_3$ anodized film, which consists of a thin dense barrier film and a porous top film with a thickness of about 4000 Å. The morphology of the micro-pores of the PAA film lends itself to excellent mechanical bonding. However, primers need to be applied prior to adhesive bonding to increase durability to an acceptable level. Commonly, these primers contain hexavalent chromium in the form of chromates. In the late 1970's and the early 1980's, extensive work was conducted both in the United States and in Europe to investigate the mechanism of adhesion. This was accomplished by characterizing the structure and morphology of the surface oxides formed during anodizing.

The state-of-the-art chemical surface treatments for adhesive bonding, which resulted from these studies, are the basis of the present high-strength and durable adhesively bonded joints. However, recent Environmental Protection Agency (EPA) and Occupational Safety and Health Administration (OSHA) regulations have imposed increasingly strict limitations on the use of wet chemical surface preparation processes. Particularly, surface treatment processes such as pickling and anodizing, which rely on wet chemistry techniques and are large water users, are subject to regulation. These processes eventually contribute to the waste water, which must be treated. Of specific concern to the environment are acids and those chemicals which contain toxic heavy metals such as chromium. Moreover, many of the primers which are presently in use, are solvent based, and are also subject to increasingly strict EPA and OSHA regulations.

In order to find replacements for the wet chemical surface treatment techniques, the Materials Directorate at Wright Laboratory (WL/MLSE) initiated a research program to develop alternative non-chemical techniques that do not produce waste, and are not detrimental to health and environment. An important requirement for such a technique is that it produces surfaces which result in mechanical strength and durability that are equal to or better than those produced by the wet chemical methods.

Thus, in order to achieve the objective of this program, a non-chemical, physical technique based on ion implantation was applied. After the feasibility of the use of Ion Beam Enhanced Deposition (IBED) to provide an alternative surface pretreatment for adhesive bonding was demonstrated, the process was further developed primarily to enhance the durability of the bond line in corrosive environments.

Based on the results of the experimental work, a process based on IBED was developed to prepare aluminum alloy surfaces for structural adhesive bonding. The adhesive bonds based on this surface treatment were shown to have mechanical strength and durability that are equal to that based on the wet chemical PAA process.

1.0 INTRODUCTION

Adhesively bonded structures are being used extensively as structural components for both military and civilian aircraft. It is essential to achieve a good bonding surface which will be the basis for high strength adhesive bonds with good durability in aggressive operating environments. Surface treatments based on wet chemical processes have been shown to create excellent surfaces for adhesive bonding and coating application, and are widely used throughout the industry. The most common surface treatment as pretreatment for adhesive bonding in the United States is the phosphoric acid anodizing (PAA) process. This anodizing process results in a $\gamma\text{-Al}_2\text{O}_3$ anodized film, which consists of a thin dense barrier film and a porous top film with a thickness of about 4000 Å. The morphology of the micro pores of the PAA film lends itself to excellent mechanical bonding. However, primers need to be applied prior to adhesive bonding to increase durability to an acceptable level. Commonly, these primers contain hexavalent chromium in the form of chromates. In the late 1970's and the early 1980's, extensive work was conducted both in the United States and in Europe to investigate the mechanism of adhesion.¹⁻⁸ This was accomplished by characterizing the structure and morphology of the surface oxides formed during anodizing. Relevant details of these studies are discussed in the *Background* section of this report.

The state-of-the-art chemical surface treatments for adhesive bonding contribute to high-strength and durable adhesively bonded joints. However, recent Environmental Protection Agency (EPA) and Occupational Safety and Health Administration (OSHA) regulations have imposed increasingly strict limitations on the use of wet chemical surface preparation processes. Particularly, surface treatment processes such as pickling and anodizing, which rely on wet chemistry techniques and are large water users, are subject to regulation. These processes eventually contribute to the waste water, which must be treated. Of specific concern to the environment are acids and those chemicals which contain toxic heavy metals such as chromium. Moreover, many of the primers which are presently in use, are solvent based, and are also subject to increasingly strict EPA and OSHA regulations.

In order to find replacements for the wet chemical surface treatment techniques, the Materials Directorate at Wright Laboratory (WL/MLSE) initiated a research program to develop alternative nonchemical techniques that do not produce waste, and are not detrimental to health and environment. An important requirement for such a technique is that it produces surfaces which result in mechanical strength and durability equal to or better than those produced by the wet chemical methods.

Thus, in order to achieve the objective of this program, a nonchemical, physical technique based on ion implantation was applied. After the feasibility of the use of Ion Beam Enhanced Deposition (IBED) to provide an alternative surface pretreatment for adhesive bonding was demonstrated, the process was further developed primarily to enhance the durability of the bond line in corrosive environments.

2.0 OBJECTIVES

The main objective of this program was to demonstrate that wet chemical pretreatments for adhesive bonding, such as PAA, can be replaced by the dry physical method of IBED. The initial goal was to demonstrate the feasibility of applying an Al_2O_3 film by IBED onto a structural aluminum alloy surface, such that a bond strength as high as that for PAA surfaces can be achieved. Once the feasibility of applying the IBED technology was demonstrated, the surface preparation process parameters were refined, in order to achieve optimal surface conditions for adhesive bonding with respect to strength and durability. The final goal of the program was to gain a mechanistic understanding of the surface parameters which contribute to a strong and durable adhesive bond.

3.0 APPROACH

In order to achieve the above objective, the program was divided into two phases. In the first phase, the feasibility of the IBED process to replace PAA as pretreatment for adhesive bonding was demonstrated. Details of this phase of the program were reported in a topical report submitted to WL/MLSE in September 1994.⁹

Following the Phase I feasibility demonstration, Phase II was initiated. Phase II consisted of two tasks, the first one being the development of a basic understanding of the mechanism of the interaction between the surface and the primer/adhesive, and the second being the refinement of the process parameters. In the mechanistic studies, the surfaces created by IBED were characterized using various surface analytical techniques such as transmission electron microscopy (TEM), scanning electron microscopy (SEM), Auger electron spectroscopy (AES), X-ray photoelectron spectroscopy (XPS), and atomic force microscopy (AFM). Electrochemical analysis techniques, such as cyclic potentiodynamic polarization (CPP) and electrochemical impedance spectroscopy (EIS) were also used to assess the durability of the surface oxide films in corrosive solutions.

The task on process refinement focused on the durability of adhesive bonds. Standard experimental techniques, such as peel and wedge testing, were used to evaluate the performance of the refinements which led to achieve a surface with optimal durability. Both tasks were performed concurrently, and the understanding of the mechanism developed in the first task served as a guideline for the process refinement.

4.0 BACKGROUND

Research of surface treatment of aluminum alloy components for adhesive bonding was conducted as early as the 1950's, when surface preparation methods were developed primarily by means of empirical approaches.¹ A significant increase in research activity and development occurred during the 1970's and 1980's, when researchers suggested that the macroscopic surface morphology, and surface oxide structure and composition are important for the bondability of aluminum alloys.²⁻⁸ Early during this period, research was concentrated on the mechanical strength and durability testing of adhesive bonds, and the relationship between adhesive bond strength and surface treatment. By the early 1980's, the technology of wet chemical surface treatment and adhesive bonding was well established, but research on the mechanism of adhesion and adhesion bond failure continued.

4.1 Aluminum Oxide Structure And Morphology

Some of the significant features of aluminum oxides were recognized as early as 1953. Keller and coworkers¹ described the basic structure of anodic oxide films as consisting of close-packed cells of oxide, predominantly hexagonal in shape, each of which contain a single pore, see Figure 1. Keller found that the pore size was a function of the type of electrolyte used, but independent of the applied voltage. The wall thickness and barrier layer thickness were found to be primarily a function of the applied voltage. Much later, in the 1970's and 1980's, transmission electron microscopy (TEM), and scanning transmission electron microscopy (STEM)^{10,11} analyses were used to gain a better understanding of the effect of surface oxide morphology on the strength and durability of adhesive bonds of aluminum alloys.

Bijlmer² described an extensive research program on the effects of different pretreatments on the surface morphology and bondability of aluminum alloys. Bijlmer investigated the surface morphology which resulted from chromic-sulfuric acid pickling and chromic acid anodizing, and generated several surface morphologies which were correlated with climbing drum peel strength. This work demonstrated that the maximum peel strength was

achieved with a surface morphology consisting of fine etch pits within coarser etch pits. The work by Herfert⁵ on various surface preparations for adhesive bonding of aluminum alloys, confirmed Bijlmer's findings, but detailed scanning electron microscopy (SEM), Auger electron spectroscopy (AES), and electron diffraction demonstrated a more complex oxide structure and surface morphology. Herfert studied five anodic processes, which created basically two different anodic films: (1) a porous film, which was obtained in phosphoric acid and chromic acid, and (2) a barrier type film, which was obtained in ammonium chromate, potassium/lithium nitrate eutectic salt, and ammonium pentaborate in ethylene glycol. Each of these anodizing treatments resulted in different aluminum oxide-hydrates:

α	-	Al_2O_3 (anhydrous)	-	corundum
γ	-	Al_2O_3 (anhydrous)		
α	-	$\text{Al}_2\text{O}_3 \cdot \text{H}_2\text{O}$	-	boehmite
α	-	$\text{Al}_2\text{O}_3 \cdot 3\text{H}_2\text{O}$	-	gibbsite
β	-	$\text{Al}_2\text{O}_3 \cdot \text{H}_2\text{O}$	-	diaspore
β	-	$\text{Al}_2\text{O}_3 \cdot 3\text{H}_2\text{O}$	-	bayerite

The most common anodizing pretreatments for adhesive bonding of aluminum alloys are chromic acid anodizing (CAA), widely used in Europe,¹²⁻¹⁴ and phosphoric acid anodizing (PAA), most commonly used in the United States.¹⁵ Both anodizing treatments are usually preceded by a pickling treatment, such as the Forest Product Laboratory (FPL) treatment or the HNO_3/HF treatment. Although both pickling and anodizing treatments result in amorphous $\gamma\text{-Al}_2\text{O}_3$,¹¹ their morphologies are quite different. Venables and coworkers¹⁰ characterized the surface morphologies resulting from the various surface treatments by conducting scanning transmission electron microscopy (STEM) studies on the various surface aluminum oxides.¹⁰⁻¹¹ Figure 2 shows an isometric drawing, based on these studies, depicting the FPL oxide morphology. The microscopic roughness of the oxide film, namely the whiskers created by the pickling process is an essential feature in establishing the bondability of the surface to a primer, adhesive or coating.

The PAA oxide morphology, as characterized in the above referenced studies, has an even greater surface roughness than the FPL oxide, as is illustrated in Figure 3. The oxide consists of a dense barrier layer with a net work of hollow, well developed hexagonally shaped pores, and whisker-type protrusions. The barrier layer is tens of Ångströms thin, while the porous layer is approximately 4000 Å thin. Chemically, the PAA oxide is amorphous Al_2O_3 , with the equivalent of a monolayer of aluminum phosphate (AlPO_4) incorporated into the surface film.¹¹ When exposed to a humid environment, water will adsorb onto the oxide film surface, changing both the chemical composition and the morphology of the oxide.

Sun and coworkers¹¹ studied the hydration of aluminum oxide formed by PAA, and developed surface behavior diagrams, based on Auger electron spectroscopy (AES) and X-ray photoelectron spectroscopy (XPS). Sun demonstrated with these diagrams that the first stage of hydration consists of a reversible process of water adsorption by the monolayer of AlPO_4 . Upon further exposure to the wet environment, the AlPO_4 dissolves, and the Al_2O_3 starts to convert to crystalline boehmite, AlOOH . During this stage, a morphological change takes place as well, as the pores of the original oxide are filled. During the final stage of the hydration process, the boehmite turns into the more hydrated oxy-hydroxide bayerite, $\text{Al}(\text{OH})_3$.

Although hydration is considered undesirable for an adhesive bond, the process is often used intentionally to seal the anodic oxide in order to make it more resistant to environmental influences. Wefers¹⁶ investigated the chemical and morphological changes of porous anodic oxide films which undergo the sealing treatment in hot water. He found that during the early stage of the sealing process, some of the anodic oxide dissolves and reprecipitates as a nonstoichiometric aluminum hydroxide gel, filling up the remaining pores. This initial step is followed by the process of aging of the hydroxide gel, where the water which results from the aging reaction migrates to the anhydrous oxide continuing the sealing process.

The chromic acid anodizing (CAA) process has been commonly used in Europe as surface treatment for adhesive bonding of aluminum alloy aircraft components.¹² The most common CAA treatment following pickling is the 45 volt anodizing process in an aqueous solution containing 5 weight percent CrO_3 . The oxide produced by CAA is denser than those produced by pickling or PAA, but appears to have less microporosity, and therefore offer less mechanical anchoring. However, primers have been shown to penetrate the oxide resulting in excellent adhesive properties. Figure 4 shows an isometric drawing of a typical CAA oxide on aluminum alloy 2024-T3. The drawing shows a relatively thick ($\sim 15,000 \text{ \AA}$) porous layer over a thin barrier layer. The porosity of the CAA surface oxide can be enhanced by varying the standard CAA process. Two notable processes are the 20 volt processes and the dual voltage process developed by Brockmann and coworkers.^{17,18}

The morphology of the aluminum surface has been shown to be a strong determining factor in the strength of the adhesive bond. Surface roughness can provide a high density of locations where the primer or adhesive can form mechanical interlocks with the adherend surface, thereby enhancing adhesion beyond that provided by physical and chemical adhesion. Surface texture on a very fine scale (tens to hundreds of Angstroms)

is provided by the current generation of wet chemical techniques. Similar microscopic features may also be generated by ion beam sputtering techniques.^{19,20} This may be achieved either by sputtering with reactive gases like oxygen or inert species like argon. Alternatively, surface roughness may be created with grit blasting.

Phosphoric acid anodizing (PAA), and CAA are currently used to develop controlled structure oxides on aluminum alloy surfaces. The IBED process can also be used to deposit controlled structure oxide films on aluminum alloy surfaces. The IBED process does not use any toxic chemicals, and will allow for better control over the crystal structure of the aluminum oxide. Adhesion of the oxide film to the alloy substrate will be better, since the oxide is initially mechanically alloyed into the substrate surface. Nonhydrated aluminum oxides can be produced, and they may be further "doped" with other species to enhance bondability and durability.

4.2 Principles Of Adhesion

Adhesion between metals and polymers is generally the result of a combination of mechanical, physical and chemical bonding at the interface layer. Adhesion of anodized aluminum alloy surfaces is considered to be primarily mechanical in nature. Bijlmer²¹ found a correlation between surface morphology, such as microroughness, and bondability. For example, a correlation between pickling time which affects the surface roughness, and the peel strength was demonstrated for aluminum alloy 5052 (see Figure 5).

Although the physical bonding is considered to be the weakest type of bonding, it is important in the development of adhesion. The van der Waals forces influence the degree of physical entanglement and surface wetting. In the mid 1970's several authors²²⁻²⁵ investigated the physical aspects of adhesion. Gledhill and Kinloch^{22,23} developed an equation that relates the thermodynamic work of adhesion to the surface free energy:

$$W_A = \gamma_a + \gamma_b - \gamma_{ab},$$

where W_A is the thermodynamic work of adhesion required to separate unit areas of two phases forming an interface, γ_a and γ_b are the surface free energies of the two phases, and γ_{ab} is the interfacial free energy. The authors used this basic equation to explain the effect of moisture on the strength of an adhesive bond, by calculating the work of adhesion in the presence of a wetting liquid. This allowed the prediction of the environmental stability of an interface.

A positive value of W_A in the presence of a liquid indicates that the interface is thermodynamically stable, whereas a negative value indicates an unstable interface, where the primer or adhesive spontaneously separates from the substrate. Thus, the value of W_{al} can predict the stability of the interface in a wet environment. Table 1 indicates that in the presence of water, the work of adhesion becomes negative for the epoxy-metal oxides listed.²³ The change from positive to negative work of adhesion creates the driving force for displacement of the adhesive by water. This mode of failure by spontaneous dissociation would only occur if the bond relied solely on dispersive forces as is the case for microscopically smooth surfaces.

Another way that water can degrade the bond strength is through hydration of the metal oxide. As discussed in the previous section, the typical natural or anodized amorphous $\gamma\text{-Al}_2\text{O}_3$ is converted to a hydrated oxide or hydroxide upon exposure to water. The composition of the hydrated oxides will range from $\alpha\text{-Al}_2\text{O}_3 \cdot \text{H}_2\text{O}$ (boehmite) and $\beta\text{-Al}_2\text{O}_3 \cdot 2\text{H}_2\text{O}$ (pseudoboehmite). Analyses of failed adhesive bonds have indicated that the hydroxide is usually attached to the adhesive suggesting that the adhesion between the metal and the hydroxide is very weak.²⁶ Brockman and coworkers^{17,18} used ultra-microtomic techniques to determine the exact failure path. They observed essentially three modes of deterioration. The first is a mainly reversible weakening effect in the primer or adhesive layer near the metal oxide surface, the second is a slow transformation of the oxide by hydration and a diffusion of hydrated oxide into the polymer, and the third is the fast transformation of the oxide due to corrosion. Figure 6 shows a schematic drawing of the fracture path due to water deterioration along the adhesive bond line.²⁶

4.3 Adhesive Joint Durability

The durability of an adhesive joint can be improved by preventing water from entering the bond line or by making the bond line more resistant to hydration. This can be accomplished by increasing the barrier to water diffusion into the bond line, by inhibiting hydration of the surface oxide, or by applying primers which contain corrosion inhibitors or coupling agents.

4.3.1 Increasing The Barrier To Water Diffusion Into The Bond Line

An obvious approach to increase the barrier to water diffusion is to select an adhesive which has low permeability and diffusivity, or to incorporate inert fillers into the adhesive, which can impede water diffusion. This approach is not often used, since by modifying polymers to decrease permeability and diffusivity, other important properties such as

wettability, mechanical strength or toughness may be decreased. Another means of inhibiting water diffusion into the bond line is to apply a bead of sealant on the outer edge of the bond line.

4.3.2 Inhibition Of Hydration Of Surface Oxide

As discussed in a previous section, natural aluminum oxide as well as those oxides obtained by anodizing readily hydrate to lower strength hydrated oxides or hydroxides. This hydration can be retarded by treating the surface with certain organic inhibitors, such as nitrilotris(methylene)phosphoric acid (NTMP), prior to adhesive bonding.²⁷

Surface oxide hydration can further be inhibited by creating crystalline Al_2O_3 , as opposed to the amorphous Al_2O_3 , which occurs naturally or is generated by the etching and anodizing processes, such as FPL, CAA, and PAA.²⁸ Crystalline aluminum oxide does not hydrate or hydrates very slowly, and is highly stable in aqueous environments.

4.3.3. Application of Primers

Often, primers are applied to the adherend surface prior to adhesive bonding to improve the durability of the bond. The most common and most effective primers are chromate containing primers. The chromate in the primer is primarily present as Cr^{6+} (hexavalent chromium), which is initially hydrophilic, but becomes hydrophobic²⁹ after 24 hours of heating to 50°C (120°F). It has been a general consensus that Cr^{6+} is the active species in chromate containing coatings, where corrosion inhibition is accomplished by reduction of Cr^{6+} to Cr^{3+} .

Other commonly used primers are the ones that contain chemical coupling agents, such as organosilanes. For example, γ -aminopropyltriethoxy silane (γ -APS) was used successfully in an aluminum-epoxy joint system.³⁰ The increased durability is directly related to the presence of metal-O-Si bonds, which are formed through the reaction of hydroxyl groups on the metal oxide surface and silanol groups.^{31,32}

4.4 Ion Beam Enhanced Deposition

Energetic ion beam based coating processes can offer the potential of alternative processes, to wet chemical techniques, for removing and rebuilding oxide films on aluminum surfaces as pretreatment for adhesive bonding and coating application. These techniques are already in wide use for the deposition of thin insulating coatings on optical

components, electronic components, and other thin film devices such as strain and temperature gauges, sensors, and transducers. These processes are highly reliable and controllable, and techniques can be developed to achieve surface oxides that are comparable to those achieved by anodizing.

There are two general classes of energetic ion beam based coating processes that may be appropriate for the controlled formation of oxide films on metallic surfaces. These are: 1) glow discharge sputter deposition, and 2) ion beam enhanced deposition (IBED). Both processes are capable of depositing oxide films on metallic substrates to thicknesses up to 10 μm . In glow discharge sputtering, oxide film adhesion is accomplished primarily by physical or van der Waals forces, and the film morphology is determined by the plasma conditions in the glow discharge. The conditions required to achieve the desired oxide structure and morphology, are difficult to control. On the other hand, oxide films deposited by the IBED process can be ballistically alloyed into the surface for optimal film-substrate bonding. Moreover, the IBED process can better control the morphology and mechanical properties of the surface film.

Ion beam enhanced deposition is a process that combines a conventional thin film deposition technique such as vacuum evaporation or ion beam sputtering with the bombardment of the growing film by a secondary, high energy flux.³³ The secondary ion flux, usually of an inert species such as argon, is incorporated into the deposition process for two reasons. First, the secondary ion beam is used to mix the initial layers of the deposited film into the substrate surface to improve adhesion of the film to the substrate. Secondly, the secondary ion beam can be used to control the film morphology as it grows from the substrate surface. Further, the secondary ion beam can be used to incorporate dopant materials into the deposited films to enhance properties of the film such as improved corrosion and fatigue resistance. For example, Natishan and coworkers³⁴ have experimented with a wide range of implanted species to inhibit pitting corrosion in aluminum alloys. They found that implanted Mo, Si, Ta, Nb, Zr, or Cr into aluminum improved the pitting performance, whereas Zn into aluminum had a detrimental effect.

Ion beam enhanced deposition is carried out in a high vacuum, at pressures of 1×10^{-6} Torr or below. With the proper choice of deposition parameters, the temperature of the parts being processed can be held below 50°C. A general diagram of the IBED process as implemented to deposit coatings is shown in Figure 7. The surface to be coated is first illuminated with a flux of high energy inert gas ions to remove surface oxides and contaminants. This high energy flux is maintained, and once the surface is cleaned, a flux of filming atoms is then directed simultaneously at the surface to be coated. The high

energy inert gas ions are used to mix the initial few atom layers of the specific species into the surface being coated. This forms a mechanically alloyed bond layer in the surface that promotes excellent adhesion of the coating to the substrate.

Once the interfacial layer is formed properly, the film or coating is allowed to grow. The high energy inert gas ion flux is used to control the morphology of the coating. This allows control over the grain structure of the film, as well as the film density and residual stresses. Conversely, the energy of the secondary beam can be reduced, or even eliminated to allow natural growth of the surface film.

Thus, the IBED process can be used to deposit controlled-structure oxide films onto aluminum alloy surfaces. Using the IBED process, the oxide can be initially mixed into the aluminum alloy surface for good oxide-substrate adhesion, and then grown in a manner such that the morphology of the oxide is highly controllable. By controlling the grain structure of the oxide film, corrosion-resistance can be optimized. Control of the film morphology may also allow the outer layers to be textured, so that stronger attachment of the adhesive is promoted.

5.0 EXPERIMENTAL APPROACH

5.1 Surface Preparation

The initial adhesive bond strength and durability depend strongly on the quality of the surface. The presence of any organic or inorganic contaminants on the surface will adversely affect the strength and durability of the adhesive bond. In addition to cleaning, surface morphology needs to be created to maximize bond strength and durability. The following pretreatments were applied to the aluminum alloy 2024-T3 surfaces:

1. Phosphoric acid anodizing (PAA)
2. Grit blasting
3. Ion beam enhanced deposition (IBED)

5.2 Phosphoric Acid Anodizing

The PAA panels were treated as follows:

Prior to PAA, the test panels were degreased in a 15:1 dilute solution of Brulin 815 MX Industrial General Purpose Cleaner at room temperature. Then they were pickled in a HNO_3/HF solution under the following conditions:

Bath composition: 500 g/l HNO_3 and 2.5 g/l HF
Bath temperature: room temperature
Exposure time: 10 minutes

Following the degreasing and pickling treatment, the panels were anodized under the following conditions:

Bath composition: 100 g/l H_3PO_4
Bath temperature: 20-25°C
Voltage: 10 V
Exposure time: 25 minutes

Following the PAA treatment, the specimens were rinsed with tap water for 5 minutes, followed by rinsing with deionized water and hot air drying.

5.3 Grit Blasting

Grit blasting of the aluminum alloy panels was conducted with 50 μm Al_2O_3 grit at a gas pressure of 50-60 psi. The carrier gas was nitrogen (N_2). The nozzle was hand held at an angle of approximately 45 degrees. Prior to and after grit blasting the surfaces were solvent cleaned.

5.4 Ion Beam Enhanced Deposition

5.4.1 Surface Cleaning

Prior to the IBED process, the surface was degreased and cleaned with an appropriate cleaning solution and solvent. Following this cleaning process, the test panels were placed in the process chamber and ion beam sputtered in order to remove the natural aluminum oxide film. The ion beam sputter cleaning was accomplished by bombarding the surface to be cleaned with inert atoms such as Argon. In this process, the surface atoms are removed by atomic collisions with the sputtering species, and the rate at which the surface is removed by sputtering is determined by the sputter yield of the base material. The sputter yield is a function of the ratio of the atomic masses of the base material and the sputtering species, and the energy of the sputtering species. The sputter yield of Al_2O_3 by 50 keV argon atoms is approximately 0.11. Once the yield is known, the dose required for removal of any thickness of the oxide film that forms on an aluminum alloy surface can be calculated, see Table 2.

For example, removal of a natural oxide film, 100 Ångstrom thick, will require a sputter dose of 1.98×10^{17} Argon atoms per square centimeter. At a delivered beam current of 2 mA, a sputter time of 110 minutes would be required. The typical natural oxide film thickness on aluminum alloys was found to be 50 - 100 Ångstrom, assuming that the temperature remains below 300°C. The natural oxide is predominantly amorphous γ oxide, and forms a good oxygen diffusion barrier. Hydroxides form easily in the top 10 - 40 Ångstrom of the oxide.¹¹

5.4.2 Ion Beam Surface Texturing

In the initial phase of the program, the aluminum alloy surface was textured after removal of the natural oxide. The removal rates of the aluminum surface atoms, and therefore the appearance of the sputter generated surface texture was determined by the sputter yield. The sputter yield of aluminum by 50 keV Argon atoms is approximately 5. Thus, given the sputter yield, the dose requirement for removal of any thickness of the aluminum surface can be calculated, see Table 3.

As the aluminum alloy surface is sputtered, dense arrays of conical structures will appear on the surface. These structures appear at sputter doses on the order of approximately 1×10^{18} Argon (at 50 keV) atoms per square centimeter and⁰ higher. The average diameter of the cones at the base was in the 0.25 to 0.5 μm range, with a peak-to-peak spacing of approximately 1 μm . It was expected that this micro-structured surface would provide a high density of structures for generating mechanical interlocking with the primer and/or adhesive, thereby improving adhesion. An attempt was made to sputter the surface of the aluminum alloy 2024-T3 test panels at these high doses to test whether bond strength could increase due to the sputter-induced surface roughness.

5.4.3 Oxide Film Deposition

The oxide film that is deposited onto the aluminum alloy surfaces must satisfy three criteria in order to promote adhesive strength and durability in aqueous environments:

1. The oxide films must adhere well to the aluminum alloy substrate,
2. The oxide films must be water and corrosion resistant, and
3. The outermost layers of the surface films must have a structure and morphology that promotes adhesive bonding and does not deteriorate in the presence of water.

Two different types of IBED oxide film structures were created on the aluminum alloy 2024-T3 substrates. In both structures, the oxide films were initially ion beam mixed into the alloy substrate to promote strong oxide-substrate adhesion. In both structures, the bulk of the aluminum oxide ($\alpha\text{-Al}_2\text{O}_3$) were grown under the influence of a high energy inert (Argon) augmenting ion flux. This produced a dense microcrystalline oxide film, which will not become hydrated and has good corrosion resistance. In the first type of structure, see Figure 8, the outer surface is designed to retain the morphology of the deposited oxide, where the outer surface is microcrystalline or amorphous and is microscopically smooth.

The second type of IBED oxide film structure was designed and deposited such that the outer surface presents a larger grained crystalline surface. This surface, see Figure 9, is formed by allowing the outer layer of the IBED oxide film to grow without the presence of the high energy augmenting beam. In this case, the outer layers of the film will grow as crystalline alumina ($\alpha\text{-Al}_2\text{O}_3$), and will present a surface which is crystalline, as opposed to a mostly amorphous structure.

5.4.4 Oxide Deposition On Grit Blasted Surface

In order to achieve optimal adhesive strength and durability, different combinations of surface treatments were applied. A promising combination was that where IBED oxide films were deposited onto Al_2O_3 grit blasted surfaces, so that both mechanical and physical bonding (van der Waals forces) could be accomplished.

5.4.5 Pre-Bond Exposure And Treatment

In order to determine the effect of surface hydration and subsequent remedial treatment on the bond strength of the surface treated panels, the panels were exposed to humid air and boiling water. Solvent (acetone, acetone + methanol), and oven treatment at 110°C for 30 minutes, were used to remove the water from the surface, and to condition the surface prior to adhesive bonding.

5.5 Adhesive Bonding

Immediately following the various surface treatments, the surfaces were primed with the chromate containing epoxy primer Cyanamid BR 127 and adhesively bonded with the epoxy adhesive Cyanamid FM 73, or directly bonded without first applying a primer.

After removal from the freezer, the chromate containing primer was allowed to reach room temperature, and after thorough shaking and stirring, the primer was applied with a soft brush. Per manufacturer's instructions, the primer was allowed to dry at room temperature for at least 30 minutes, after which the curing process was completed at a temperature of 120°C for 30 minutes. After priming, the test panels were stored in a desiccated cabinet to prevent any moisture pick up that may be detrimental to the adhesion between the oxide and the primer/adhesive.

The panels, with or without the primer, were bonded with FM 73 at a pressure of 40 psi and a temperature of 120°C. Adhesive bonding was accomplished over a total time of 75 minutes.

5.6 Mechanical Testing

In order to assess the initial mechanical strength of the adhesive bonds, standard mechanical tests were conducted. These tests were:

1. the floating roller peel test, and
2. the single lap shear tests.

5.7 Peel Testing

The floating roller peel test (ASTM D 3167)³⁵ is intended to determine the relative peel strength of adhesive bonds between one rigid adherend and one flexible adherend. Due to the nature of the specimen configuration and loading mode, the highest stresses are exerted on the interface between the flexible adherend and the adhesive. Thus in this program, the flexible adherend was the test alloy with the various surface treatments, while the rigid adherend was kept the same for all tests, namely, 0.063 inch thick 2024-T3 sheet with HNO₃-HF pickling treatment. The flexible adherend was 0.025 inch thick 2024-T3 sheet with the various surface treatments. The advantage of this test is that it is particularly well suited to evaluate the quality of the various surface treatments rather than the adhesive itself.

5.7.1 Test Specimens

Figure 10 shows the test panel and test specimen configuration for peel testing. The test panels are 0.5 inch wide strips cut with a band saw from the bonded panel. The edge strips were not used for testing. After cutting, the unbonded end of the flexible adherend was bent perpendicular to the rigid adherend to clamp in the grip of the testing machine.

5.7.2 Test Apparatus and Procedure

The peel tests were conducted in a servo-hydraulic tensile machine using the roller drum peel test fixture shown in Figure 11. After the test specimen was inserted into the test fixture, the specimen was peeled at a cross head speed of 6 inches/minute. During the peel test, the load is recorded as a function of cross head displacement. The peel strength (lbs/inch) is then calculated, plotted as a function of the cross head displacement (inch).

5.8 Durability Testing

The operating environment of adhesively bonded aircraft components plays an important role in the durability of these structures. The initial mechanical joint strength may be significantly reduced when the joint is exposed to various environments. As discussed in the "Background" section, water is the most detrimental environment. Although water tends to plasticize polymers, such as the epoxy resins used in this program, it exerts its most detrimental effect on the adherend-adhesive interface.

In order to evaluate the effects of aggressive environments on the durability of adhesive bonds, various test methods can be applied, the most common being peel testing and wedge testing. In the first type of test, peel specimens are exposed to an environment for some period of time, after which the peel strength is determined. The peel strength and degree of disbonding apparent on the fracture surface, provide indications of the resistance of the bond line to environmental attack.

5.8.1 Wedge Testing

A simple test method to determine the durability of bond lines stressed under Mode I condition, is the Boeing wedge test, which is also an ASTM standard test method (ASTM D3762)³⁶. The self stressing is induced by the insertion of a wedge, which creates the initial crack length a , see Figure 12. As the crack propagates, the effective load or stress at the crack tip decreases. The decrease in effective load provides a self arrest capability for the wedge test which enables the establishment of the threshold level in terms of the mode I load (P).

5.9 Electrochemical Testing

In order to gain a better understanding of the ability of the different surface oxides to prevent corrosion of the substrate, electrochemical testing was conducted. The techniques

which were used during this evaluation were cyclic potentiodynamic polarization (CPP) and electrochemical impedance spectroscopy (EIS). These techniques are described below.

5.9.1 Cyclic Potentiodynamic Polarization

Cyclic potentiodynamic polarization (CPP) is a direct current (DC) electrochemical technique, which permits the measurement of the polarization behavior of a surface in an electrolyte by continuously scanning the potential while monitoring the current response. With this technique, a potentiostat adjusts the applied polarizing current to control the potential between the working electrode and a reference electrode, generally a saturated calomel electrode (SCE). A CPP diagram, as shown in Figure 13, is able to indicate the susceptibility of an alloy to uniform and localized corrosion in specific environments. Hysteresis in the curve between the forward scan and the reverse scan is generally an indication of susceptibility to pitting or crevice corrosion. The important parameters in a CPP diagram which relate to pitting corrosion are the pitting potential (E_{pit}), protection potential (E_{prot}), and corrosion potential (E_{cor}).

5.9.2 Electrochemical Impedance Spectroscopy

Electrochemical impedance spectroscopy (EIS) is an alternating current (AC) electrochemical technique, which allows the quantification of corrosion rates over a broad range from fast to very slow. The technique is particularly well suited to determine the very low corrosion rates in well protected systems such as coated and anodized material. Various surface film properties such as impedance and capacitance can also be measured with this technique. The laboratory evaluations of both IBED and PAA treated aluminum alloy surfaces are performed in a cell which consists of the test alloy, an inert (platinum) counter electrode and a reference electrode (standard calomel electrode or SCE). The electrochemical potential of the working electrode is perturbed by a small sinusoidal potential, which is produced by an AC signal between the metal and the counter electrode. The current response to this perturbation is measured as a function of the frequency of the potential input from which various parameters can be calculated.

The alloy in the corrosive solution usually behaves as circuit comprised of resistors and capacitors. Figure 14 shows a simple equivalent electrical circuit, where R_s represents the electrolyte or solution resistance, and the parallel elements R_p and C_p represent the resistive and capacitive aspects of the interface between electrode and electrolyte. The results can be presented in two different ways. If the real component Z' and the negative of the imaginary component Z'' , measured as a function of the frequency, are plotted

against each other for a simple corrosion process the plot would appear as in Figure 15, This type of plot is called the Nyquist plot. An alternative method of plotting the circuit in Figure 14 is by means of Bode plots. A typical plot, shown in Figure 16, plots the logarithm of the impedance, Z , as a function of the logarithm of the frequency. Characteristics of the Bode plots can be used to obtain the circuit elements, R_s (solution resistance), R_p (polarization resistance), and C (capacitance).

5.10 Surface Analysis

Several surface analytical techniques were used to characterize the physical and chemical state of the various PAA and IBED treated aluminum alloy surfaces. These techniques included high magnification, high resolution scanning electron microscopy (SEM) and atomic force microscopy (AFM) to characterize the surface morphology of the surfaces.

Transmission electron microscopy (TEM) was used to study the morphology and structure of the surface oxides. The technique used study of the morphology was the direct carbon replica technique. The TEM specimens were prepared by coating the surface with a nominally 20 Å thick Au-40Pd film, deposited at an acute angle of 30 degrees, and by coating with a carbon film of a nominal thickness of 400 Å. Following the filming process, the carbon films were lifted off the surface in a methanol-2.5% bromine solution. In order to determine the crystal structure of the oxide the PAA and IBED films were deposited on aluminum foil, which was dissolved in the methanol-bromine solution. The electron diffraction technique was used to determine the oxide structure.

X-ray photoelectron spectroscopy (XPS) and Fourier transform infrared (FTIR) spectroscopy were used to evaluate the chemical state of the oxide surface, and to determine the change in chemical state, if any, as a result of exposure to aqueous environments.

Auger electron spectroscopy (AES) was used to determine the elemental composition of oxide films and to determine their thickness.

Atomic force microscopy (AFM) is one of the scanning probe microscopic techniques that can be used for imaging surfaces of solid materials with "atomic" resolution.³⁷ AFM measures the short-range interatomic forces (van der Waals forces) between the surface and a probe mounted on a flexible cantilever.³⁸ In this technique, the force between a probe or tip and a specimen surface is monitored as a function of the displacement of the sample relative to the probe, Figure 17 shows the principle in force measurements using

the AFM. A laser beam is reflected from the end of the cantilever probe to a position sensitive photodetector. The position of the sample surface is controlled by a piezoelectric actuator. By simultaneously collecting the voltage applied on the actuator and the signal from the photodetector, i.e. the deflection of the cantilever, it is possible to calculate the force acting on the probe as a function of surface separation, so that an atomic scale profile can be generated.

6.0 RESULTS

The results of this research program are divided into four separate sections, namely:

1. the effect of surface treatment on the mechanical strength of the bond,
2. the effect of surface treatment on durability of the bond,
3. surface analysis of the oxide surfaces, and
4. corrosion performance of the different treated surfaces.

6.1 Mechanical Strength

In order to assess the effects of the various surface treatments on the mechanical strength of the adhesive bonds, floating roller peel testing was used. For reference purposes, aluminum alloy panels were pickled using the HNO_3 -HF and FPL processes, and anodized using the PAA process. The results of the peel tests of these reference specimens, shown in Figure 18 indicate that the peel strength of the HNO_3 -HF treated surfaces is very low with an average peel strength of around 25 lbs/inch. The FPL etched specimens yielded somewhat higher peel strengths, ranging from 25 to 45 lbs/inch. These values are well below the manufacturer specified peel strength for the alloy-adhesive combination. When the etching treatment, HNO_3 -HF in this case, is followed by PAA, the peel strength is increased significantly into the range of 70-90 lbs/inch, which values are well above the minimum peel strength specified by the manufacturer for the FM 73 adhesive.

In order to develop a nonchemical alternative to PAA, using ion beam enhanced deposition, a stepwise approach was taken. First, after degreasing the surface with an appropriate degreasing solution, the aluminum alloy surface was ion beam cleaned to remove the natural oxide film. This cleaning process was achieved with a high energy argon (Ar) beam with beam doses of 5×10^{16} Ar atoms/cm² and 1×10^{17} Ar atoms/cm². The results of the peel tests on these surfaces, shown in Figure 19, indicate a low peel strength with values ranging from 15 to 25 lbs/inch.

Following the ion beam cleaning process, it was decided to evaluate the effect of ion beam texturing on the peel strength. The intent of this treatment was to create micro-roughness on an otherwise smooth surface which could serve as an anchor pattern for the primer/adhesive. The beam doses used to texture the surface ranged from 2×10^{17} to 1×10^{19} Ar atoms/cm.² The results of the peel tests, shown in Figure 20 show relatively low peel strength values for all of the texturing treatments. Thus, this approach to create an appropriate surface for adhesive bonding of aluminum alloys was not further pursued.

Following the work on surface texturing, a different direction was taken by applying an IBED film directly onto the ion beam cleaned surface. First, the IBED film was applied to the ion cleaned surface to a thickness of 4,000 Ångstrom, after which the panels were bonded. The surface cleaning prior to IBED deposition appears to have a significant effect on the peel strength. Figure 21 shows the low peel strength of aluminum alloy panels treated with a degreasing solution (Burlin) prior to the IBED treatment. When the panels were treated with a stronger degreaser (acetone-methanol) prior to IBED, the average peel strength increased.

As will be demonstrated in a later section in this report, the IBED film is amorphous with a very smooth surface, so that little mechanical anchoring is provided for mechanical bonding. Thus, the next step was to allow the oxide film to grow freely in a crystalline mode after a 3,000 Ångstrom thick barrier film was deposited, by turning off the Ar augmenting beam. In order to reduce the variability in mechanical strength of the adhesive bonds, the vacuum chamber was backfilled with dry nitrogen gas, rather than ambient air which can have various levels of humidity. The above described surface treatment resulted in high, reproducible values for peel strength, see Figure 22.

6.2 Durability

As was discussed in the Background Section, the durability of an adhesive bond interface is an important and critical property of an adhesively bonded structure. In order to assess the durability of the adhesive/primer-aluminum oxide interface with different aluminum oxide structures and morphologies, various tests were conducted in humid air and NaCl salt environments.

The following types of tests were conducted:

1. Exposure of wedge test coupons to both humid air and salt spray.
2. Exposure of peel specimens to humid air and salt spray.

Wedge panels with different surface treatments were exposed to a 60°C, 98% RH water vapor environment. The various surface treatments which were investigated, are in the following sections. The initial durability tests were conducted on IBED treated specimens using the process, which yielded high mechanical strength, namely, a 1,000 Ångstrom thick amorphous or micro-crystalline barrier layer, with a 3,000 Ångstrom thick crystalline top coat. The results of the wedge tests indicated that the durability of the bond line between this surface oxide and the primer/adhesive was extremely poor. In fact, Figure 23 shows that the crack jumps ahead a significant distance as soon as the loaded wedge specimen is exposed to the humid environment. A photograph of the fracture surfaces of one of these specimens suggests that fracture occurred along the oxide-adhesive interface, virtually unzipping the bond, see Figure 24. The exact fracture path was confirmed using XPS, which will be described in detail in a later section. By comparison, the crack growth in PAA wedge specimens was minimal, and no or little disbonding was observed between the adhesive/primer and the substrate (See Figure 25).

In order to improve the durability of the IBED treated surfaces, some modifications were made to the surface to either enhance the chemical bonding or the mechanical bonding. It was attempted to achieve the former by doping the IBED treated surface with silicon (Si), titanium (Ti), or chromium (Cr). The surface concentration with these elements was approximately 30% (atomic). The results of peel tests after exposure to the humid environment for 14 days, shown in Figure 26, clearly demonstrate that only Si has some beneficial effect, while the presence of Cr in the oxide appears to be actually detrimental to the durability. Further work to assess the effect of surface concentration of Si, demonstrated an increased benefit of higher Si concentration up to 60% (atomic), but no additional benefit could be derived from further increasing the Si concentration, see Figure 27. Figure 28, which shows crack extension data of wedge specimens with 60 and 100% silicon on the surface demonstrates only a slight increase in crack growth for the 100% treatment. This may suggest that a Si concentration of approximately 60% is optimal.

An alternative approach to improve the durability of the bond line was to roughen the aluminum alloy surface prior to the IBED treatment by grit blasting with fine grit Al_2O_3 . Figure 29, which shows the wedge test results for the grit blasted surfaces, demonstrates a marked improvement over the smooth IBED surface. The figure shows the crack growth of wedge specimens with grit blasted surfaces and with or without primer. Clearly, the presence of the chromate containing primer has again a significantly beneficial effect on the durability of the bond line. This effect of the primer is also demonstrated in Figure 30, which compares the durability of adhesive bonds with PAA treated and primed surfaces with PAA treated and not-primed surfaces.

Although a marked improvement in durability of adhesive bonds could be achieved by promoting mechanical bonding, the objective of obtaining the consistency in durability of PAA treated aluminum alloy adhesive bonds was not achieved with the above described surface treatments. Since aluminum oxide is known to be very hygroscopic, it was therefore suspected that water would readily adsorb from the environment onto the surface. If not removed, a thin film of water could be trapped between the oxide film and the primer, and result in a weak interface. In order to achieve consistently good durability of the bond line, the surface water film needs to be removed either by solvent wiping or boiling off.

In order to pursue different possible approaches to remove water, aluminum alloy panels were immersed in boiling water for 5 minutes, after which they were solvent cleaned in acetone or acetone + methanol, or dried in an oven at 110°C (230°F) for 30 minutes. After these treatments, the surfaces were immediately primed and bonded for peel test specimen preparation. Figure 31 shows that the peel strength completely recovered once the water was removed from the surface, suggesting that no or little hydration of the aluminum oxide ($\alpha\text{-Al}_2\text{O}_3$) had occurred. In order to further assess the durability of bond lines subjected to these treatments, wedge test specimens were prepared as well. The results of the durability tests on the wedge test specimens demonstrated that removal of the water film from the surface by either method resulted in durable bond lines, see Figure 32.

The reproducibility of the water removal process was evaluated with the post-IBED oven treatment. Figure 33 demonstrates that the IBED treatment over a grit blasted surface followed by 30 minutes in 110°C air, results in a strong and durable bond line. Moreover, specimens which were exposed to boiling water for 5 minutes, and were subsequently oven dried at 110°C, also demonstrated extremely good durability. Finally, Figure 34 presents the results of wedge tests in 98% RH, 60°C (140°F) humid air illustrating the progression of the surface treatment development. The figure compares the poor bond durability of the IBED treated surface with the excellent bond durability of the PAA treated surface. Also, the figure clearly demonstrates that grit blasting and oven drying of the IBED treated surface prior to primer again results in excellent durability. The excellent durability of the bond line with this surface treatment is further illustrated by the photograph in Figure 35, which shows cohesive failure during exposure to the humid air environment.

6.3 Electrochemical Testing

Electrochemical testing was conducted on both PAA and IBED treated surfaces to assess the resistance of these films to deterioration by corrosive environments. The techniques used were cyclic potentiodynamic polarization (CPP), and electrochemical impedance spectroscopy (EIS). The results of these experiments are presented in the following sections.

6.4 Cyclic Potentiodynamic Polarization

Figures 36 to 38 show CPP curves for as-received, PAA treated, and grit blasted + IBED treated aluminum alloy 2024-T3 in a 3% aqueous NaCl solution. Relevant parameters from these diagrams, such as E_{cor} , i_{cor} , E_{pit} , and E_{prot} are presented in Table 4. The CPP diagrams indicate that pitting occurred readily on all three surfaces. The three CPP curves appear to be very similar. Specifically, the curves show pitting potentials in the range of -570 to -610 mV vs. SCE, and considerable hysteresis loops. These loops are indicative of active localized corrosion or pitting, even after the potential drops below the pitting potential. Inspection of the surface, after running the CPP curves, indicated that the localized attack on both the bare and anodized surfaces appeared to be at inclusions, whereas corrosion on the IBED treated surfaces appeared to spread along ridges on the alloy surface.

6.5 Electrochemical Impedance Spectroscopy

Electrochemical impedance spectroscopy (EIS) was conducted on as-received, anodized (PAA), and IBED treated surfaces, exposed to 0.5% and 3% aqueous NaCl solutions. The polarization resistance (R_p) was determined from the log impedance vs. log frequency (Bode) plots, examples of which are given in Figures 39 and 40. The Bode plots of the PAA and IBED treated specimens are similar, with that of the IBED treated specimens indicating a greater impedance at low frequencies. The capacities for the two surfaces are also similar and both surfaces produced a low frequency inductance. This inductance is likely caused by the relatively thick oxide films on the surface.

Figures 41 - 43 show the values of R_p of aluminum alloy 2024-T3 with three different surface oxides as a function of exposure time to aqueous solutions with two different NaCl concentrations. The diagrams indicate that, immediately after exposure, the R_p decreases significantly, and in most cases, continues to decrease during the exposure. A decreasing R_p corresponds to increasing corrosion rates. This decrease in R_p appears to be the

greatest for the as-received aluminum alloy, and the least for the IBED surface treated alloy. The diagrams for both the as-received and anodized material demonstrate expected behavior, where lower R_p values (higher corrosion rates) are observed for the higher chloride concentration solution. Moreover, the R_p values continue to decrease with increased exposure time.

Figure 43 shows a different behavior for the IBED surface treated alloy. Although there is again an initial sharp decrease in R_p , the value remains fairly constant after approximately 8 hours of exposure. Moreover, no significant difference in polarization resistance R_p was found, when the IBED treated aluminum alloy coupons were exposed to either 0.5 or 3 % NaCl solutions.

6.6 Surface Analysis

In this section the results of various different surface analyses are presented. These analyses include scanning electron microscopy (SEM), transmission electron microscopy (TEM), Auger electron spectroscopy (AES), X-ray photoelectron spectroscopy (XPS), Fourier transform infrared (FTIR) spectroscopy, and atomic force microscopy (AFM). The objective of conducting these analyses was to determine the surface morphology, surface oxide structure, and oxide composition at oxidation state.

6.6.1 Scanning Electron Microscopy

Scanning electron microscopy was conducted on IBED treated coupons. Scanning electron micrographs, shown in Figures 44 and 45, demonstrate the smooth nature of the surfaces. Specific features on the surface deserve mentioning. Figure 44 shows the morphology of an aluminum alloy surface, which has been IBED treated only. The photograph shows blister-like features on an otherwise smooth surface. As was demonstrated with the peel experiments, the adhesive properties of this surface were relatively poor. The scanning electron micrographs in Figure 45 shows the surface morphology of an IBED treated surface where the top layer was allowed to grow in the absence of the augmenting Argon beam. The micrographs show that the macroscopically smooth IBED surface exhibited considerable micro-roughness, which could account for the improved mechanical strength of these surfaces.

It was described in previous sections that exposure of the IBED treated alloy to boiling water followed by oven drying at 250°F resulted in excellent durability of the adhesive bond. Scanning electron microscopy was used to characterize the morphology of the

surface resulting from this treatment. Figure 46 shows an IBED Al_2O_3 surface after exposure to boiling water and subsequent oven drying. The micrograph clearly demonstrates microscopic roughening of the surface as a result of this treatment.

Finally, in order to shed some light on the corrosion behavior of the IBED treated aluminum alloy, SEM studies were conducted on the IBED treated aluminum alloy's surface. Figure 47 shows micrographs with characteristic localized attack where mud cracking surrounded pit-like features. From the SEM micrograph, shown in Figure 48, it appears that corrosion does not penetrate into the material, but rather spreads out on the surface. The mud cracking indicates formation of hydrated oxide. It may be speculated that the crystalline top layer hydrates and forms mud cracking, while the barrier α Al_2O_3 remains intact.

6.6.2 Transmission Electron Microscopy

Carbon replicas of different oxide surfaces were examined in the TEM in order to determine the morphology of the surfaces created by pickling, PAA, and IBED. Figures 49 to 51 show TEM micrographs of the surfaces of a detergent cleaned, HNO_3 -HF pickled, an PAA treated surfaces, respectively. The micrographs clearly indicate that the as-received detergent cleaned, as well as the pickled surfaces have a relatively smooth appearance. Also the photomicrographs show extensive residual natural oxide. The pickled surface shows some evidence of microetching. The PAA treated surface, shown in Figure 50, shows the well developed and uniformly microetched surface which can provide an excellent anchor pattern for mechanical adhesive bonding.

Figure 52 shows a TEM photomicrograph of a carbon replica of an ion beam cleaned surface, indicating a very smooth surface with no residual oxides remaining on the surface. Deposition of the α - Al_2O_3 onto the cleaned surface with IBED resulted in a smooth surface. As indicated in the photomicrograph in Figure 53, this smooth surface oxide has some signs of microroughness, although not to the extent of the PAA treated surface. It is suspected that the profile of this surface is too fine to provide an adequate anchoring profile for adhesive bonding.

The structures of the surface oxides were determined with electron diffraction in a TEM. Sections of the surface oxide were removed from the alloy surface by dissolving the alloy substrate, and retaining the oxide for electron diffraction analysis. The electron diffraction patterns, such as shown in Figure 54, show a mixture of micro-crystalline or amorphous and crystalline α - Al_2O_3 , confirming earlier statements that the IBED film consists of a micro-crystalline oxide base layer, while the top layer is a crystalline oxide.

6.6.3 Atomic Force Microscopy

Atomic force microscopy (AFM) was used to further study the morphology of the IBED oxide surfaces. Figures 55 and 58 show AFM profiles of aluminum alloy 2024-T3 with a 2,000 Å α -Al₂O₃ IBED film, and with a 3,000 Å α -Al₂O₃ IBED film (2,000 Å barrier film and 1,000 Å top film), respectively. The AFM diagrams indicate that both films are microscopically smooth, and at the lower magnification, the morphological features appear to be similar. However, when comparing these two surfaces at much higher magnification, differences in surface morphology become more apparent. Figures 56 and 59 show that the surface structure of the IBED surface is much finer than that of surface with the grown oxide in absence of the augmenting argon beam. This difference in surface profile is quantified with a height profile line scan across A-A and B-B, respectively, see Figures 57 and 60.

6.6.4 Auger Electron Spectroscopy

The composition and thickness of the IBED oxide film was determined with AES. Figure 61 shows the AES depth profile of an IBED oxide film on the aluminum-copper alloy 2024-T3, which has a 1,000 Å barrier film and a 3,000 Å top film. The AES depth profile indicates that the oxide film consists of only aluminum and oxygen and that the major alloying element copper is not present in the oxide. The absence of copper is significant, since it is always present in natural and anodized oxide films on 2024-T3. Since copper is known to promote pitting corrosion in these aluminum alloys, its absence of copper in the oxide film may suggest a higher resistance to pitting corrosion.

The AES depth profile further confirms a total aluminum oxide film thickness of approximately 4,000 Å.

6.6.5 X-Ray Photoelectron Spectroscopy

X-ray photoelectron spectroscopy (XPS) was performed to study various aspects of bondability and bond durability. Specifically, XPS analyses were conducted to study the effects of water on the oxide state on the surface of the aluminum alloy. The IBED (1,000 Å + 3,000 Å) treated coupons were exposed to the following conditions:

1. Fifteen minutes in boiling deionized water,
2. fifteen minutes in boiling deionized water, followed by oven heating at 230°F (110°C) for 30 minutes, and
3. oven heating at 230°F (110°C) for 30 minutes.

Typical XPS scans are shown in Figures 62 and 63 for IBED treated surfaces as received and exposed to boiling water and subsequently oven dried.

The XPS results, which are summarized in Table 5, show significant increases in the O/Al ratios for the samples which were exposed to the boiling water (treatment #1) as compared to the as-received samples. Also, the samples which received treatment #2, show a slightly lower O/Al ratio than those which had received treatment #1. Although this difference is slight, it does appear to be significant. The results of these XPS analyses suggest that the $\alpha\text{-Al}_2\text{O}_3$ is hydrated during exposure to boiling water, but that this hydration is partially reversible.

6.6.6 Fourier Transform Infrared Spectroscopy

Fourier Transform Infrared Spectroscopy (FTIR) was conducted to determine whether water adsorbed onto the $\alpha\text{-Al}_2\text{O}_3$ IBED surface could change the oxidation state of the oxide. Figures 64 and 65 show FTIR spectra of an IBED treated aluminum alloy 2024-T3 (1,000 Å barrier film and 3,000 Å top film) after exposure to boiling water for 15 minutes, and subsequent oven drying at 230°F (110°C). These figures show the presence of hydroxyl peaks at wavelengths of 3,300 cm^{-1} and 1,050 cm^{-1} , respectively following exposure to the boiling water. Oven drying at 230°F (110°C) for up to 60 minutes did not appear to reverse this process, see Figure 66. These observations suggest that at least in part, the top part of the deposited oxide film will be irreversibly hydrated, when exposed to a wet environment.

7.0 DISCUSSION AND CONCLUSIONS

The results of this work have clearly demonstrated that a viable alternative to the wet chemical phosphoric acid anodizing (PAA) process can be developed as pretreatment for adhesive bonding of aircraft aluminum alloys. This alternative process is based on an ion beam enhanced deposition (IBED) process, which does not require the use of toxic materials and does not generate waste material. The surface created with this process was designed such that adhesive bonding was achieved by a combination mechanical and physical bonding.

It was first demonstrated that the smooth $\alpha\text{-Al}_2\text{O}_3$, which was obtained with the IBED process on as-received aluminum alloy surfaces, could achieve high initial mechanical strength. A strong oxide film was formed by direct IBED deposition of a dense amorphous or micro-crystalline barrier film (1,000 Ångstrom), followed by growth of a crystalline oxide adding an additional 3,000 Ångstrom. The bond strength of this surface could be primarily

attributed to physical or van der Waals forces. Although the physical bonding is considered to be the weakest type of bonding, compared to chemical and mechanical bonding, it is important in the development of adhesion. The van der Waals forces influence the degree of physical entanglement and surface wetness. As discussed in the *Background* Section, Gledhill and Kinloch (5,6) developed a relationship between the thermodynamic work of adhesion and the surface free energy:

$$W_A = \gamma_a + \gamma_b - \gamma_{ab},$$

where W_A is the thermodynamic work of adhesion required to separate unit areas of two phases forming an interface, γ_a and γ_b are the surface free energies of the two phases, and γ_{ab} is the interfacial free energy. This relationship was used to explain the poor durability characteristics of the van der Waals type bond. In the presence of water, the work of adhesion (W_A) becomes negative, and the bond between the oxide and the primer/adhesion becomes unstable and disintegrates. This mode of failure by spontaneous dissociation between the substrate oxide and the primer or adhesive, would only occur if the bond relied solely on the physical or van der Waals forces, as is the case for microscopically smooth surfaces.

The durability of an adhesive joint can be improved by preventing water from entering the bond line or by making the bond line more resistant to hydration. The first can be accomplished by increasing the barrier to water diffusion into the bond line, by providing an arduous path for water diffusion, which was accomplished by grit blasting the surface prior to oxide implantation.

An obvious approach to increase the barrier to water diffusion is to select an adhesive which has low permeability and diffusivity, or to incorporate inert fillers into the adhesive, which can impede water diffusion. This approach is not often used, since by modifying polymers to decrease permeability and diffusivity, other important properties such as wettability, mechanical strength or toughness may also be decreased. Another means of inhibiting water diffusion into the bond line is to apply a bead of sealant on the outer edge of the bond line.

Often, primers are applied to the adherend surface prior to adhesive bonding to improve the durability of the bond. The most common and most effective primers are chromate containing primers. The chromate in the primer is primarily present as Cr^{6+} (hexavalent chromium), which is initially hydrophilic, but becomes after 24 hours of heating to 120°F (50°C) hydrophobic. It has been a general consensus that Cr^{6+} is the active species in

chromate containing coatings, where corrosion inhibition is accomplished by reduction of Cr^{6+} to Cr^{3+} . It was demonstrated in this work that a corrosion inhibiting primer which keeps water from the bond line, such as the chromate containing primer BR127, is essential for acceptable durability both for PAA and IBED treated surfaces. Also, it was found incorporation of silicon in the IBED oxide film improved the durability of the bond. It may be speculated that, as in the case of silanes, the silicon forms an oxirane bond (metal O-Si) which improves bond strength and durability. However, the bonds may be hydrophylic and attract water to the bond line.

Based on the results of the experimental work, a process based on IBED was developed to prepare aluminum alloy surfaces for structural adhesive bonding. The adhesive bonds based on this surface treatment were shown to have mechanical strength and durability equal to or better than that based on the wet chemical PAA process. The process which resulted in both high mechanical strength and excellent durability, is described as follows:

1. Clean surface with appropriate degreasing medium,
2. Grit blast with 50 μm Al_2O_3 grit at N_2 gas pressure of 50-60 psi,
3. Clean again,
4. Sputter clean the surface at the sputter dose of 1×10^7 Ar atoms per square centimeter for 30 minutes.
5. Apply a 1,000 Å thick $\alpha\text{-Al}_2\text{O}_3$ barrier film by using the IBED process.
6. Allow a 3,000 Å thick top layer of $\alpha\text{-Al}_2\text{O}_3$ to grow by shutting off the Ar augmenting beam,
7. Following oxide growth, backfill the vacuum process chamber with dry N_2 gas,
8. Immediately prime or,
9. If the part is left exposed to the atmosphere for some time, oven dry at 230°F (110°C) for 30 minutes, and then prime.

The results of the experimental work have suggested that, after the oxide application, exposure to hot water followed by oven drying may have a further beneficial effect on the strength and durability of the adhesive bond. This could be attributed to partial hydration of the surface. Upon drying of the hydrated oxide surface, microscopic roughening was observed on the surface, which could provide additional mechanical anchoring for mechanical adhesive bonding.

Finally, it was found with electrochemical and surface analytical experiments, that the IBED process can create a dense $\alpha\text{-Al}_2\text{O}_3$ film which resists corrosion. In fact, it was found that hydration and spalling of the crystalline top film occurred upon exposure to a chloride containing environment and spread over the surface but did not penetrate through the IBED barrier $\alpha\text{-Al}_2\text{O}_3$ film.

8.0 REFERENCES

1. F. Keller, M. S. Hunter, and D. L. Robinson, "Structural Features of Oxide Coatings on Aluminum," *J Of Electrochemical Society*, September, 1953, pp. 411-419.
2. P. F. A. Bijlmer, "Influence of Chemical Pretreatments on Surface Morphology and Bondability of Aluminum," *J. Adhesion*, 1973, Vol/ 5, pp. 391-331.
3. W. J. Russell, "A Chromate-Free Process for Preparing Aluminum Substrates for Adhesive Bonding - A Preliminary Study," Report No. PA-TR-4861, July 1976, p. 57, Picatinny, Arsenal, Dover, NJ.
4. T. P. Remmel, "Characterization of Surfaces Prior to Adhesive Bonding," Report No. NOR-76-58, July 1976, p. 92, Northrop Corporation, Hawthorne, CA.
5. R. E. Herfert, "Fundamental Investigation of Anodic Films as a Surface Preparation for Adhesive Bonding," Report No. NOR-76-101, August 1976, p. 111, Northrop Corporation, Hawthorne, CA.
6. W. L. Russell and C. A. L. Westerdahl, "Characterization of Chromic-Acid Anodized 2024-T3 Aluminum Adherents," Report No. ARLCD-TR-77040, September 1977, p. 35, Army Armament Research and Development Command, Dover, NJ.
7. B. B. Bower, R. E. Herfert, and K. C. Wu, "Development of Corrosion Resistant Surface Treatments for Spot Welding Bonding," Report No. NOR-75-51, March 1975, p. 125, Northrop Corporation, Hawthorne, CA.
8. T. Smith, "Surface Treatment for Aluminum Bonding," Report No. SC 5180.17FTR, October 1979, p. 204, Rockwell International, Thousand Oaks, CA.
9. G. H. Koch and A. Deutchman, "Non-Chemical Surface Treatment for Aluminum, Titanium, Copper, Phase 1: Feasibility Study," Contract No. F33615-93-C-5323, WL/MLSE, September 1994.
10. J. D. Venables, D. K. McNamara, J. M. Chen and T. S. Sun, "Oxide Morphologies on Aluminum Prepared for Adhesive Bonding Applications," *Surface Science*, Vol 3:1, 1979, p. 88.

11. T. S. Sun, G. D. Davis, J. D. Venables, and J. M. Chen, "Effects of Surface Morphology and Chemical Composition on the Durability of Adhesively Bonded Aluminum Structures," Final Report MMLTR81-45C, October 1981, Martin Marietta Corporation, Baltimore, MD, p. 34.
12. R. J. Schliekelman, "Structural Aspects in Applications of Adhesive Bonding," (German) VD1-Berichte, No. 360, 1980, p. 137.
13. H. E. Franz, "Characterization of Aluminum Oxide Layers (Pre-Treatment of Plated Aluminum Sheet Metal for Adhesive Bonding)," (German) Messerschmitt-Boelkow-Blohm G. M. B. H., Ottobrunne (Germany), 1983.
14. J. Odories, "Study of Surface Treatments Before Adhesive Bonding of Light Alloys," (French), 1987, (ETM-88-9243) NTIS.
15. D. B. Arnold and C. S. Carter, "Service History of Phosphoric Acid Anodized Aluminum Structure," 27th National SAMPE Symposium, 1982, Asuza, CA, p. 769.
16. K. Wefers, "The Mechanism of Sealing of Anodic Oxide Coating on Aluminum," *Aluminum*, Vol. 49(8)(9), 1979.
17. W. Brockmann, "Durability of Adhesion Between Metals and Polymers," *Adhesion*, 1989, Vol. 29, p. 53.
18. O. D. Hennemann and W. Brockmann, "Weak Boundary Zones in Metal Bonds," 14th National SAMPE Technical Conference, October 12-14, 1982, p. 302.
19. Radiation Effects on Solid Surfaces, Manfred Kaminsky, Ed., *American Chemical Society* (Advances in Chemistry Series #158), Washington, D.C., 1976, pp. 1-63.
20. O. Auciello, "Ion Interaction with Solids: Surface Texturing, Some Bulk Effects and Their Possible Applications," *J. Vac. Sci. Technol.*, 19(4), 1981, P. 841.
21. P. F. A. Bijlmer, "Surface Potential Difference Measurements on Aluminum Alloys and Their Relationship to Bondability," Chapter 4, Adhesion 2, ed., K. W. Allen, 1978.

22. R. A. Gledhill and A. J. Kinloch, "Environmental Failure of Structural Adhesive Joints, *Adhesion*, 1974, Vol 6, p. 315.
23. A. J. Kinloch, "Interfacial Fracture Mechanical Aspects of Adhesion Bonded Joints - Review," *J. Adhesion*, Vol. 10, 1979, p. 193.
24. E. H. Andrew and N. E. King, "Adhesion of Epoxy Resins to Metals," *J. Of Materials Science* 11, (1976), p. 2004.
25. J. Comyn, "A Review of Certain Recent Work on the Durability of Aluminum Alloy Bonded with Epoxide and Phenolic Adhesives," *J. Adhesion*, 1989, Vol. 29, p. 121.
26. J. D. Venables, "Review - Adhesion and Durability of Metal-Polymer Bonds," *J. Material Science*, Vol. 19, 1984, p. 243.
27. G. D. Davis, T. S. Sun, J. S. Ahearn and J. D. Venables, *J. Material Science*, Vol. 17, 1982, p. 807.
28. N. H. Sung, "Moisture Effects on Adhesive Joints," Adhesives and Sealants, Vol. 3, ASM International, 1990, p. 622.
29. K. A. Korinek, "Chromate Conversion Coatings," *Metals Handbook*, Vol. 13, *Corrosion*, p. 389, ASM International, 1987.
30. A. Kaul, N. H. Sung, I. J. Chin, and C. S. P. Sung, "Effect of Bullic Structure of Amino Silane Primer on the Strength and Durability of Al/Epoxy Joints," *Polym. Eng. Sci.*, Vol. 26, 1986, p. 768.
31. M. Gettings and A. J. Kinloch, *J. Material Science*, Vol. 12, 1977, p. 2511.
32. M. Gettings and A. J. Kinloch, *Surface Interface Anal.*, Vol. 1, 1979, p. 189.
33. J. A. Thornton, "Coating Deposition by Sputtering Deposition Technologies for Films and Coatings," R. F. Bunshah ed., Noyes Publication, NJ, 1988.
34. P. M. Natishan, E. McCafferty and G. K. Huber, "Ion Beam Alloying of Aluminum for Corrosion Resistance," Proceedings of the 1987 Tri-Service Conference on Corrosion, ed., F. H. Meyer, Jr., May 1987, pp. 303-332.

35. "Standard Test Method for Floating Roller Peel Resistance of Adhesives," ASTM D3167-76 (1986), ASTM, Philadelphia, PA.
36. "Standard Test Method for Adhesive Bonded Surface Durability of Aluminum (Wedge Test)," ASTM D3762-79 (1988), ASTM, Philadelphia, PA.
37. G. Binning, C. F. Quate, and Ch. Gerber, *Phys. Rev. Lett.*, Vol. 56, 1986.
38. J. Y. Josefowicz, G. C. Farrington, V. S. Agarwala and J. J. DeLuccia, *Material Characterization*, Vol. 34:2, March, 1995.

Table 1. Work Of Adhesion Values For Various Interfaces.⁽²³⁾

Interface	Work of Adhesion			
	In inert medium		In water	
	mJ/m ²	ft · lbf/in. ² × 10 ⁻⁶	mJ/m ²	ft · lbf/in. ² × 10 ⁻⁶
Epoxy-ferric oxide	291	138	-255	-121
Epoxy-silica	178	85	-57	-27
Epoxy-aluminum oxide	232	110	-137	-65
Epoxy-carbon fiber	88-90	42-43	22-44	10-21

Table 2. Sputter Dose Required For Surface Cleaning (Argon On Al₂O₃).

Oxide Layer (Angstroms)	Argon Sputter Dose (X10 ¹⁵) atoms/cm ²	Sputtering Time Required (minutes)			
		Beam Current (2 mA)	Beam Current (3 mA)	Beam Current (4 mA)	Beam Current (5 mA)
1	1.98	1.1	0.73	0.55	0.44
100	198	110	73	55	44
500	999	550	367	275	220
1000	1980	1,100	733	550	440

**Table 3. Sputter Dose Required For Aluminum Layer Removal
(Argon On Aluminum).**

Oxide Layer (Angstroms)	Argon Sputter Dose (X10 ¹⁴) atoms/cm ²	Sputtering Time Required (minutes)			
		Beam Current (2 mA)	Beam Current (3 mA)	Beam Current (4 mA)	Beam Current (5 mA)
1	1.2	<1	<1	<1	<1
100	120	6.7	4.5	3.3	2.7
500	600	33.3	22.2	16.7	13.3
1000	1,200	66.7	44.5	33.3	26.7

Table 4. Electrochemical Parameters For Anodized, IBED Treated And Bare Aluminum Alloy 2024-T3 In A 3% NaCl Aqueous Solution.

	E_{corr} mV, SCE*	I_{corr} $\mu A/cm^2$	E_{pit} mV, SCE	E_{prot} mV, SCE	Comments
PAA	-767	0.008	-580	<830	Pits
IBED	-833	0.03	-573	<-873	Numerous pit-like feature
Natural Oxide	-920	0.07	-608	-929	Pits

* Standard Calomel Reference Electrode.

Table 5. Atom Percent Surface Composition Of IBED Samples, As Determined By XPS.

SAMPLE	C	O	Al	O/Al
As-Received				
BR-98	20.3	53.6	26.1	2.06
BR-99	20.9	52.7	26.4	2.00
BR-100	15.0	57.1	27.9	2.05
BR-101	19.1	54.5	26.5	2.06
15 min Boiling Water				
BR-99	12.7	60.6	26.7	2.27
BR-100	14.1	59.3	26.6	2.23
15 min Boiling Water, 30 min @ 230°F Air				
BR-98	24.0	52.2	23.8	2.19
BR-101	23.5	52.6	23.9	2.20
BR-98 (#2)	27.0	50.2	22.7	2.21
30 min @ 230°F Air				
BR-101	21.1	52.6	26.4	1.99
Boehmite (AlOOH)	14.4	58.1	27.5	2.11

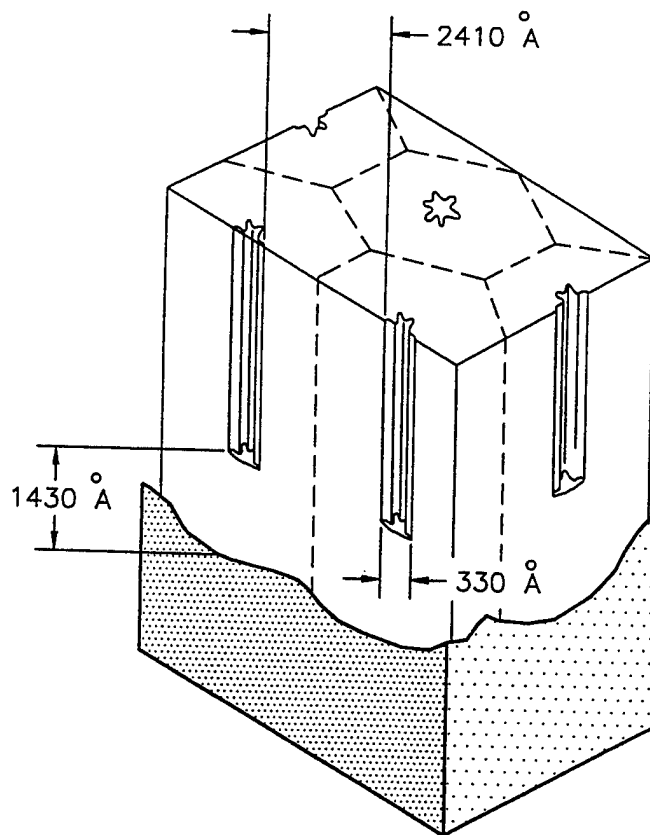


Figure 1. Structure Of 120-Volt Phosphoric Acid Coating Constructed On Cross Section Of Cell Base Pattern. The Dimensions Of Pore, Cell, Cell Wall and Barrier are Shown.¹

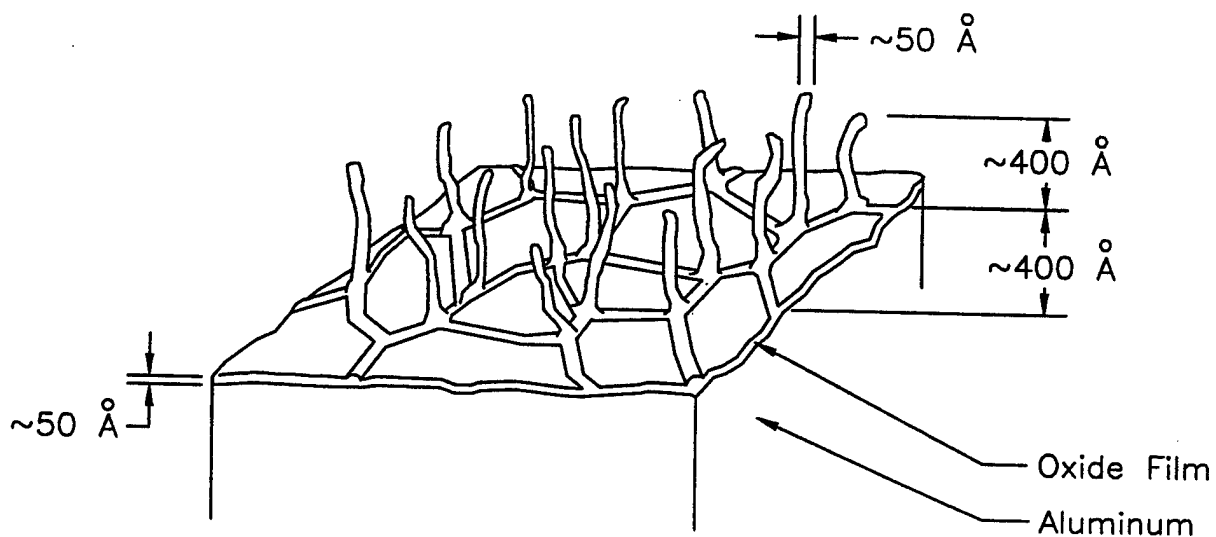


Figure 2. Schematic Representation Of Oxide Morphology Of An Aluminum Surface After Pickling With FPL Process.^{10,11}

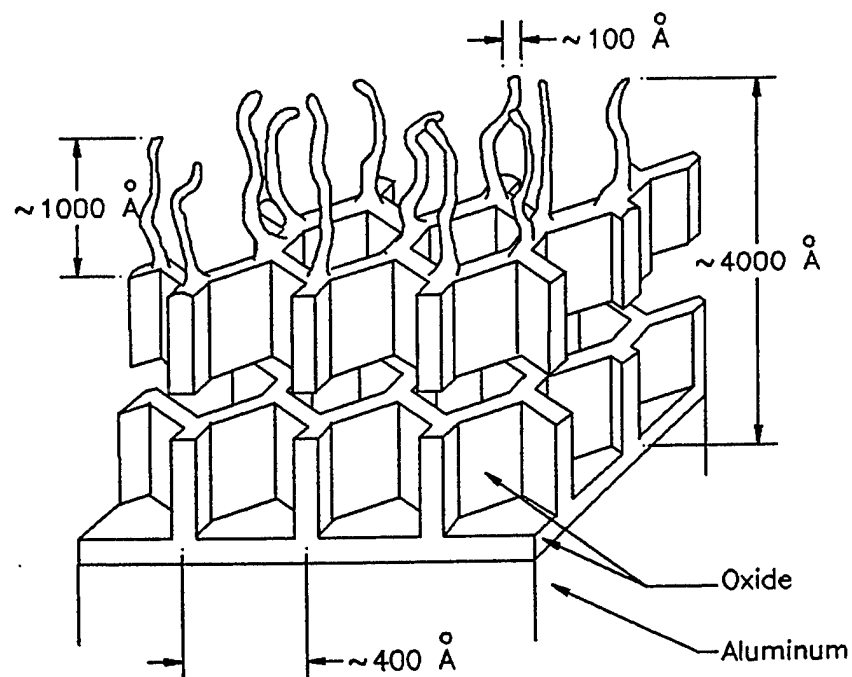


Figure 3. Schematic Representation Of Oxide Morphology On An Aluminum Surface After Phosphoric Acid Anodizing.^{10,11}

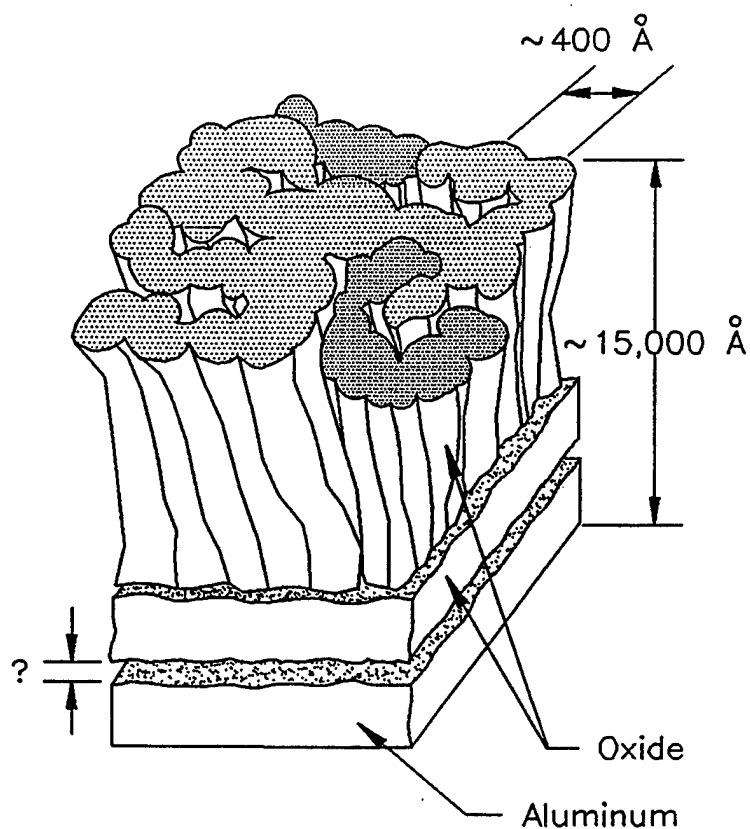


Figure 4. Schematic Representation Of Oxide Morphology On An Aluminum Surface After Chromic Acid Anodizing.^{10,11}

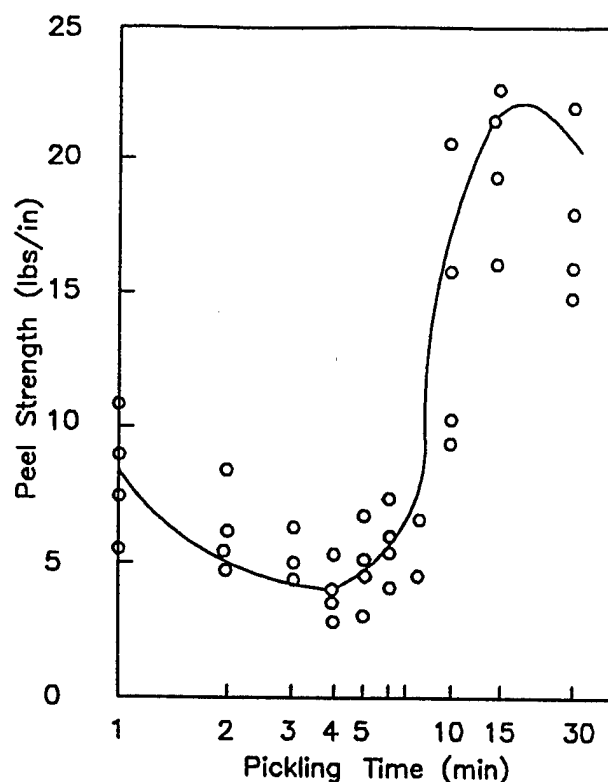


Figure 5. Peel Strength After Pickling Aluminum Alloy 5052 In A Sulfuric Acid-Chromic Acid Solution.²¹

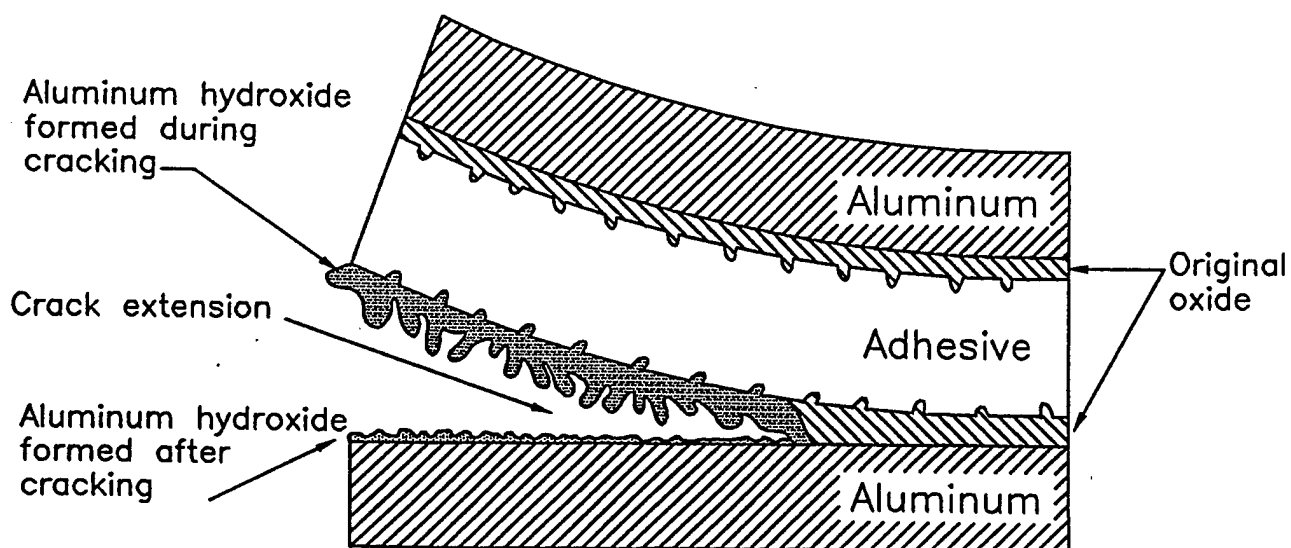


Figure 6. Schematic Drawing Of The Failure Mechanism In An Aluminum/ Polymer Joint System During Wedge Testing In Humid Environment.²⁶ The Original Oxide Is Converted To Hydroxide, Which Adheres Poorly To The Aluminum Substrate.²⁶

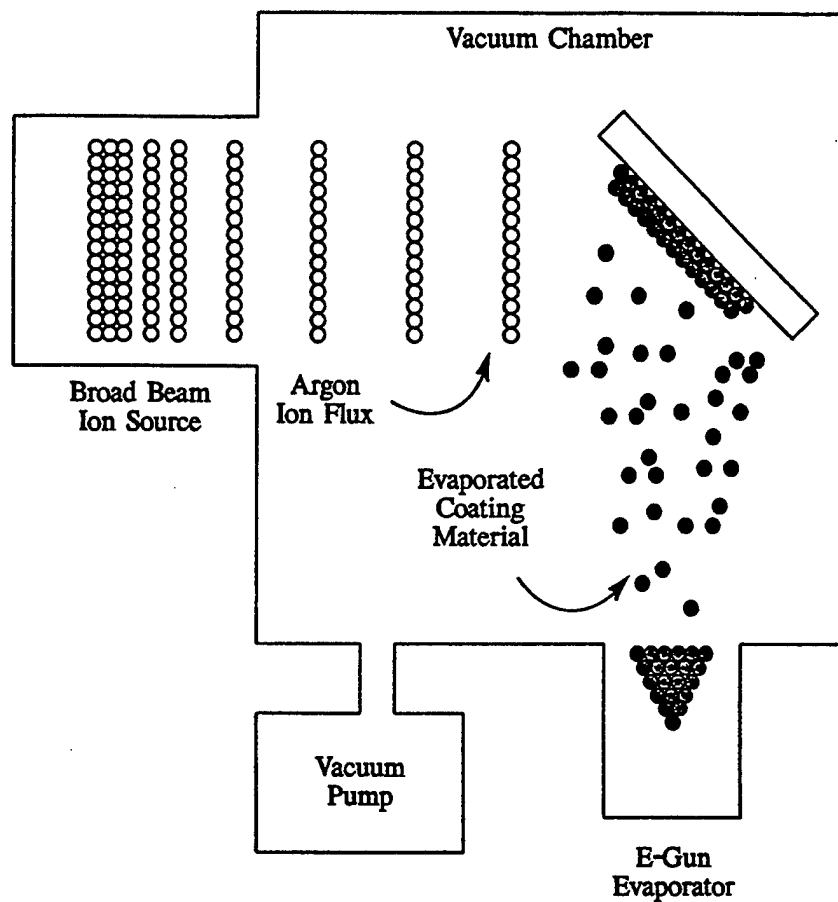


Figure 7. Schematic Drawing Of Ion Beam Enhanced Deposition (IBED) Process.

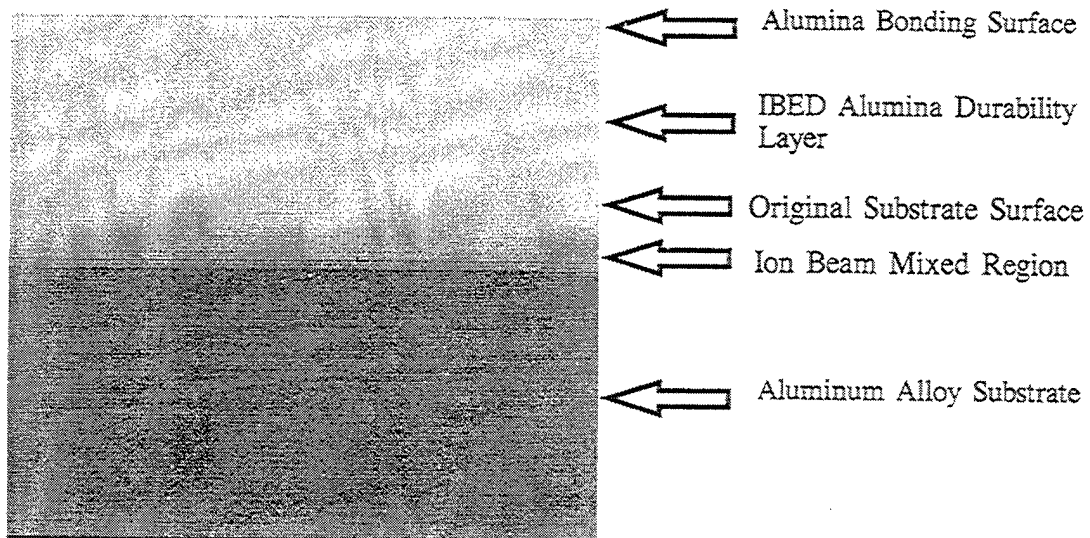


Figure 8. Schematic Diagram Showing Amorphous Bonding Surface, Resulting From Oxide Growth Under Influence Of Augmenting Ion Beam.

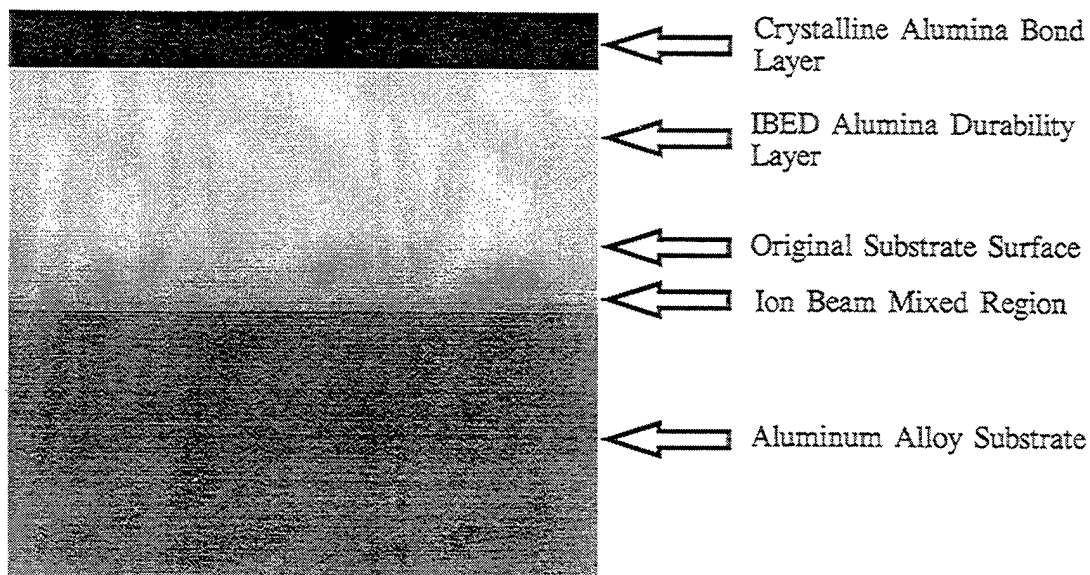


Figure 9. Schematic Diagram Showing Crystalline Bonding Surface, Resulting From Outer Oxide Growth Without The Influence Of The Augmenting Ion Beam.

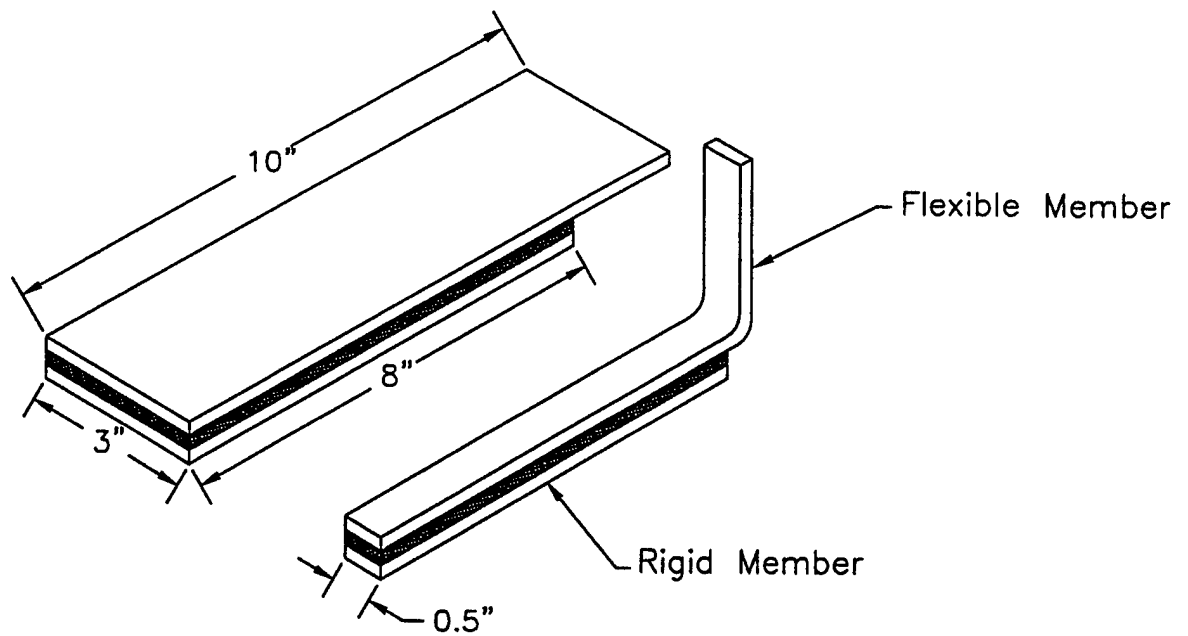


Figure 10. Test Panel And Test Specimen For Peel Testing.³⁵

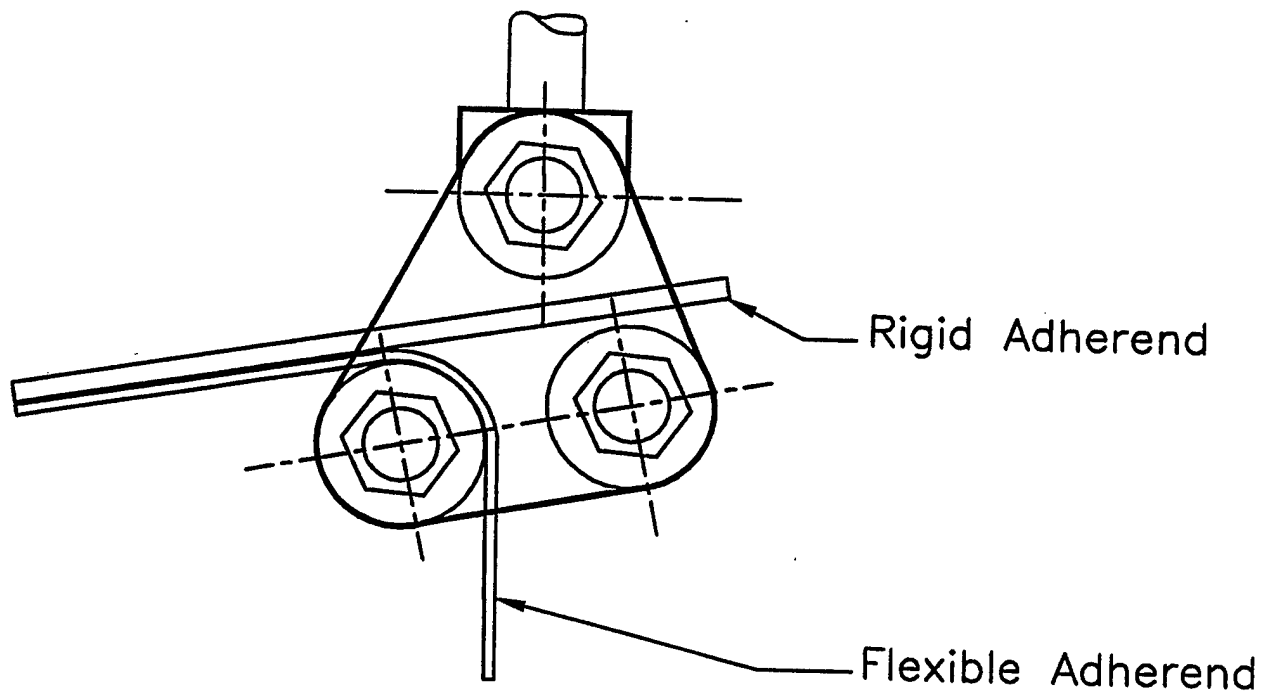


Figure 11. Roller Drum Peel Test Fixture.³⁵

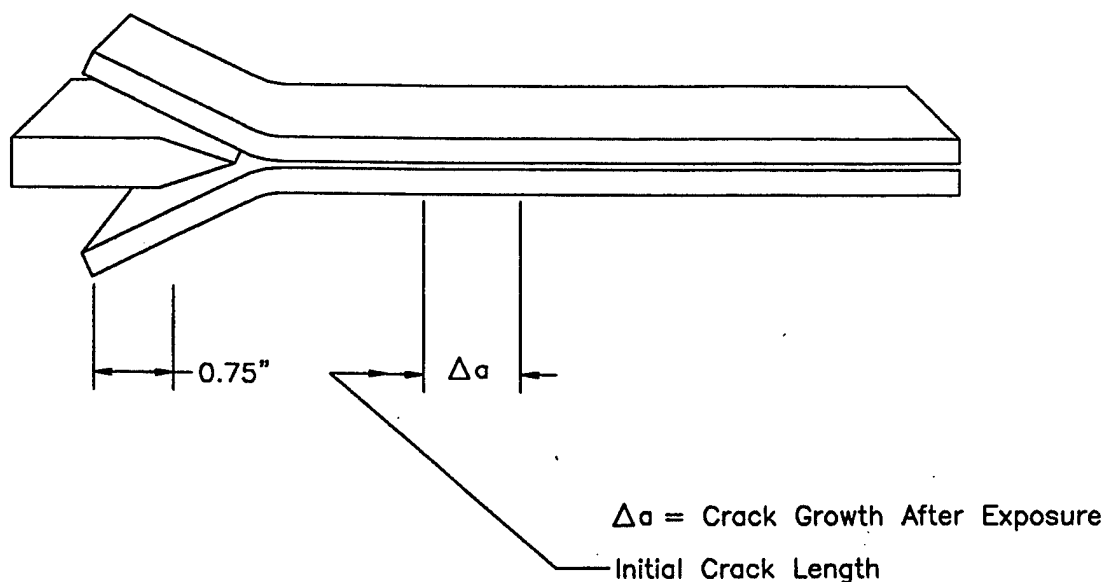


Figure 12. Wedge Test Specimen Configuration.³⁶

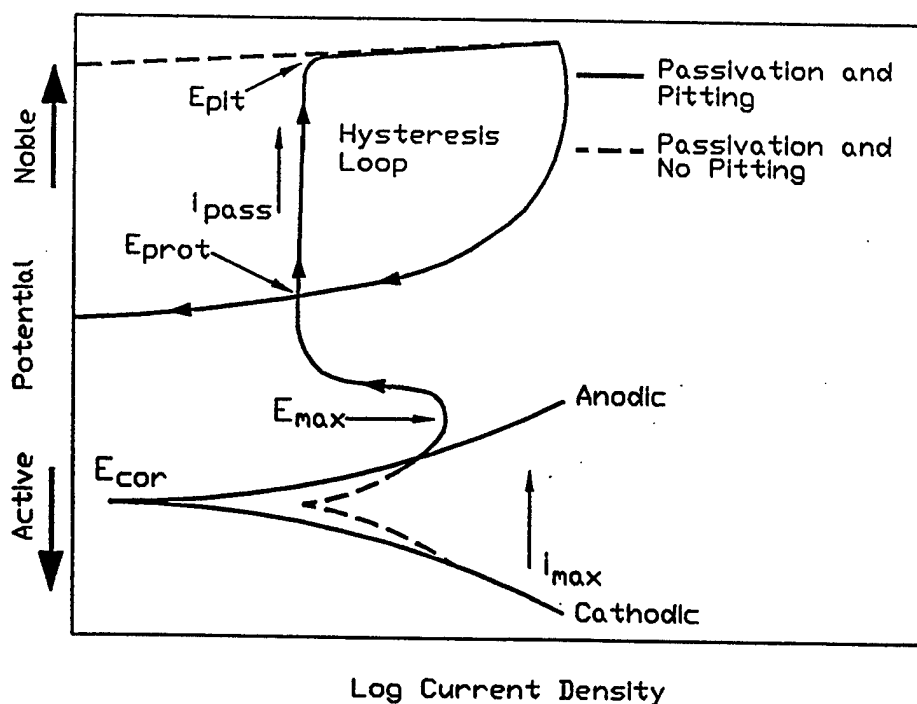
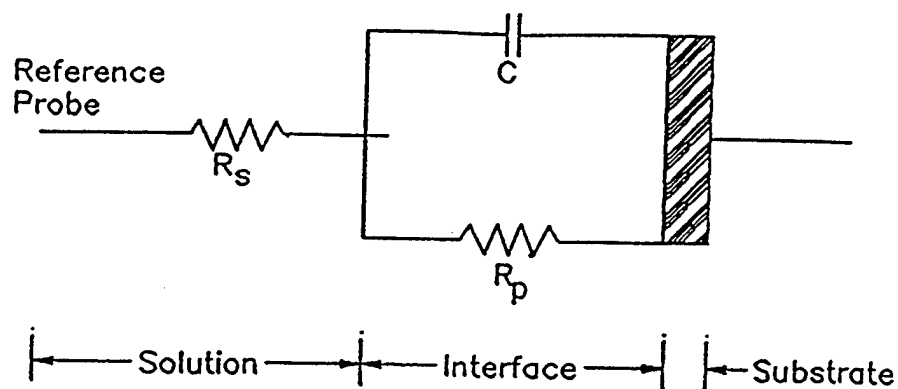


Figure 13. Schematic Diagram Of Typical Potentiodynamic Polarization Curve Showing Important Polarization Parameters.

E_{cor} = corrosion potential; E_{pk} = potential at which pits form on forward scan; E_{prot} = potential at which pits repassivate on scan; i_{cor} = corrosion current density; i_{max} = current density active peaks; i_{pass} = current density in passive range.



R_s = Uncompensated Resistance
 R_p = Polarization Resistance
 C = Capacitance

Figure 14. Analog Circuit For Single Time Constant Corroding Interface.

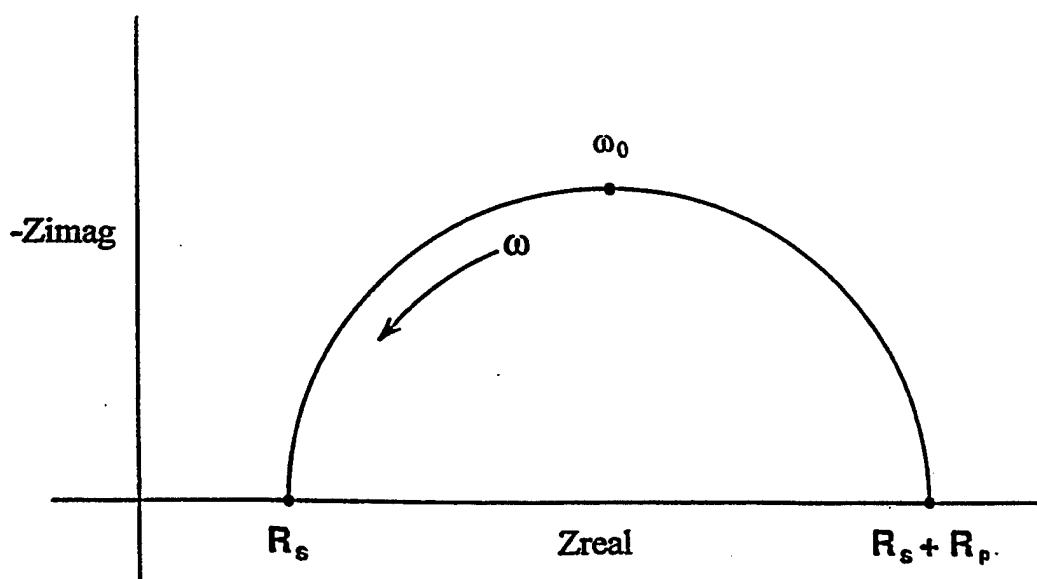


Figure 15. "Nyquist" Plot Corresponding To Simple Circuit Of Figure 14.

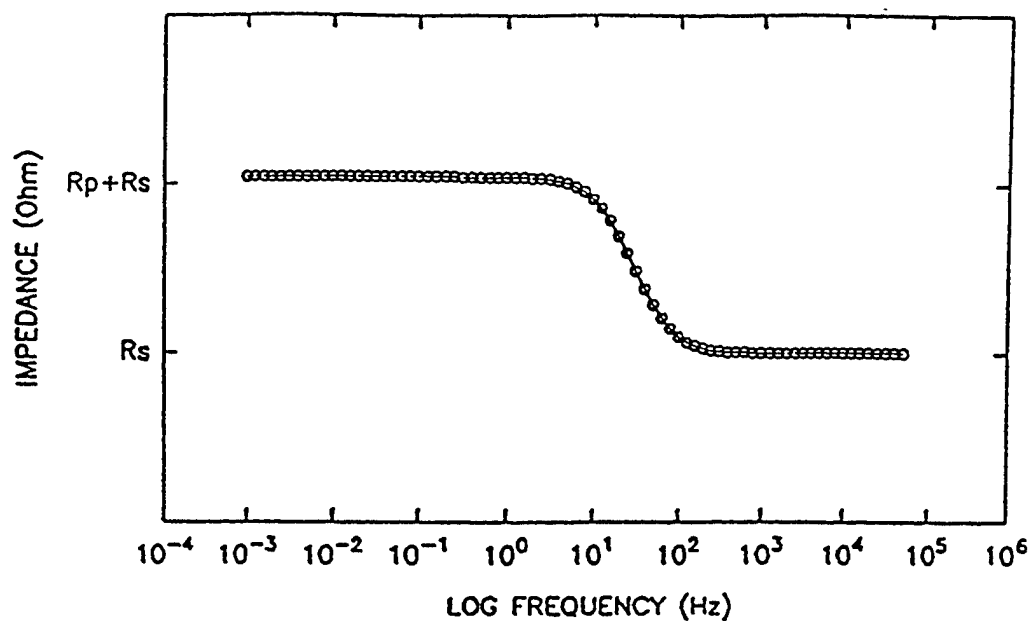


Figure 16. Typical "Bode" Plot Produced By EIS Corresponding To Circuit in Figure 14.

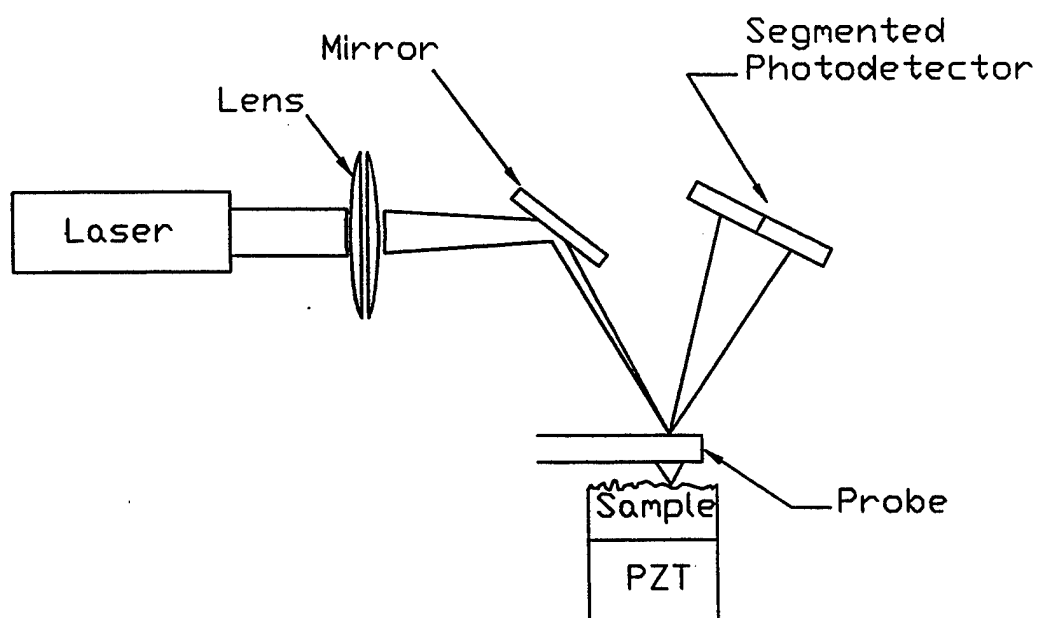


Figure 17. Schematic Drawing Of Atomic Force Microscope.

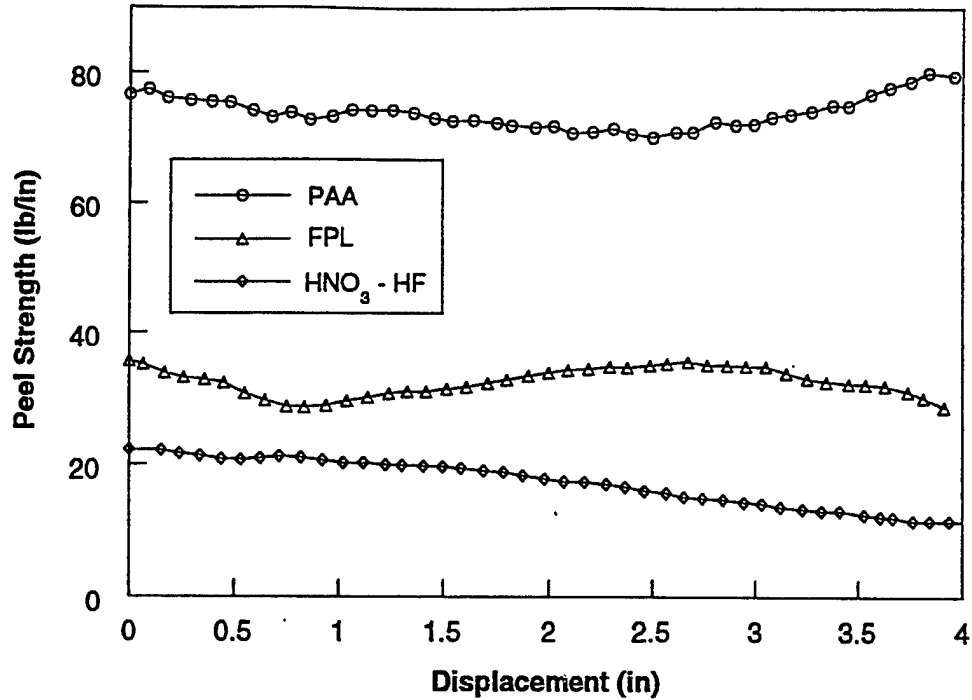


Figure 18. Peel Strength Diagram Of Aluminum Alloy 2024-T3 With FPL Pickled Surface, HNO₃ - HF Pickled Surface And PAA Treated Surface.

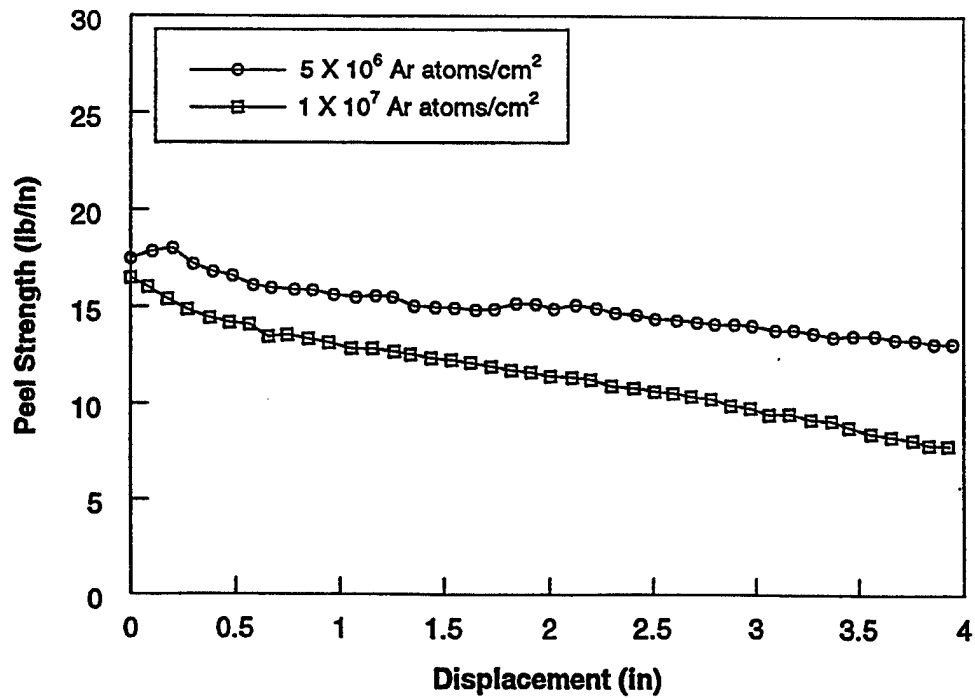


Figure 19. Peel Strength Diagram Of Aluminum Alloy 2024-T3 With Sputter Cleaned Surfaces (5×10^{16} Ar Atoms/cm², 50kev and 1×10^{17} Ar Atoms/cm², 50kev).

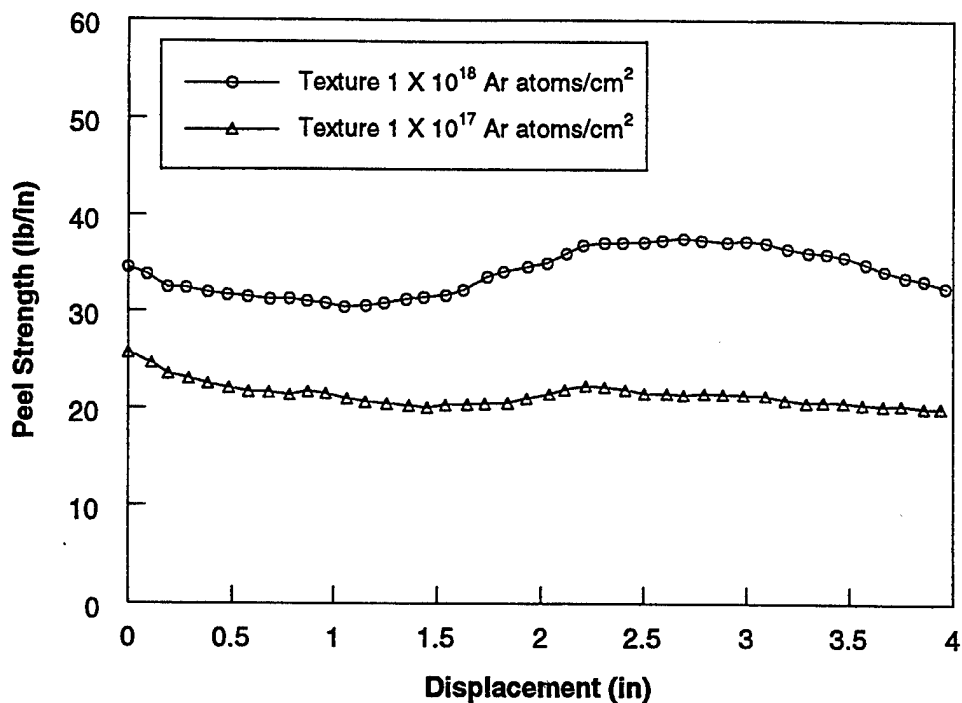


Figure 20. Peel Strength Diagram Of Aluminum Alloy 2024-T3 With Textured Surfaces (Sputter Dose 2×10^{17} Ar Atoms/cm², Texture Dose 1×10^{17} and 1×10^{18} Ar Atoms/cm²).

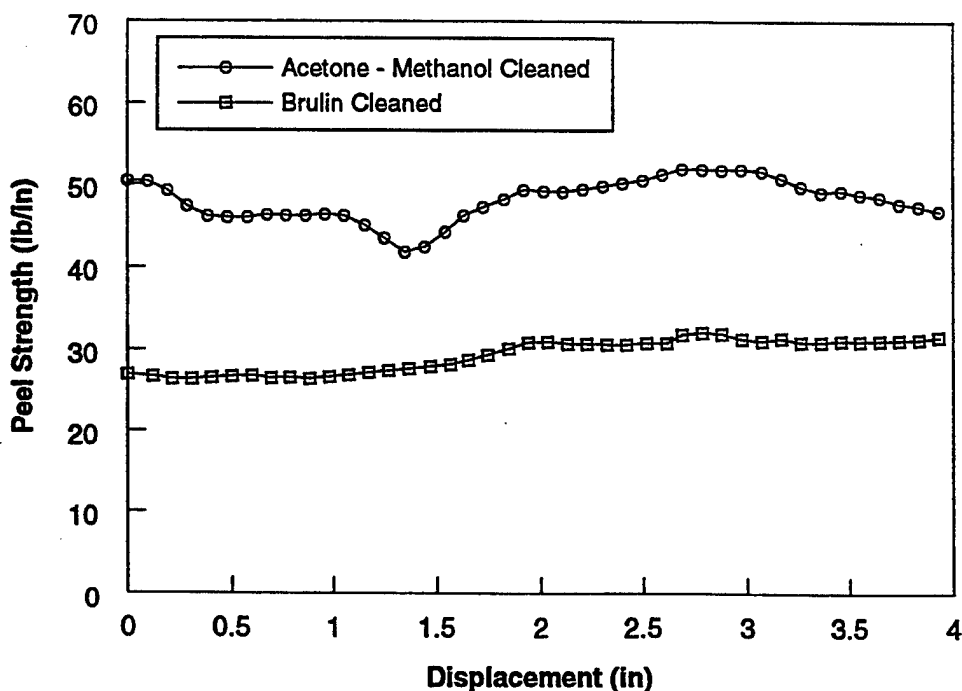


Figure 21. Peel Strength Of Aluminum Alloy 2024-T3 With A 5000 Å IBED Film Directly Deposited On Brulin And Acetone - Methanol Cleaned Surface.

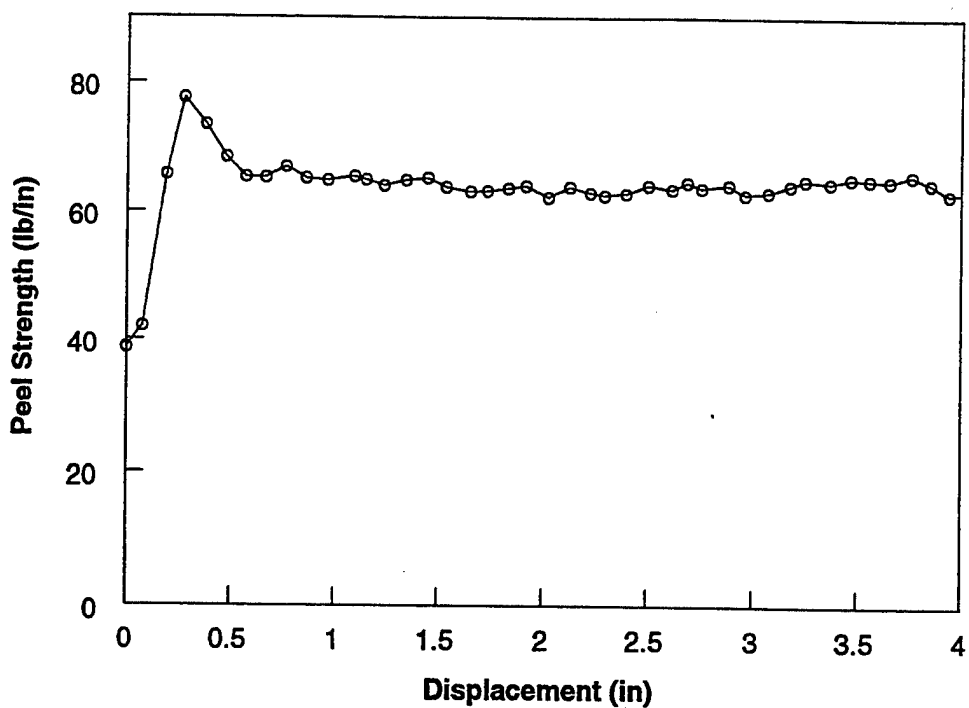


Figure 22 Peel Strength Diagram Of Aluminum Alloy 2024-T3 With A 5000 Å IBED Film Deposited Under Optimal Conditions.

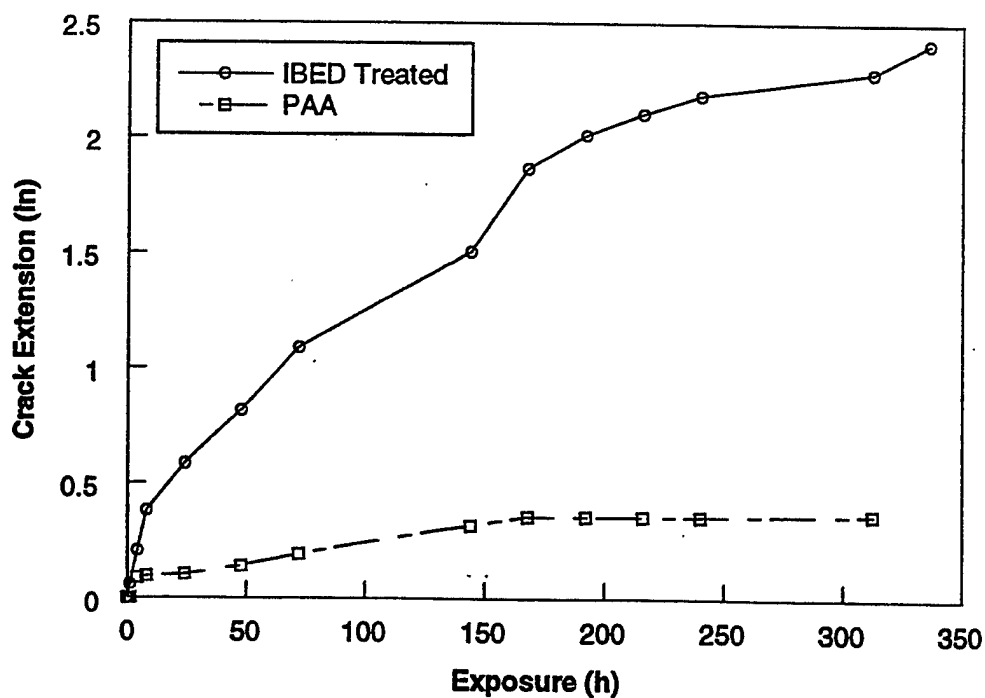


Figure 23. Crack Extension Diagram Of IBED And PAA Treated Aluminum Alloy 2024-T3 Wedge Specimens Exposed To 98% RH, 120°F Air.

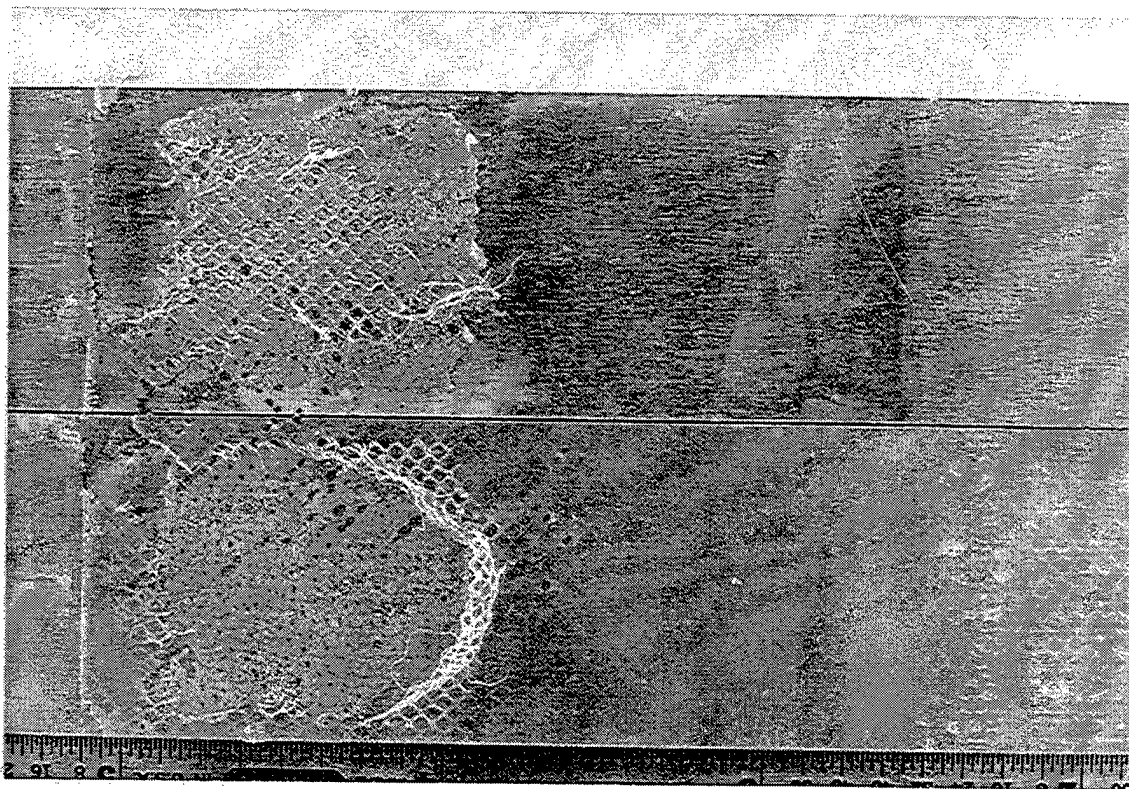


Figure 24. Photograph Of Wedge Specimen Fracture Surface Of IBED Treated Aluminum Alloy 2024-T3.

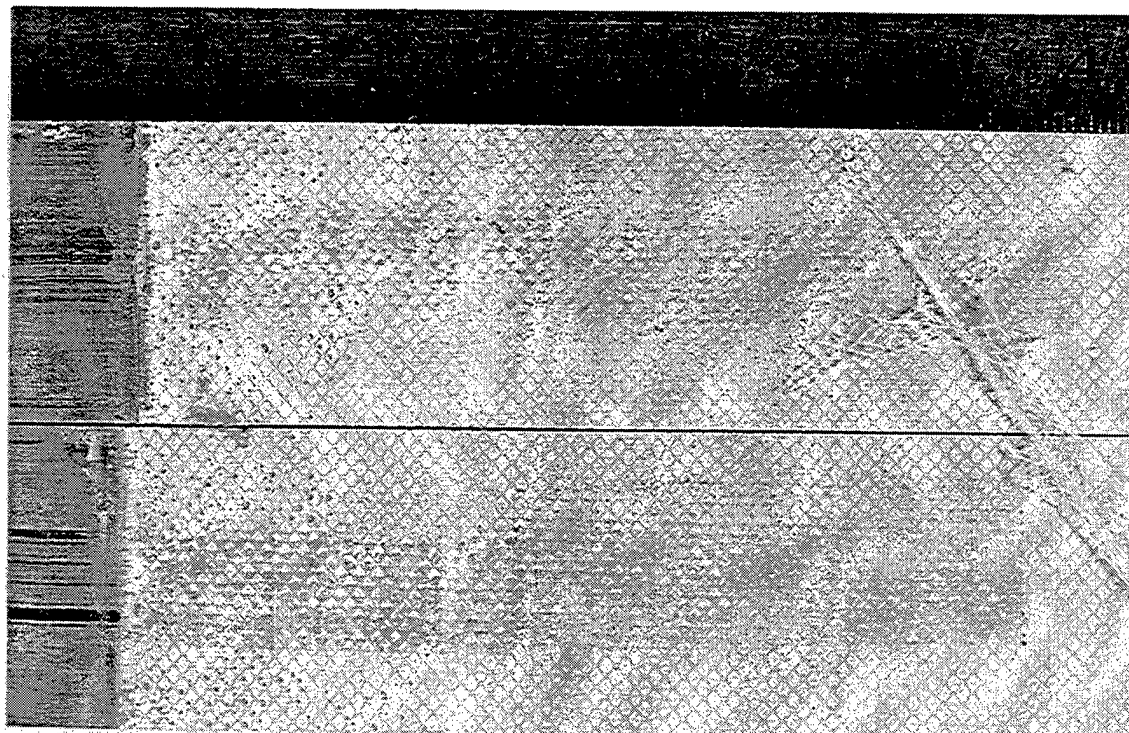


Figure 25. Photograph Of Wedge Specimen Fracture Surface Of PAA And Primed Aluminum Alloy 2024-T3.

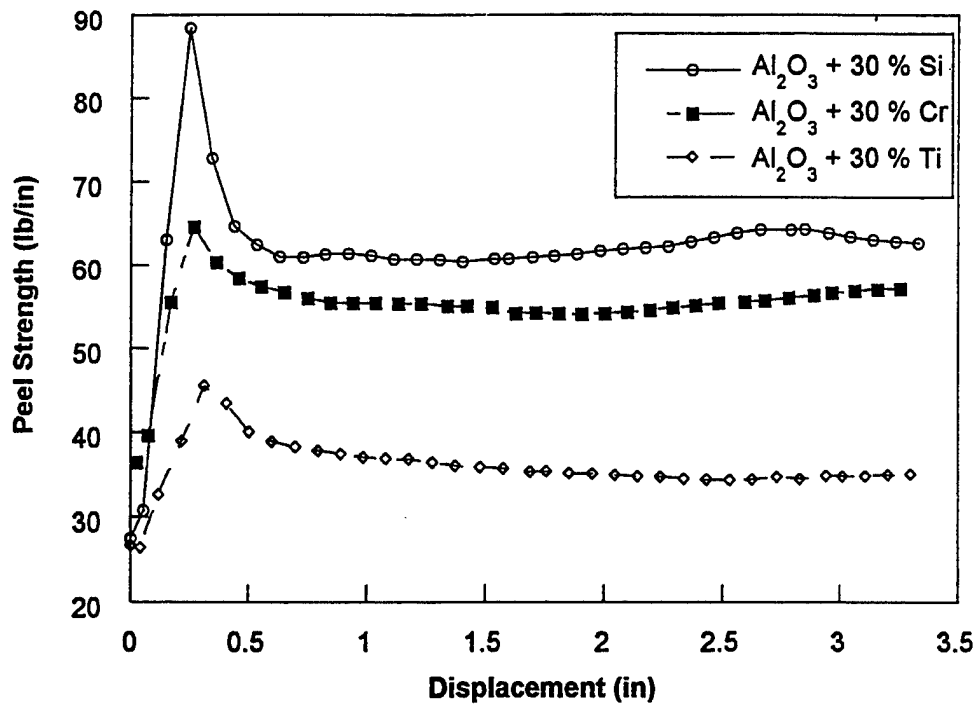


Figure 26. Peel Strength Diagrams After 14 Days Exposure To Humid Air Of IBED Treated Aluminum Alloy 2024-T3 With The Surface Oxides Doped With 30% Silicon, 30% Chromium, And 30% Titanium.

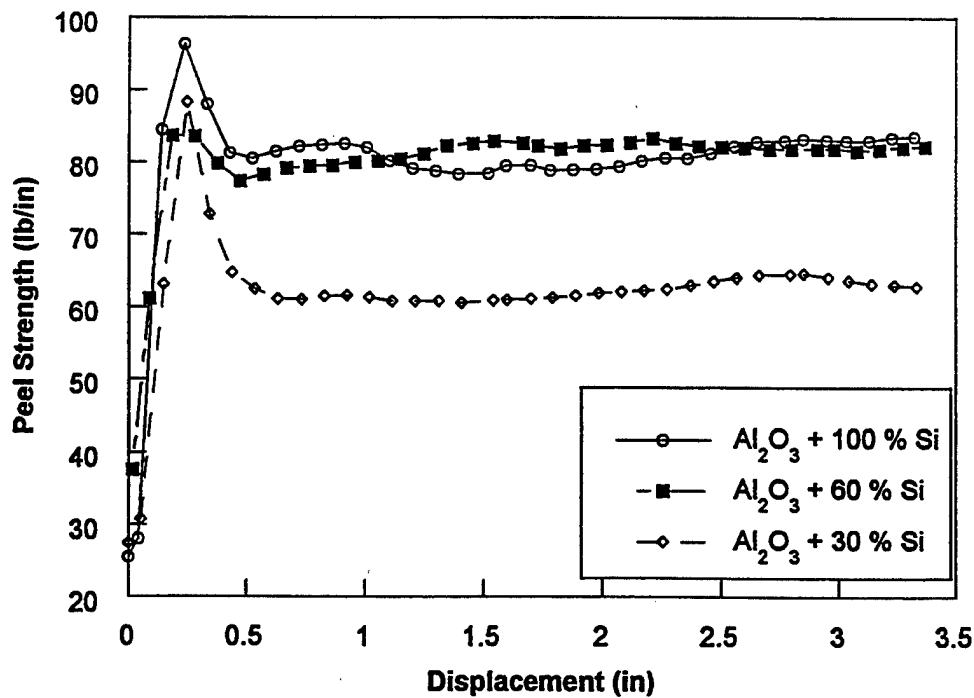


Figure 27. Peel Strength Diagram After 14 Days Exposure To Humid Air Of IBED Treated Aluminum Alloy 2024-T3 Where The Surface Oxides Were Doped With 30%, 60% And 100% Silicon.

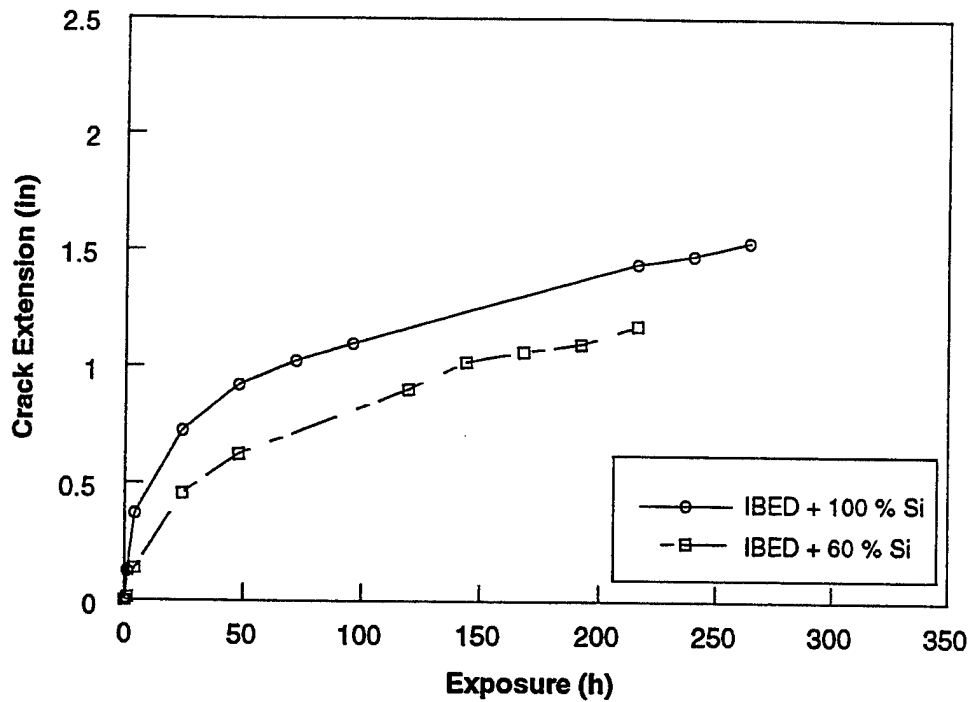


Figure 28. Crack Extension Diagram Of IBED Treated, Silicon Doped Aluminum Alloy 2024-T3 Wedge Specimens, Exposed To 98% RH, 120°F Air.

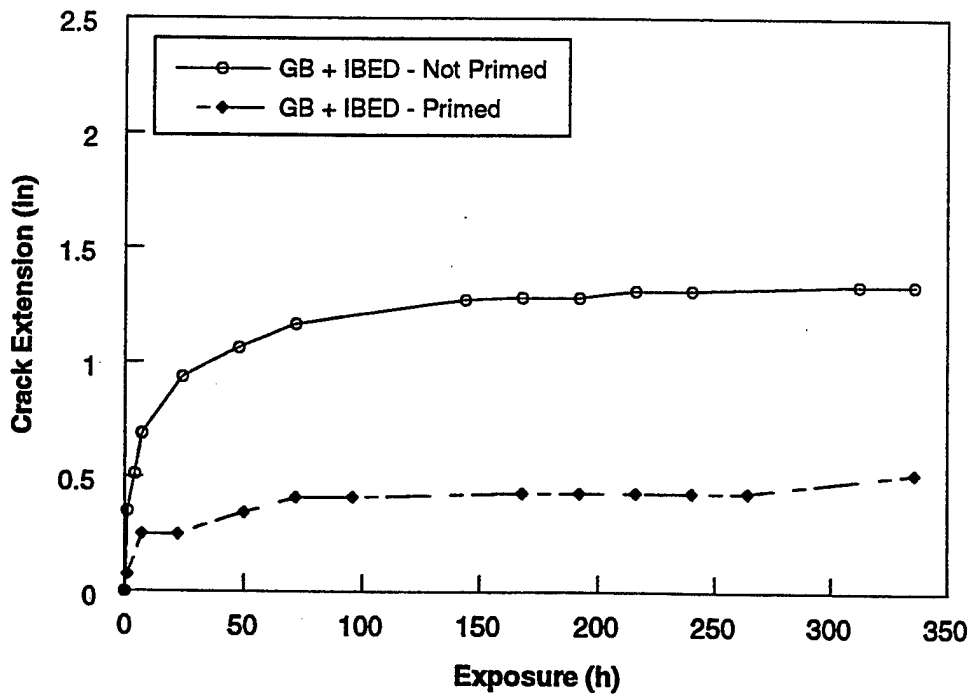


Figure 29. Crack Extension Diagram Of Grit Blasted And IBED Treated Wedge Specimens Exposed To 98% RH, 120°F Air, Comparing Primed And Not-Primed Surfaces.

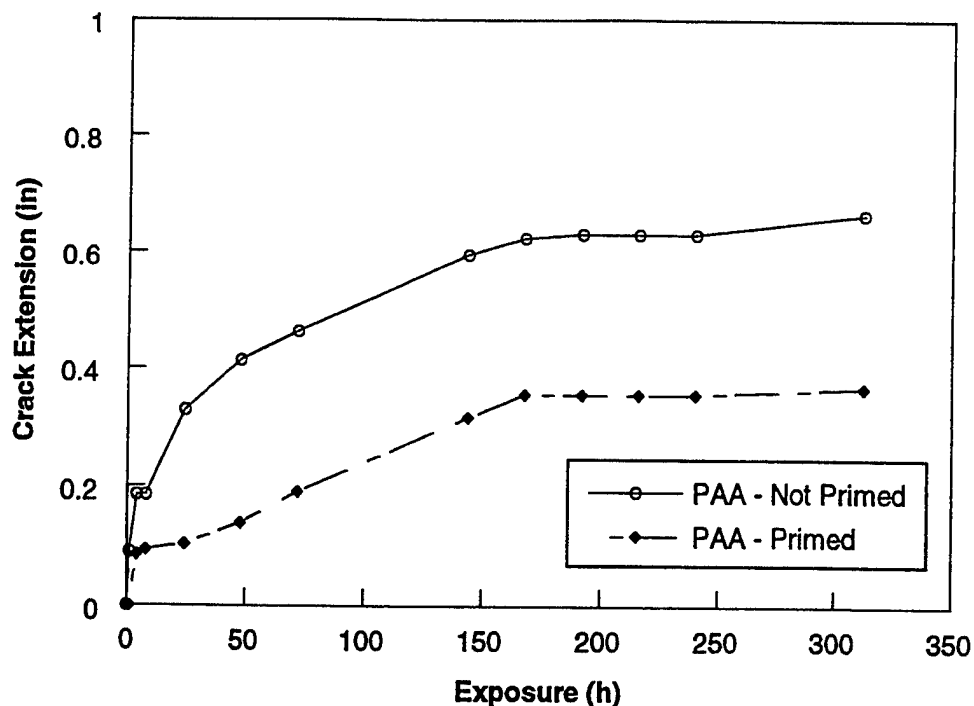


Figure 30. Crack Extension Diagrams Of PAA Treated Wedge Specimens Exposed To 98% RH, 120°F Air, Comparing Primed And Not-Primed Surfaces.

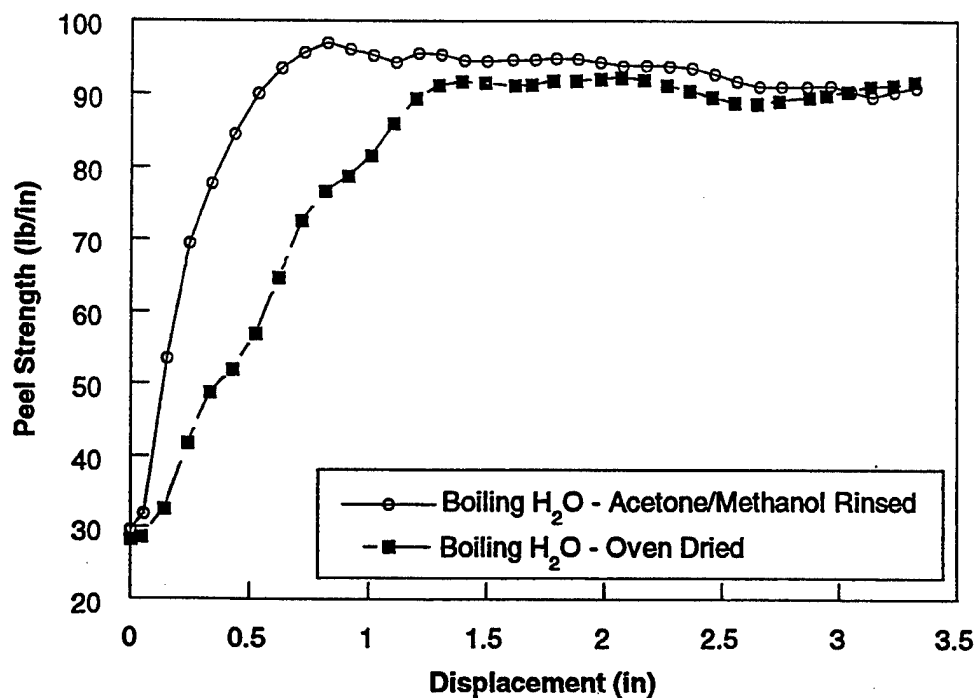


Figure 31. Peel Strength Diagram Of Grit Blasted And IBED Treated Aluminum Alloy 2024-T3 After 14 Days Exposure To 98% RH, 120°F Air. Prior To Bonding, The Surfaces Were Exposed To Boiling Water For 5 Minutes And Dried With Acetone And Methanol Or In A 250°F Oven For 30 Minutes.

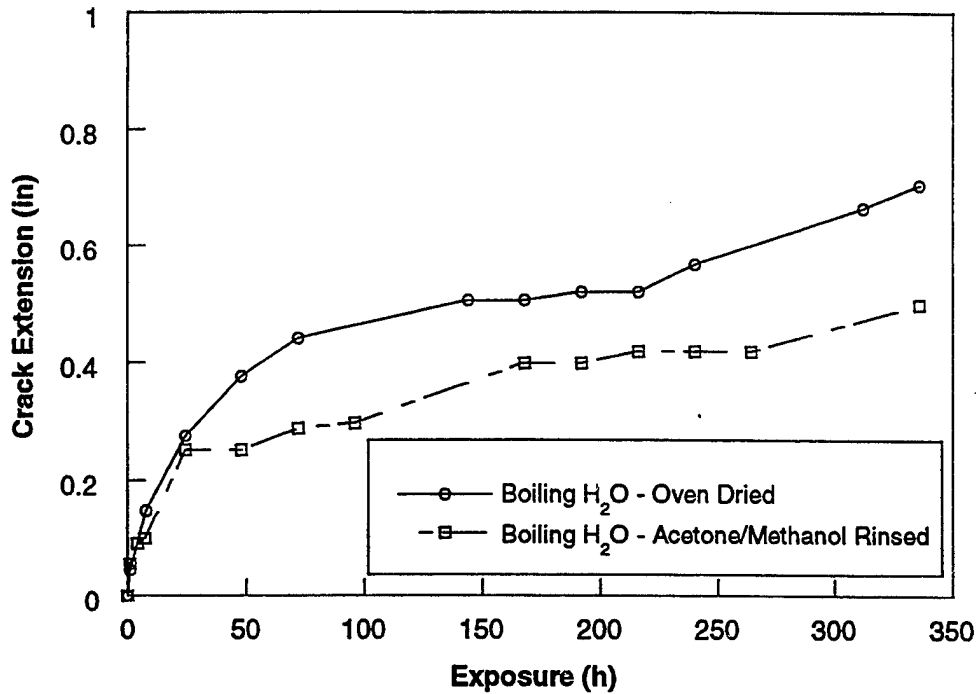


Figure 32. Crack Extension Diagram Of Grit Blasted And IBED Treated Aluminum Alloys Exposed To 98% RH 120°F, Comparing The Effect Of Different Prebond Drying Treatments (see Figure 31).

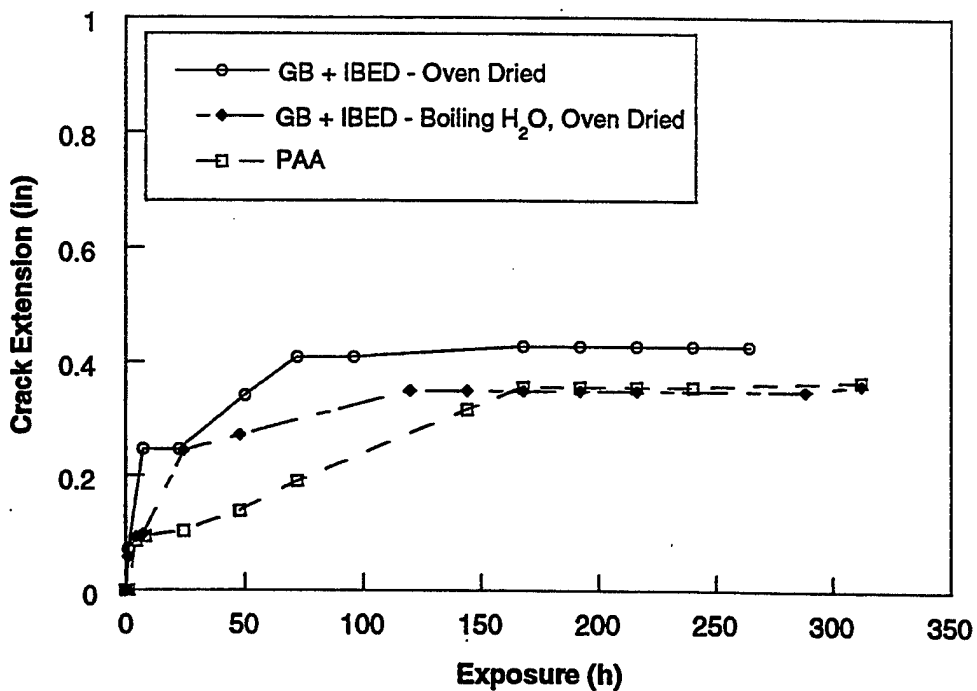


Figure 33. Crack Extension Diagram Comparing The Optimal Non-Chemical Surface Treatments With PAA. Exposure Environment Is 98% RH, 120°F Air.

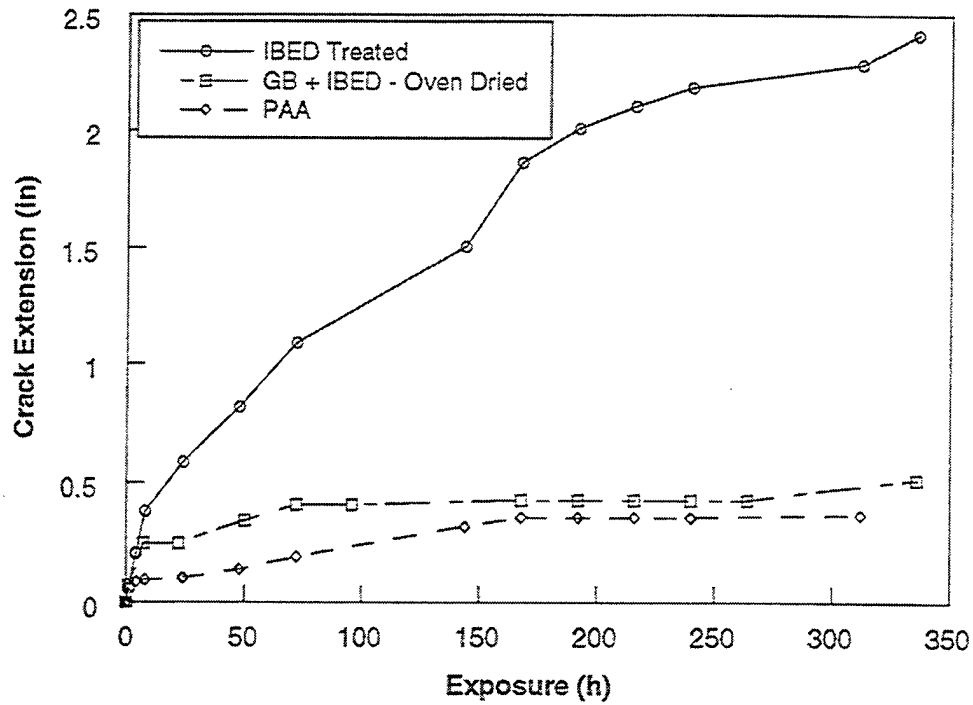


Figure 34. Crack Extension Diagram Demonstrating The Progression Of IBED Treatment To The Optimal Combination Of Grit Blasting And IBED Treatment Compared With PAA. Exposure Environment Is 98% RH, 120°F Air.

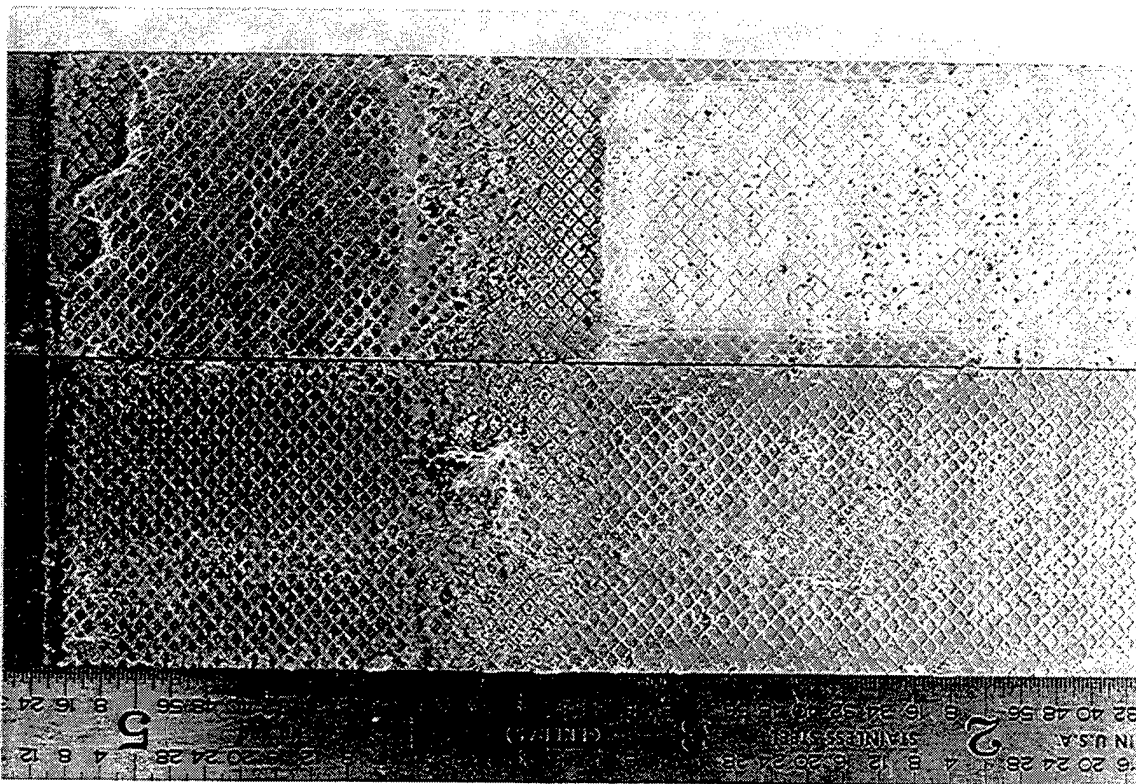


Figure 35. Photograph Of Wedge Specimen Fracture Surface Of Grit Blasted IBED Treated, Oven Dried And Primed Aluminum Alloy 2024-T3.

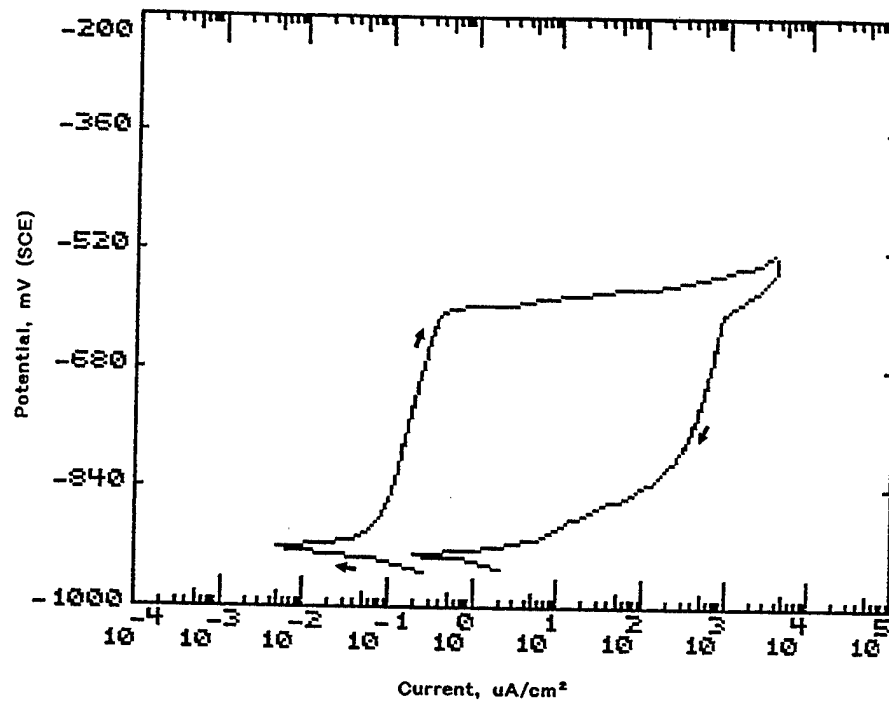


Figure 36. Cyclic Potentiodynamic Polarization Curve Of Aluminum Alloy 2024-T3 With Natural Oxide Film. The CPP Test Is Conducted In A Deaerated 3% NaCl Aqueous Solution.

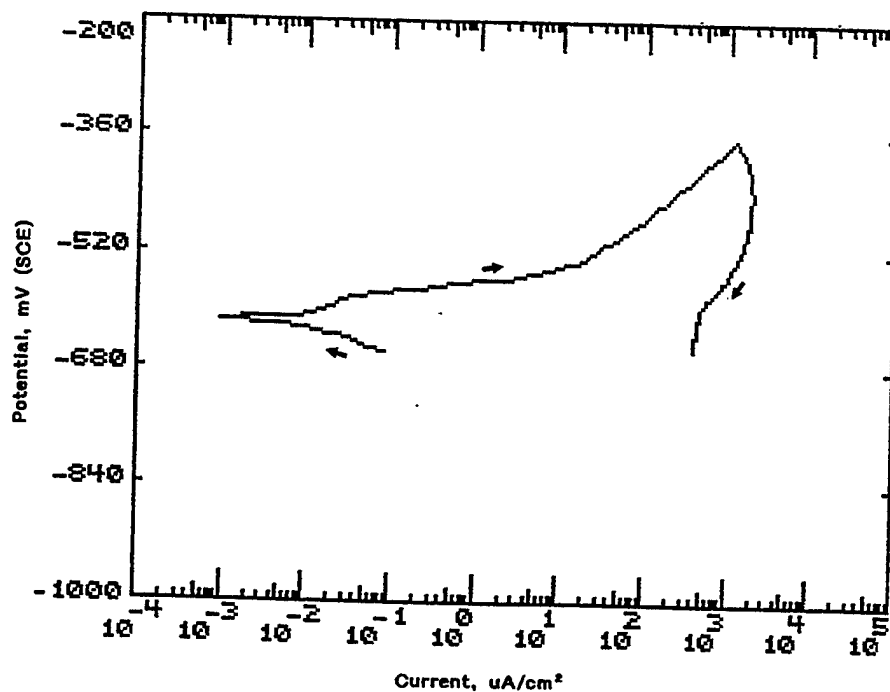


Figure 37. Cyclic Potentiodynamic Polarization Curve Of Aluminum Alloy 2024-T3 With PAA Surface. The CPP Test Is Conducted In A Deaerated 3% NaCl Aqueous Solution.

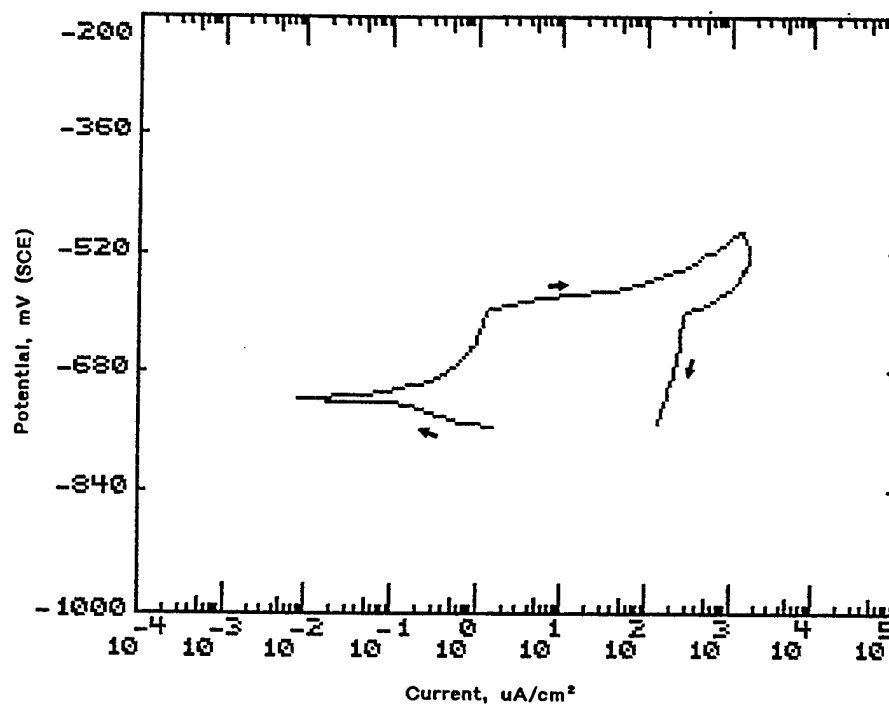


Figure 38. Cyclic Potentiodynamic Polarization Curve Of Aluminum Alloy 2024-T3 With IBED Oxide Surface. The CPP Test Is Conducted In A Deaerated 3% NaCl Aqueous Solution.

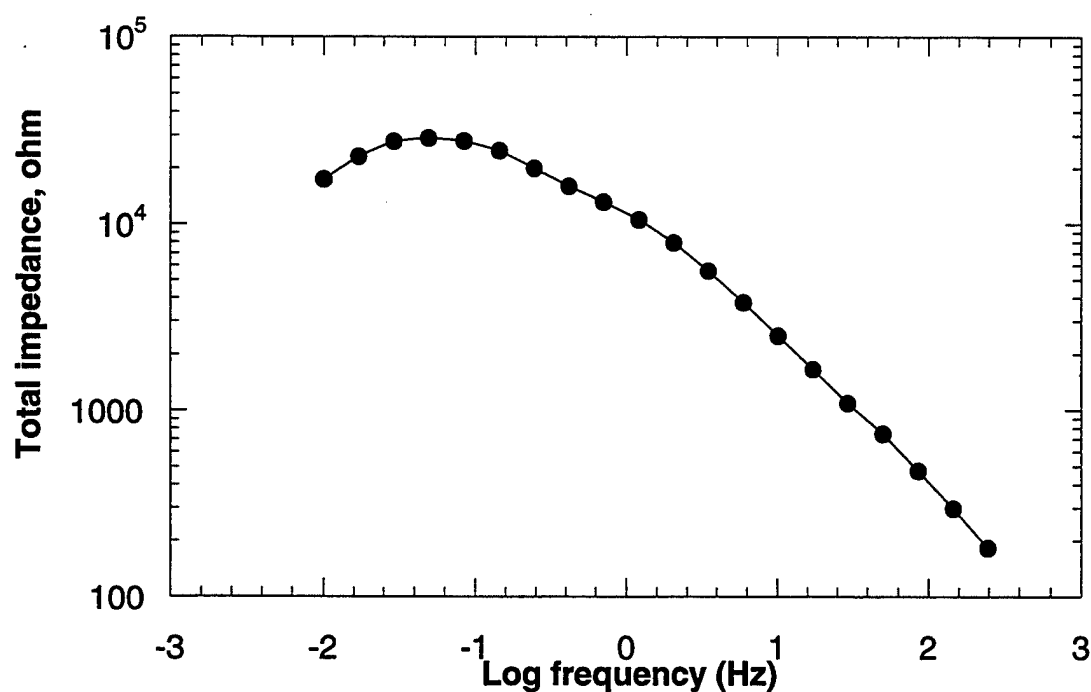


Figure 39. Impedance (Bode) Diagram Of IBED Treated Surface After Exposure To A 3% NaCl Aqueous Solution For 1 Hour.

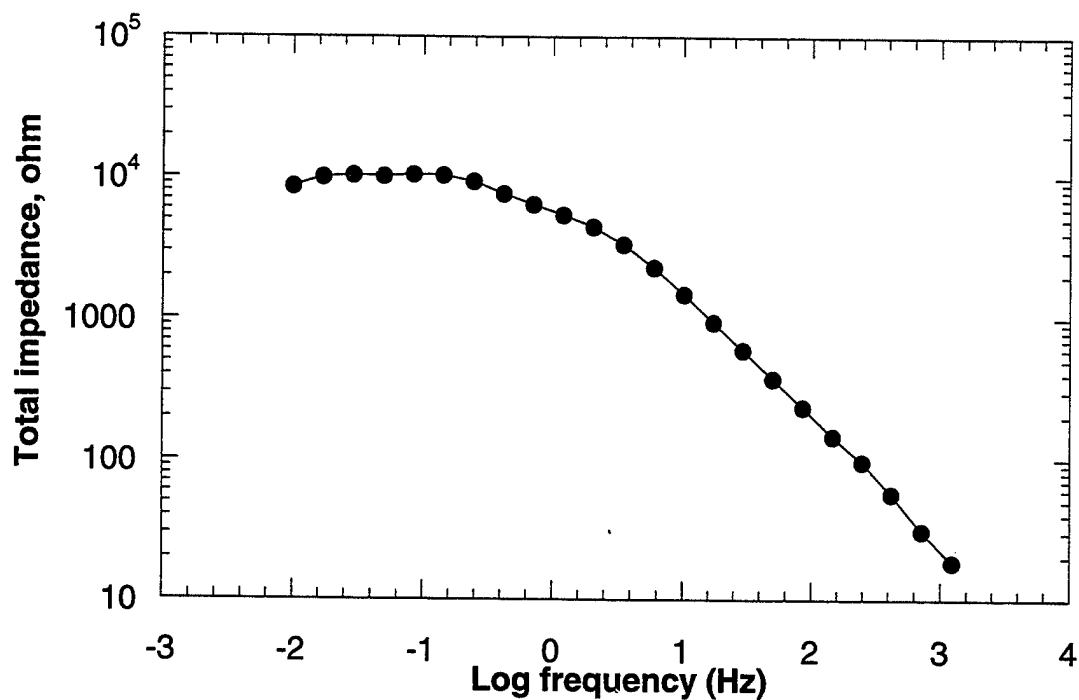


Figure 40. Impedance (Bode) Diagram Of PAA Treated Surface After Exposure To A 3% NaCl Aqueous Solution For 1 Hour.

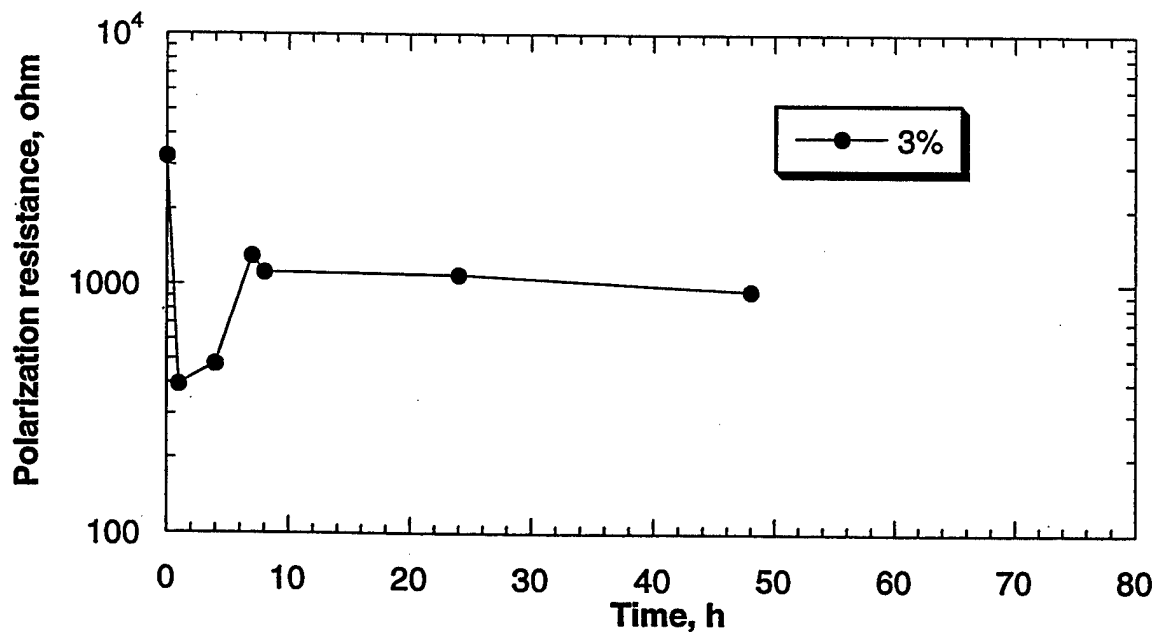


Figure 41. Polarization Resistance (R_p) Of Naturally Oxidized Aluminum Alloy 2024-T3 As A Function Of Exposure Time To A 3% NaCl Aqueous Solution.

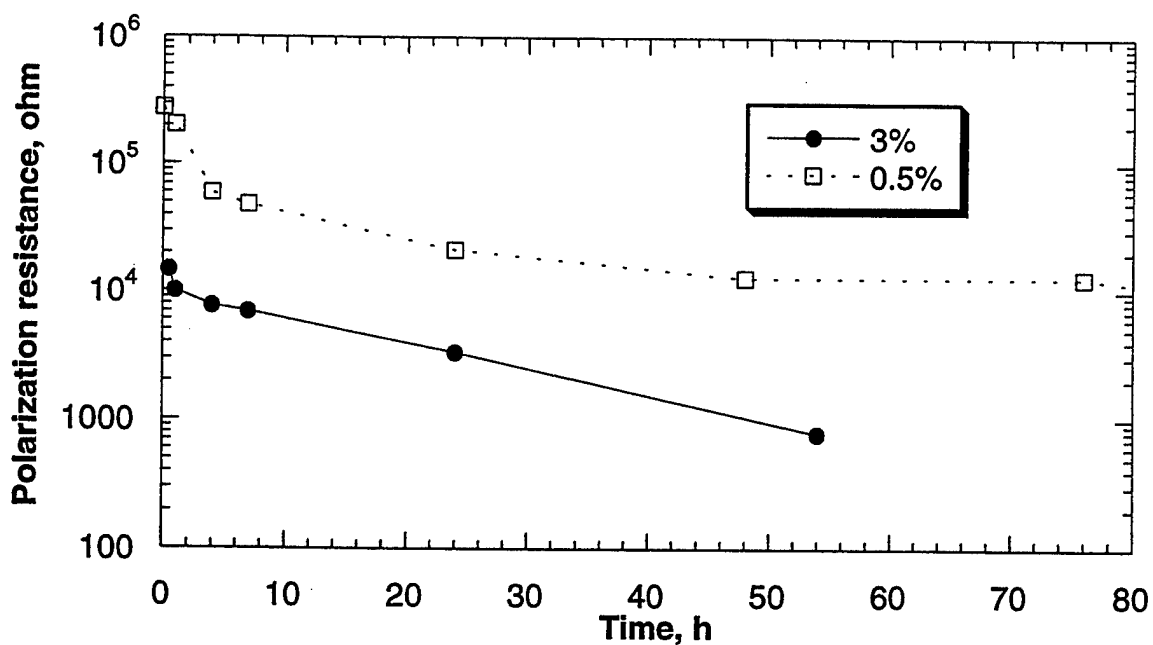


Figure 42. Polarization Resistance (R_p) Of PAA Treated Aluminum Alloy 2024-T3 As A Function Of Exposure Time To A 0.5% and 3% NaCl Aqueous Solution.

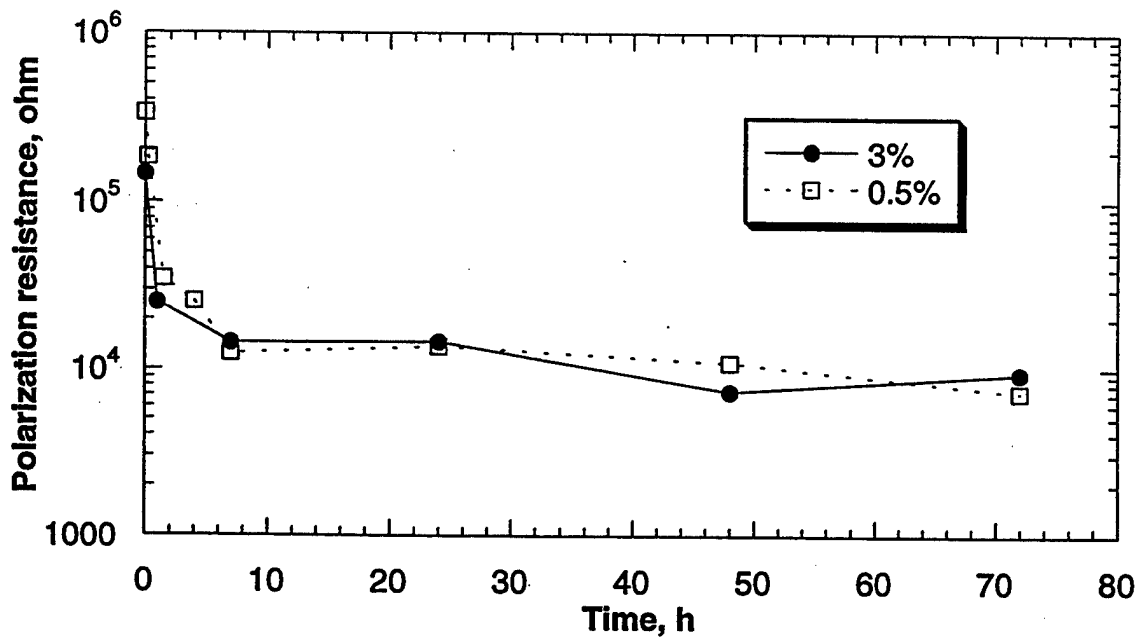


Figure 43. Polarization Resistance (R_p) Of IBED Treated Aluminum Alloys 2024-T3 As A Function Of Exposure Time To A 0.5% and 3% NaCl Aqueous Solution.

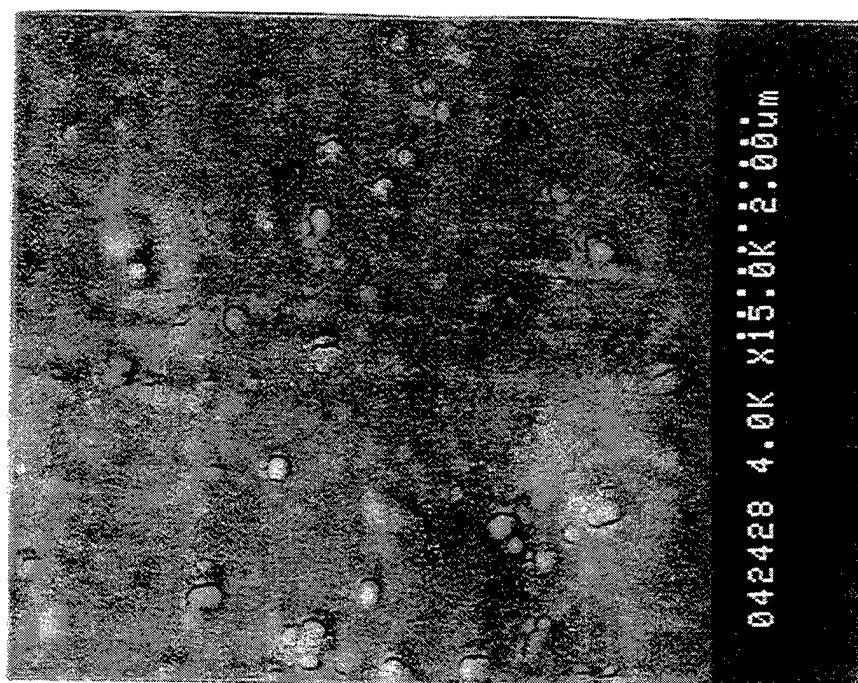
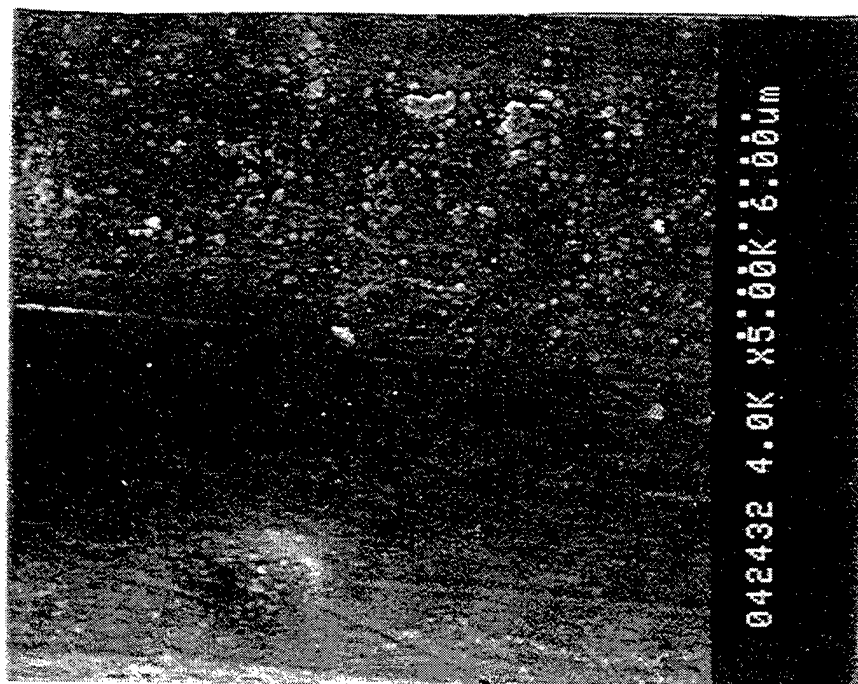


Figure 44. Scanning Electron Micrographs Of IBED Treated Surface.

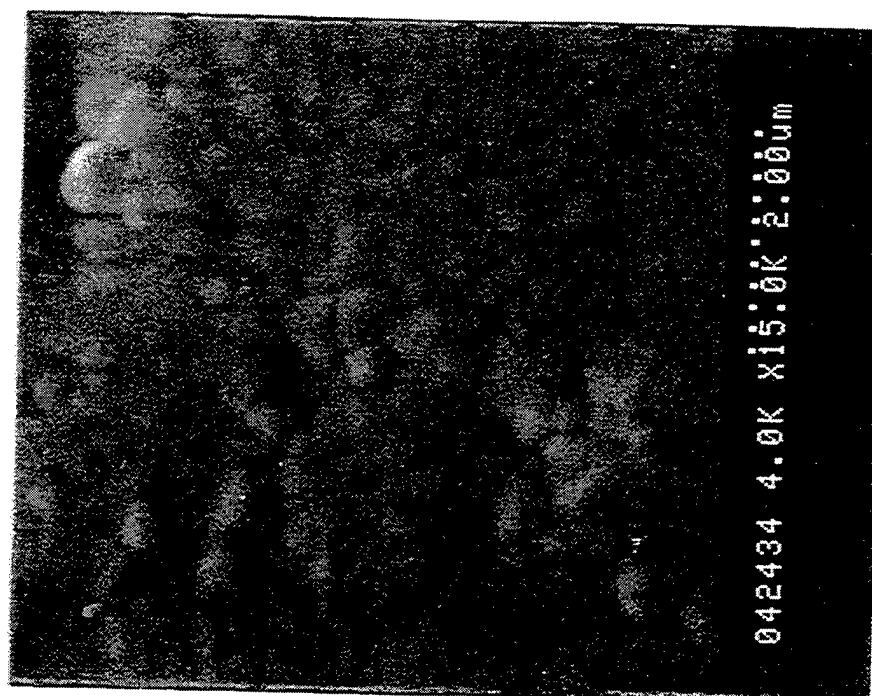
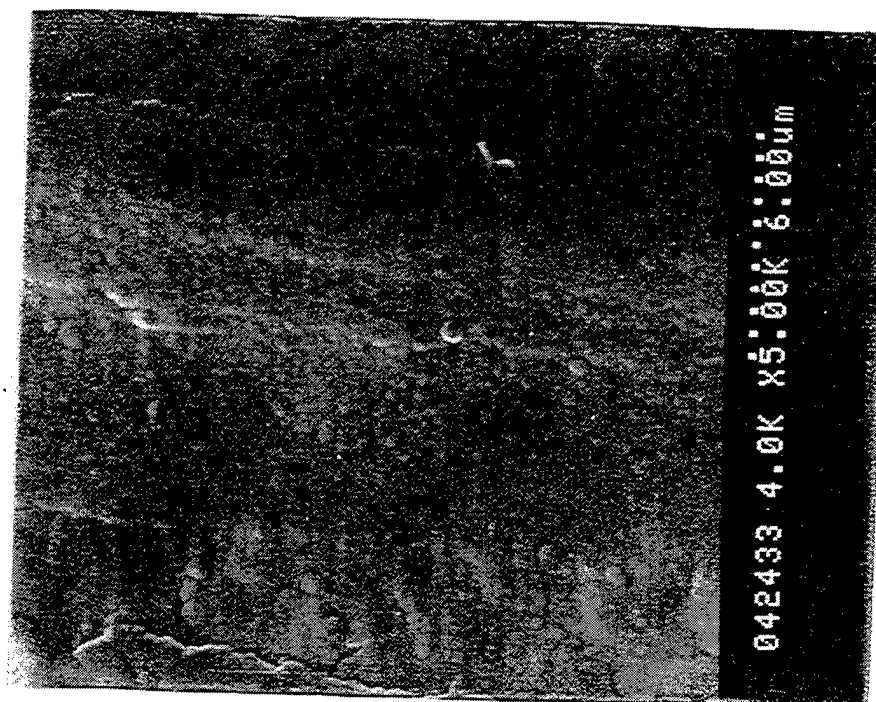


Figure 45. Scanning Electron Micrographs Of IBED Treated Surface Where The Top Layer Was Allowed To Grow Without Argon Beam Augmentation.

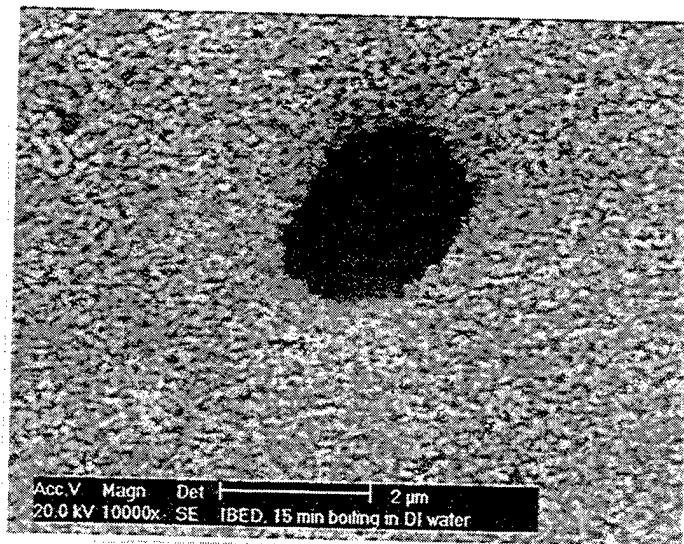


Figure 46. Scanning Electron Micrograph Of IBED Treated Aluminum Alloy 2024-T3 Exposed To Boiling Water For 15 Minutes.



Figure 47. Scanning Electron Micrographs Of IBED Treated Aluminum Alloy 2024-T3 Exposed To A 3% NaCl Aqueous Solution For 24 Hours.

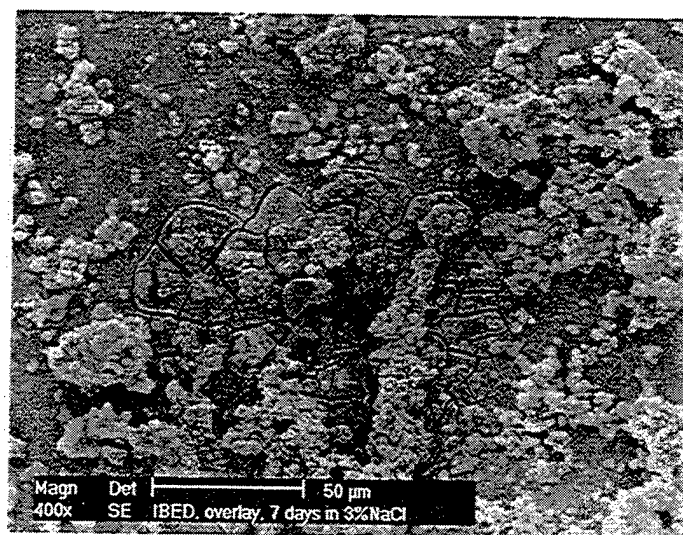


Figure 48. Scanning Electron Micrograph Of Surface Shown In Figure 45 After 7 Days Of Exposure To A 3% NaCl Aqueous Solution.

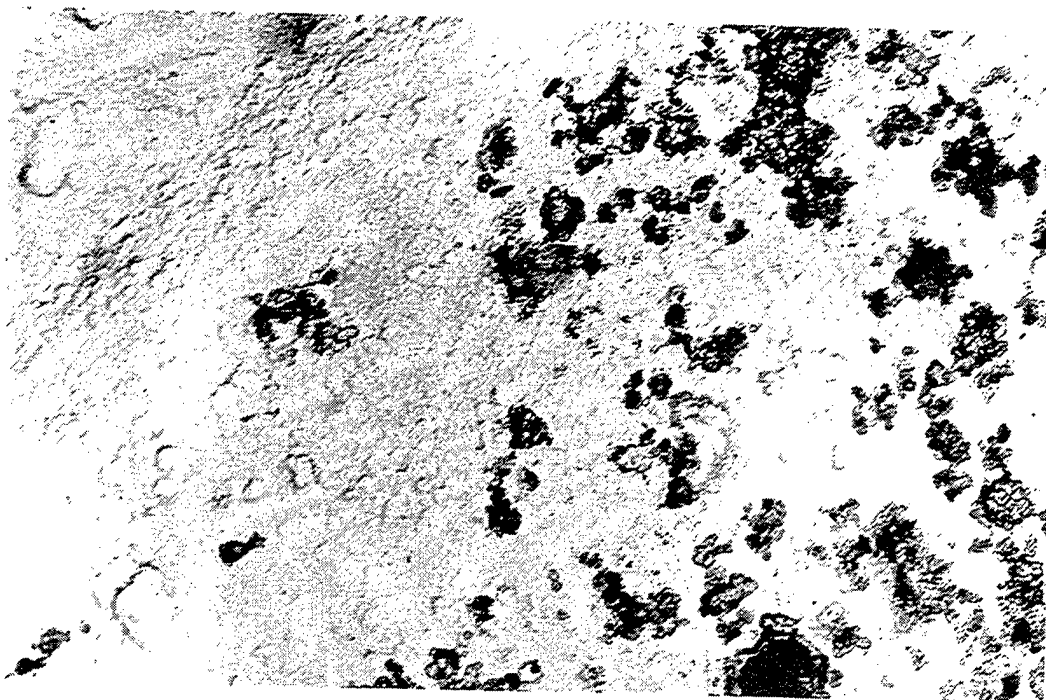


Figure 49. TEM Micrograph Of Carbon Replica Of Detergent Cleaned Aluminum Alloy 2024-T3 Surface. (Magnification 80,000 X)

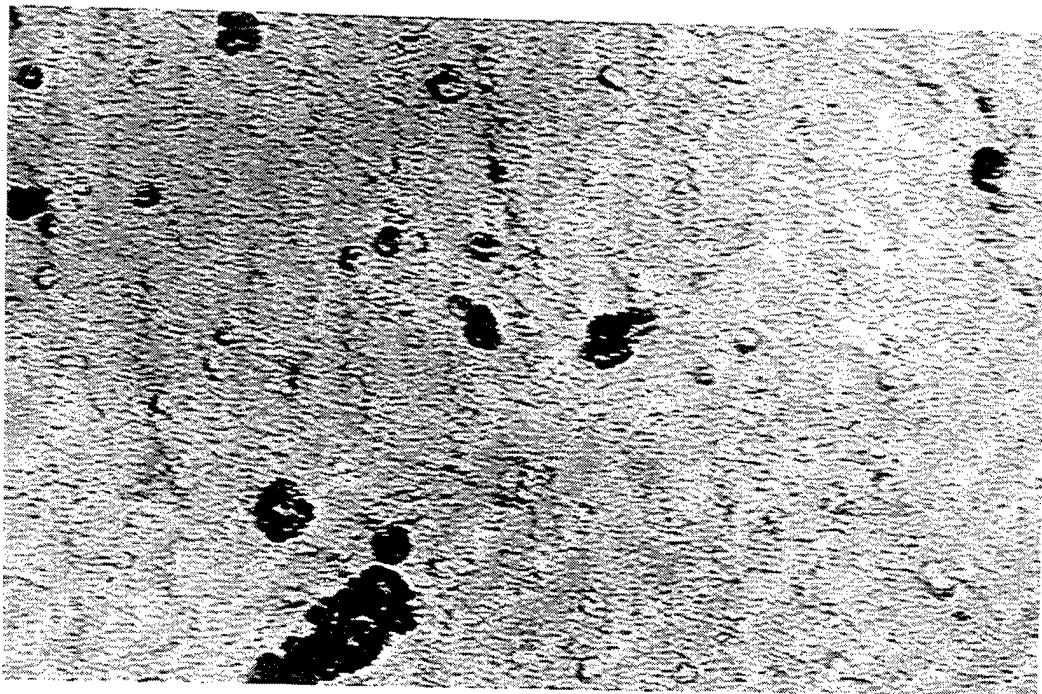


Figure 50. TEM Micrograph Of Carbon Replica Of HNO₃ - HF Pickled Aluminum Alloy 2024-T3 Surface. (Magnification 80,000 X)

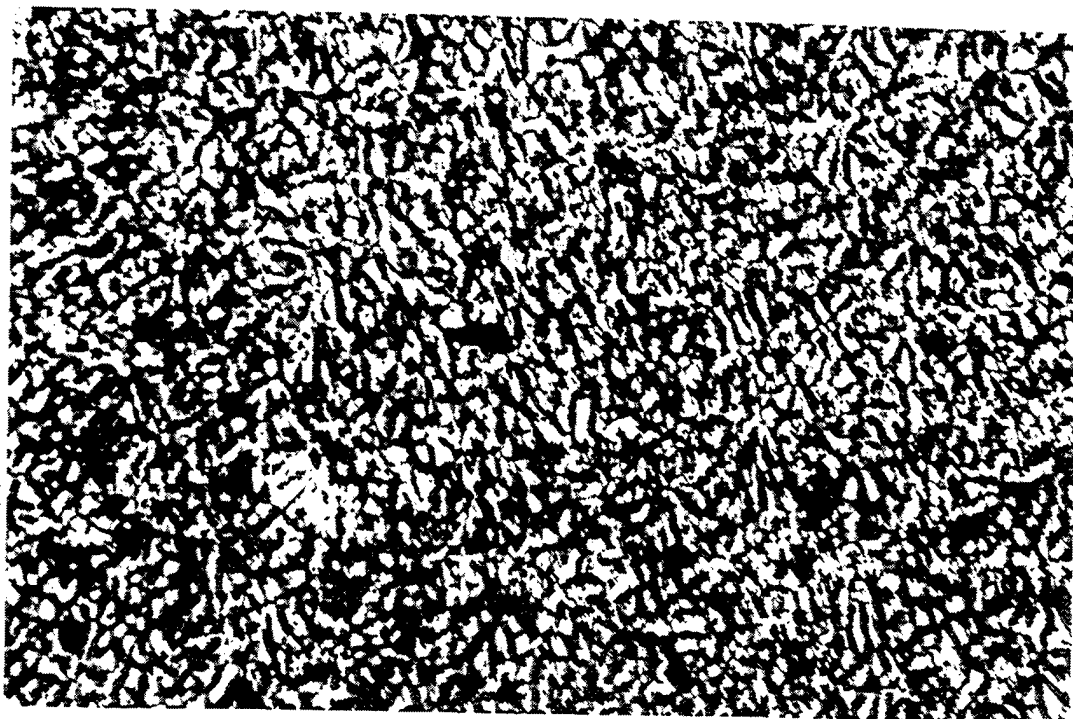


Figure 51. TEM Micrograph Of Carbon Replica Of PAA Treated Aluminum Alloy 2024-T3 Surface. (Magnification 80,000 X)

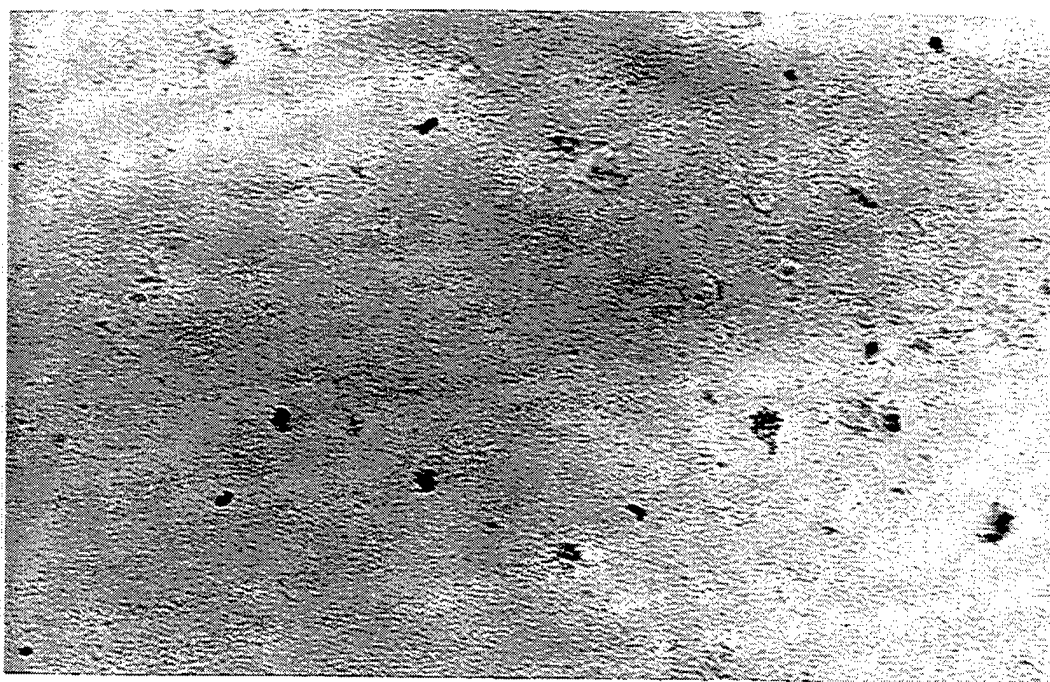


Figure 52. TEM Micrograph Of Carbon Replica Of Ion Beam Cleaned Surface Of Aluminum Alloy 2024-T3. (Magnification 80,000 X)

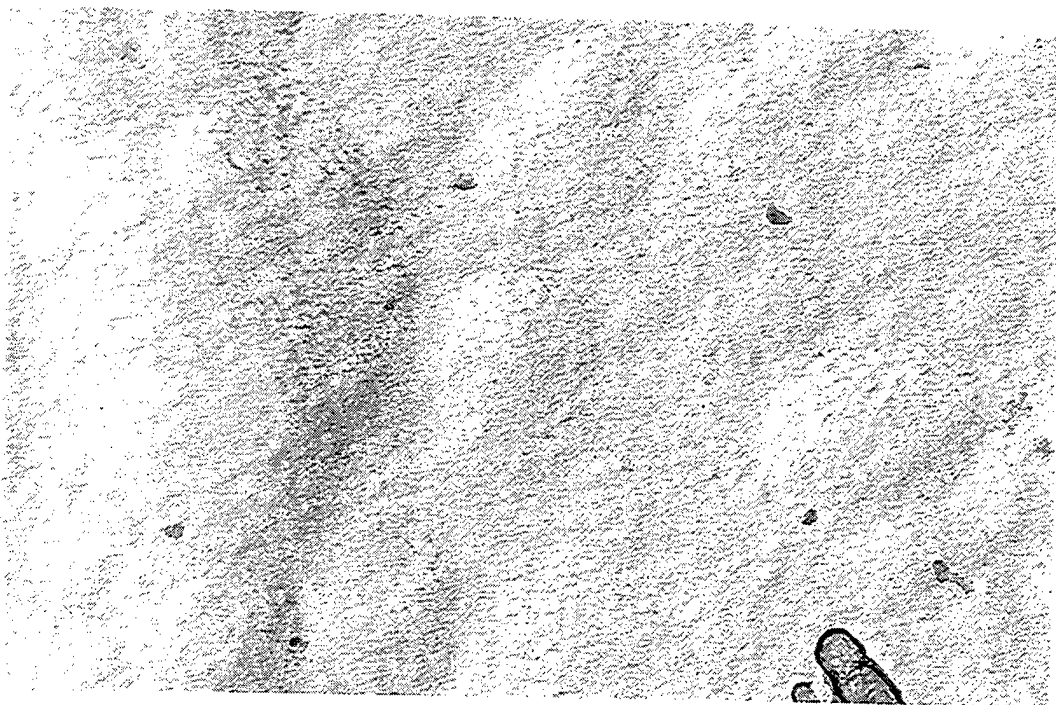


Figure 53. TEM Micrograph Of Carbon Replica Of IBED Treated Surface Of Aluminum Alloy 2024-T3. (Magnification 80,000 X)

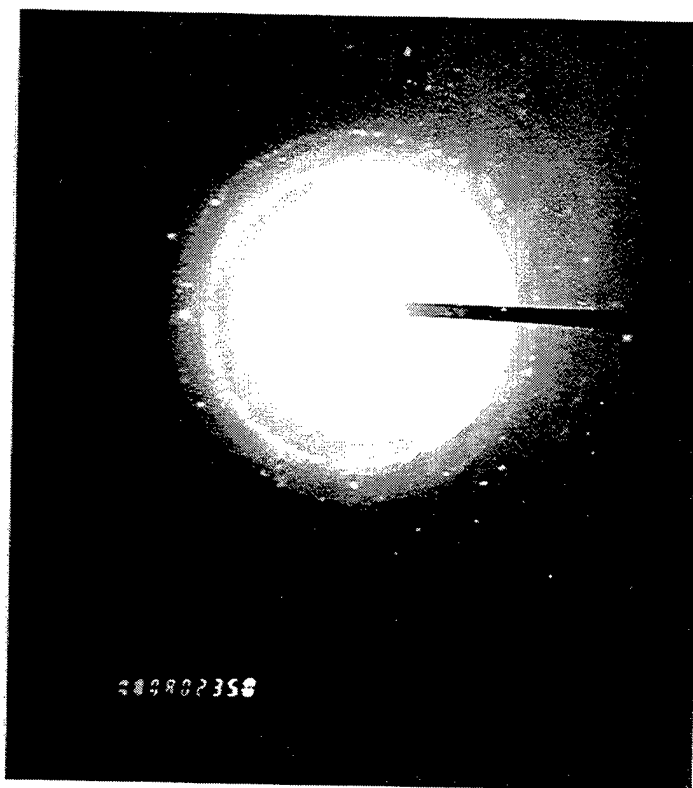


Figure 54. Electron Diffraction Pattern Of Surface Oxide Resulting From The IBED Process And Oxide Growth Without Augmenting Beam.

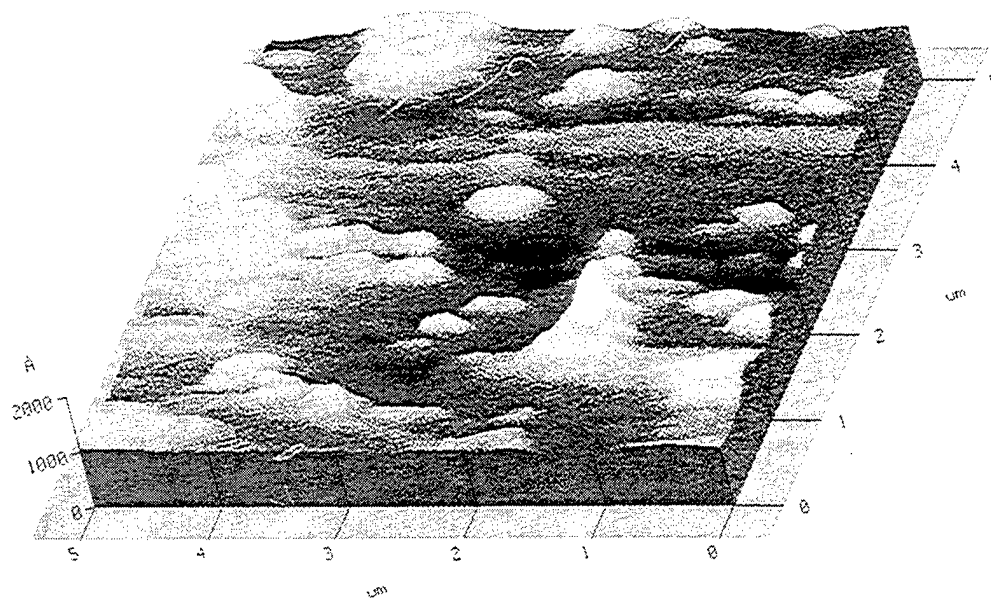


Figure 55. Profile Of Aluminum Alloy 2024-T3 With 2,000Å IBED Film, Generated With AFM.

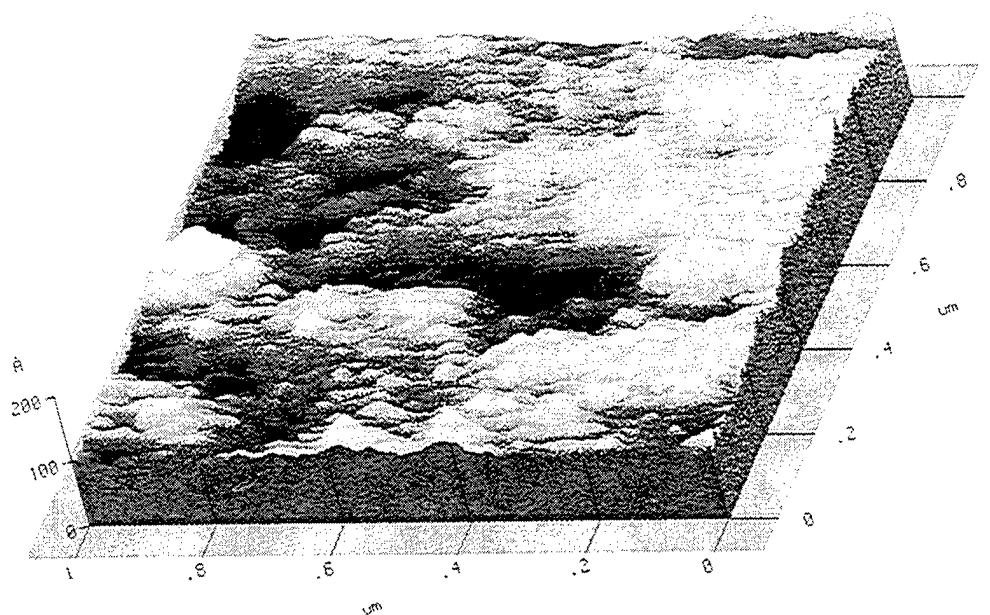


Figure 56. High Magnification Profile Of Area In Figure 55.

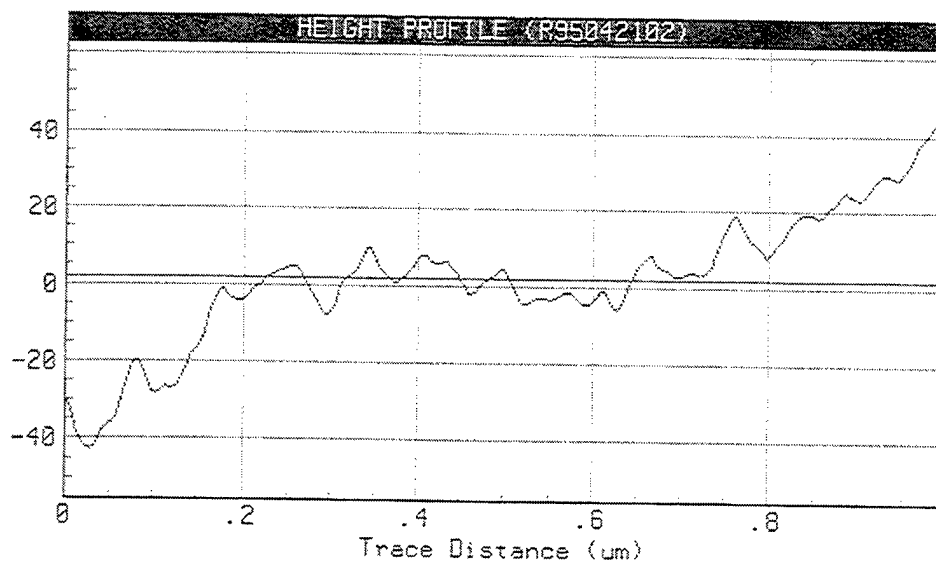
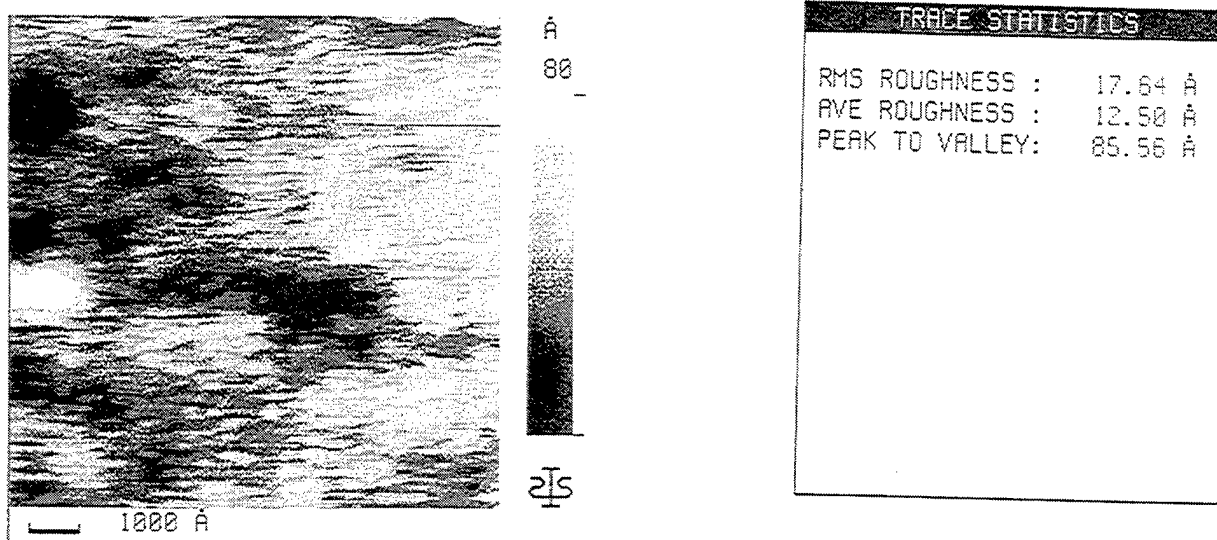


Figure 57. Height Profile Of A Typical Scan Across The Profile In Figure 56.

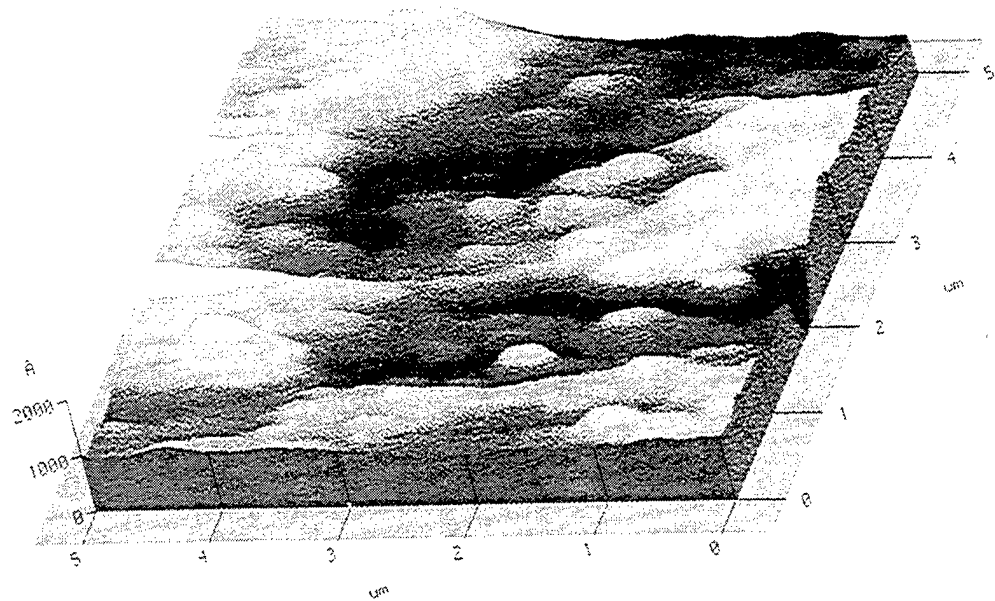


Figure 58. Profile Of Aluminum Alloy 2024-T3 With 3,000Å IBED Film (2,000Å Barrier Film And 1,000Å Top Film)

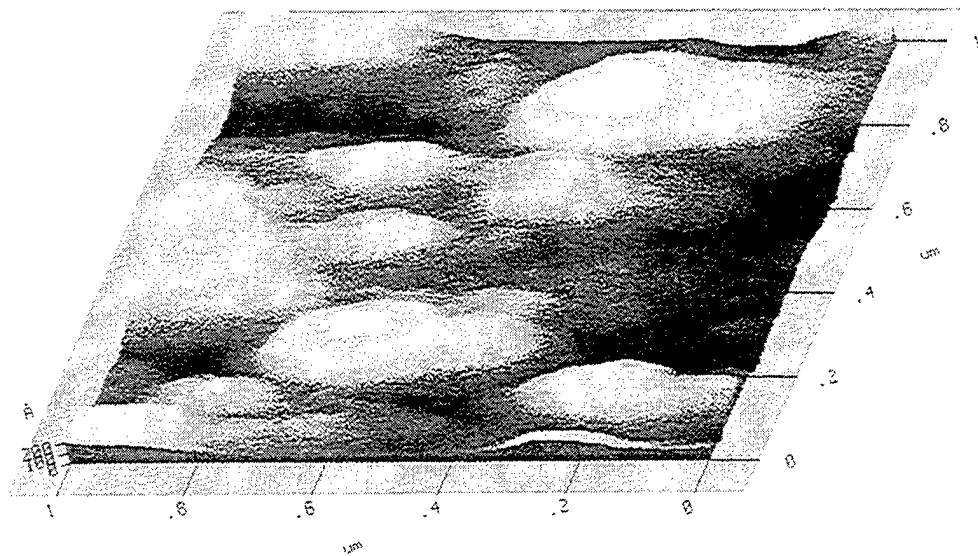


Figure 59. High Magnification Profile Of Area In Figure 58.

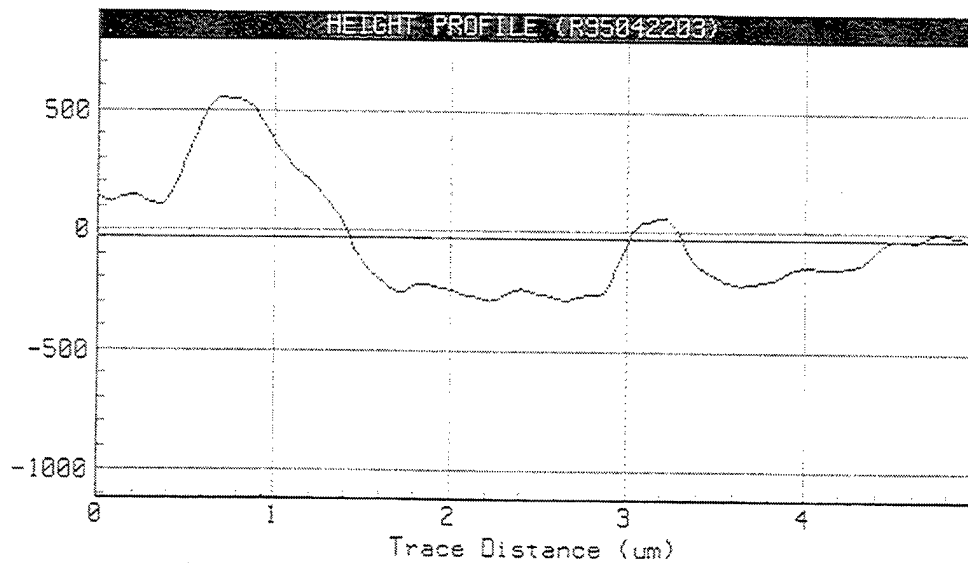
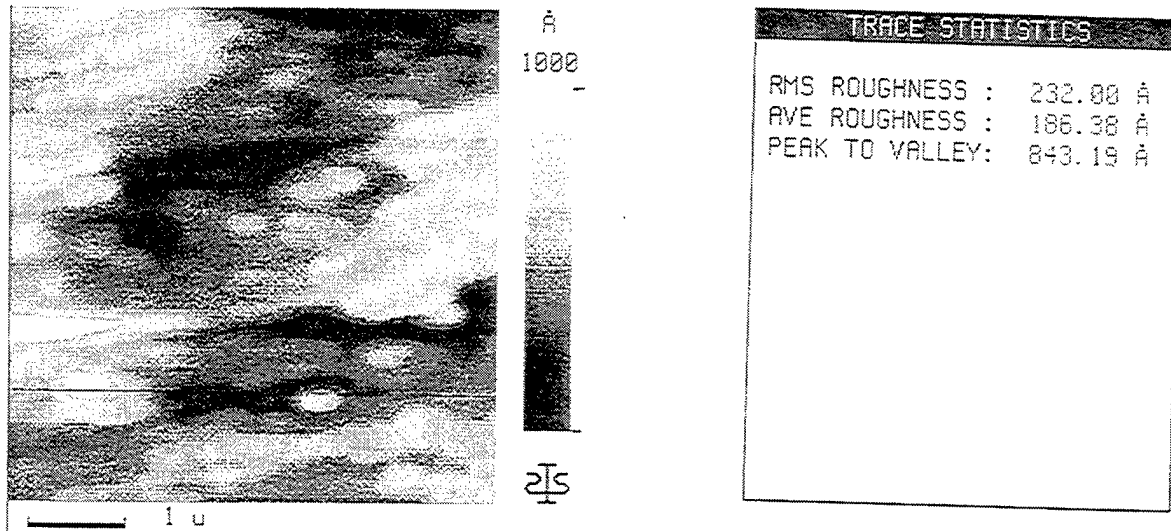


Figure 60. Height Profile Of A Typical Scan Across The Profile In Figure 59.

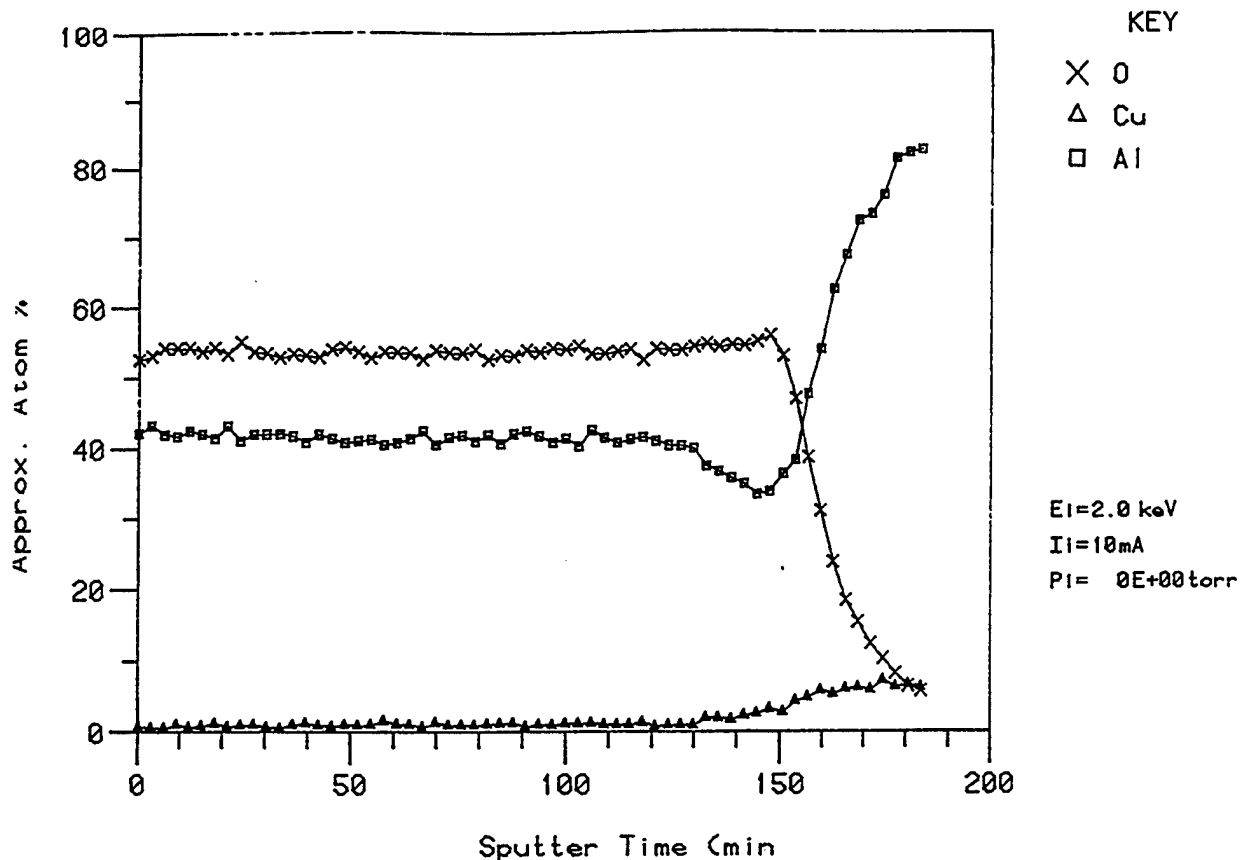


Figure 61. Auger Electron Spectrograph Depth Profile Across The Aluminum Oxide Indicating Oxide Thickness. A Copper Scan Indicates The Absence Of Copper In The Oxide.

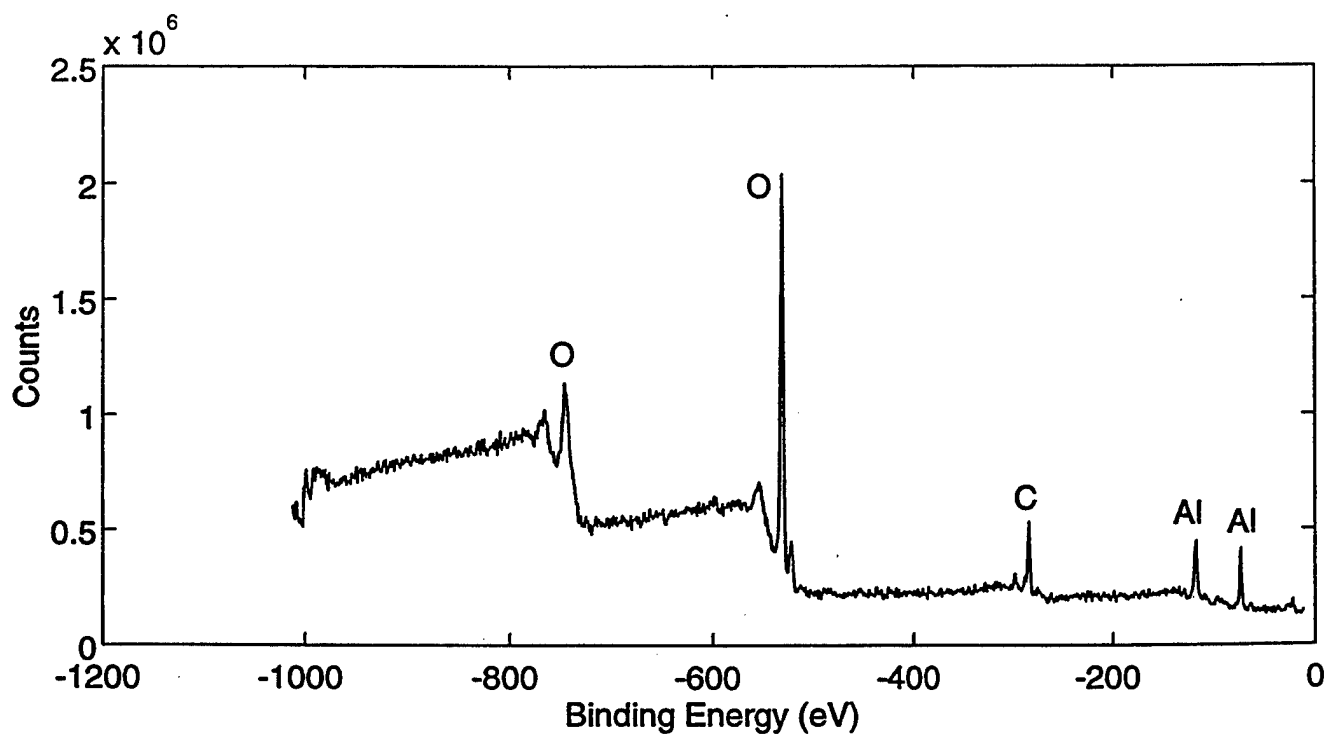


Figure 62. XPS Scan Of IBED Treated Aluminum Alloy 2024-T3.

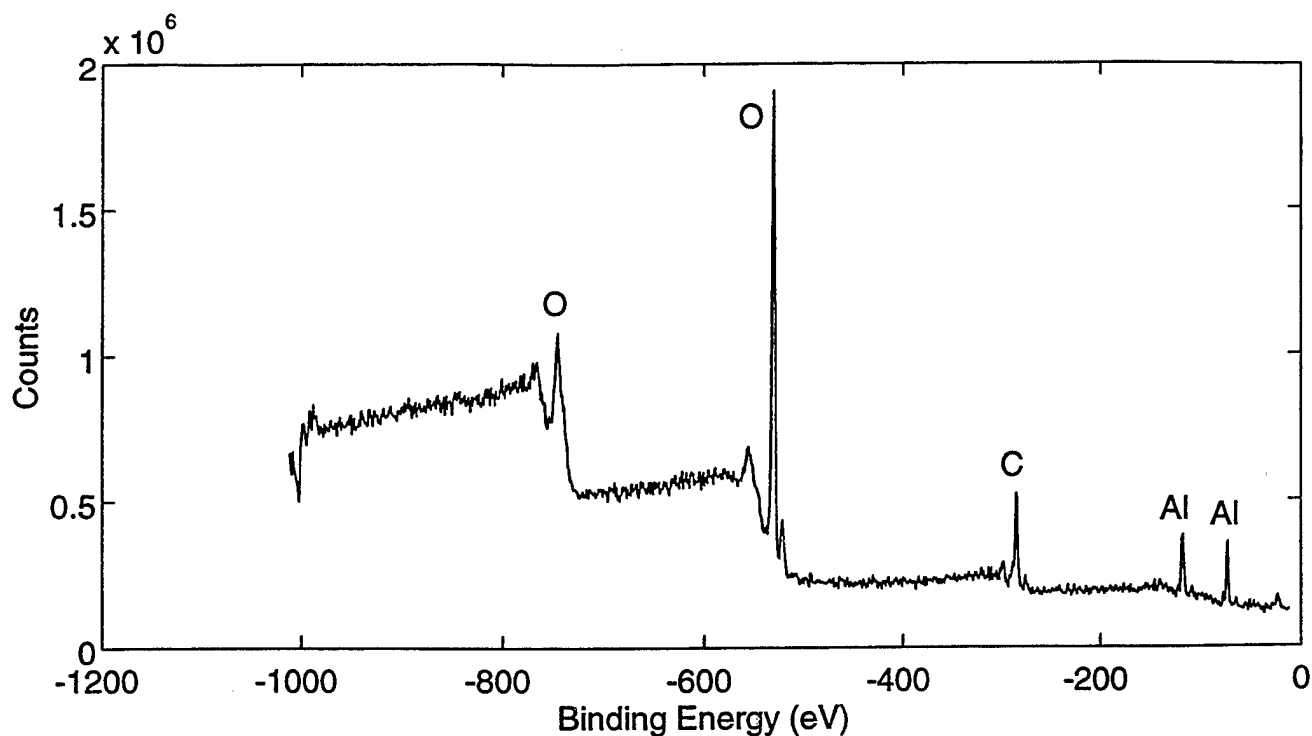


Figure 63. XPS Scan Of IBED Treated Aluminum Alloy 2024-T3 After Exposure To Boiling Water For 15 Minutes Then Dried In 110°C (230°F) Air.

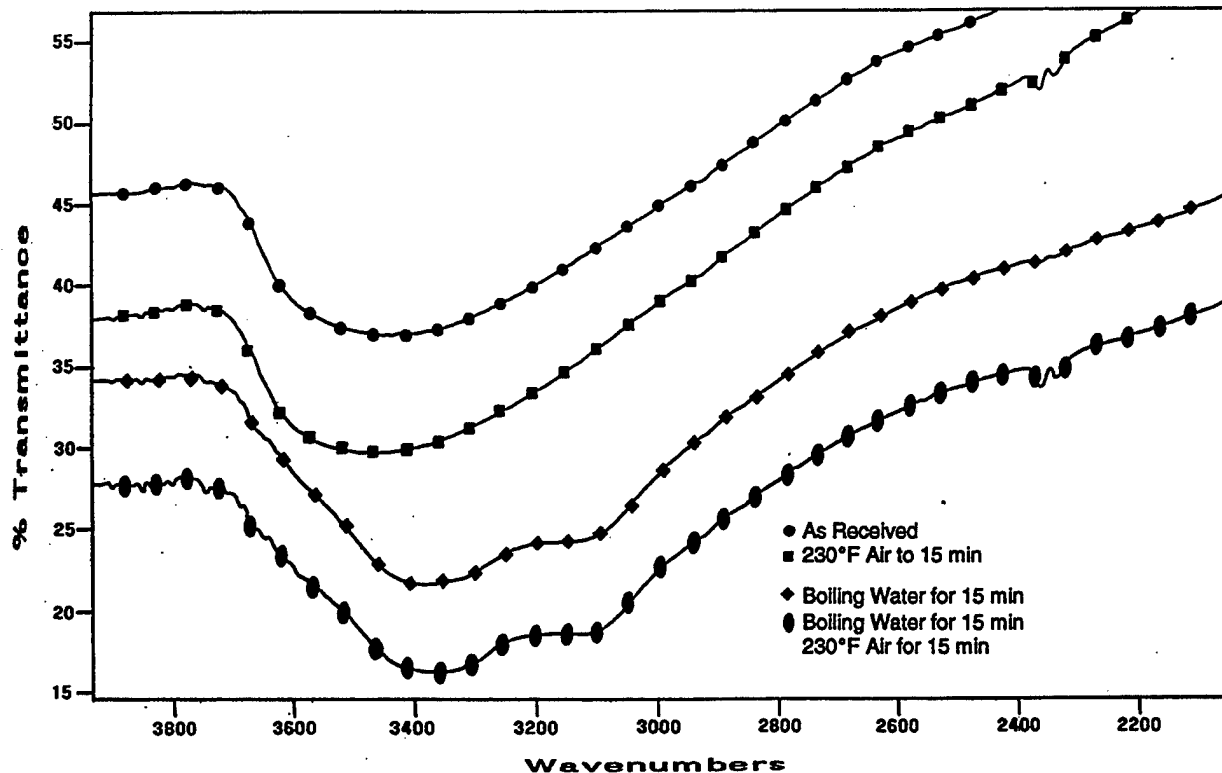


Figure 64. FTIR Spectra Of IBED Treated Aluminum Alloy 2024-T3 Exposed To Boiling Water And 110°C (230°F) Air.

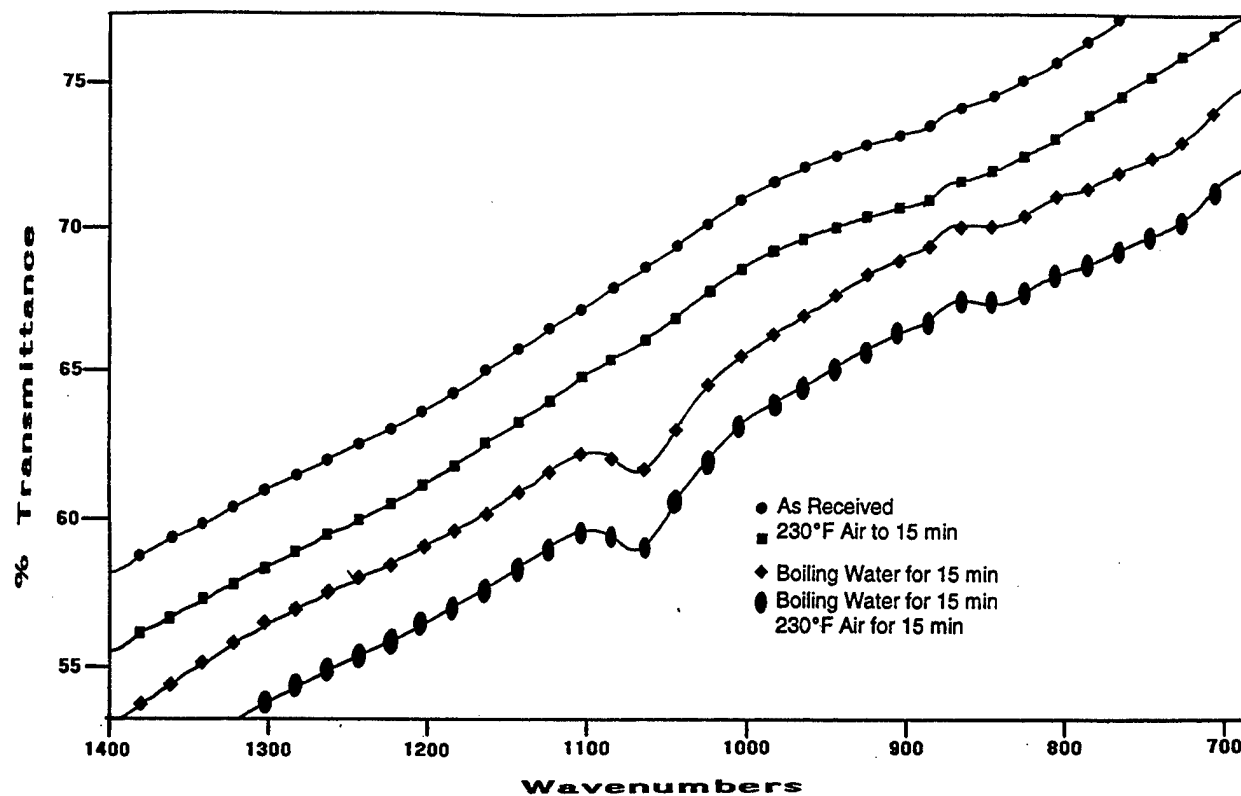


Figure 65. FTIR Spectra Of IBED Treated Aluminum Alloy 2024-T3 Exposed To Boiling Water And 110°C (230°F) Air.

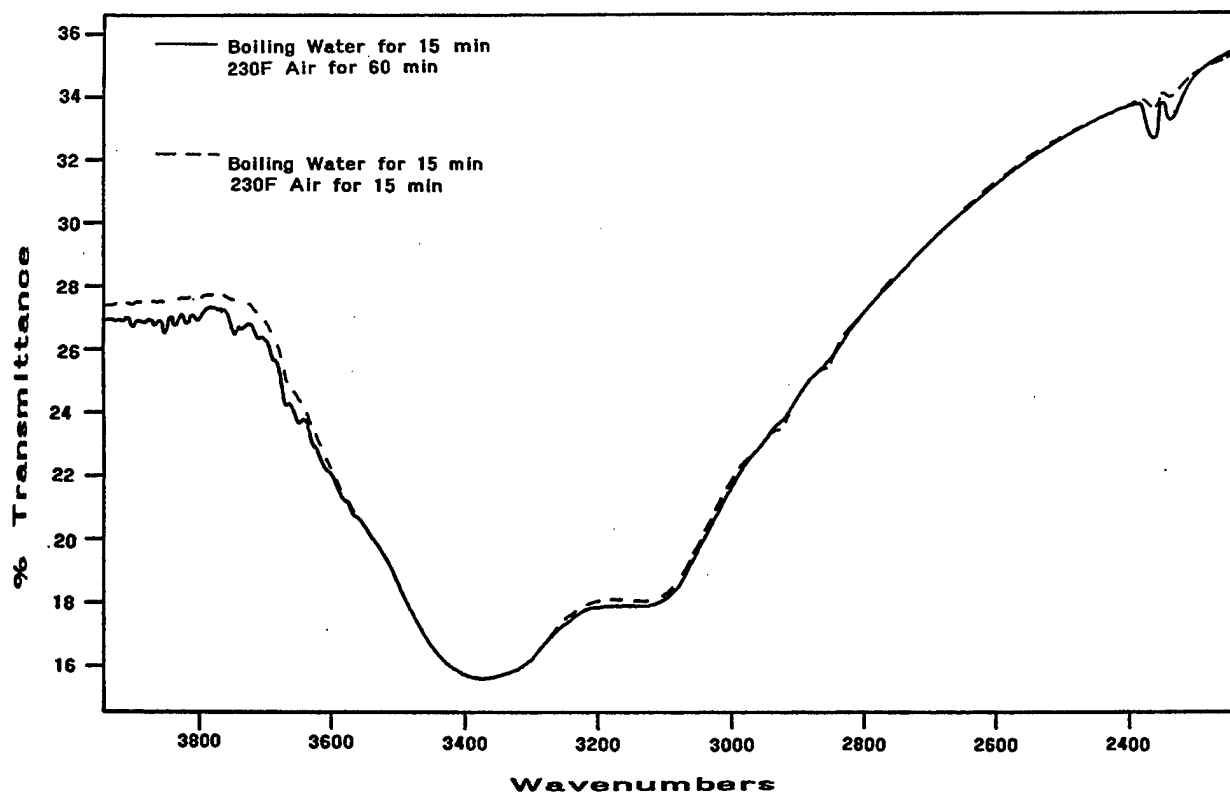


Figure 66. FTIR Spectra Showing The Effect Of Exposure Time To 110°C (230°F) Air On The Hydroxyl Peak.